

PART I  
THE INFRARED SPECTRA AND STRUCTURE OF CYANAMIDE

PART II  
THE INFRARED SPECTRA OF FORMAMIDE, N,N-DIDEUTEROFORMAMIDE,  
AND N-METHYLFORMAMIDE

Thesis by  
Hector Rubalcava

In Partial Fulfillment of the Requirements  
for the Degree of  
Doctor of Philosophy

California Institute of Technology  
Pasadena, California

1956

## ACKNOWLEDGMENTS

It is a pleasure to express my sincere gratitude to the many people who have helped me during the period of my graduate studies. In particular, I would like to thank Professor Richard M. Badger for his patient guidance, instruction, and encouragement during all phases of this work. I also wish to acknowledge my debt to my fiancée, Miss Magdalen Belton, for drawing many of the figures, and to my sister, Miss Gloria Rubalcava, for typing the rough draft of this thesis. My sincere thanks are also extended to the Dow Chemical Company for sponsoring a fellowship which I enjoyed during the academic year 1951-1952.

## ABSTRACT

1. The prismatic spectra of crystalline cyanamide and of methylene chloride solutions of cyanamide were obtained from 2 to 15 microns, and of gaseous cyanamide from 2 to 6.5 microns. High dispersion spectra in the three micron region were obtained for all these substances. The rotational structure of the antisymmetric  $\text{NH}_2$  stretching vibration shows an intensity alternation which implies that cyanamide has a planar structure, belongs to the symmetry point group  $\text{C}_{2v}$ , and has the structural formula  $\text{H}_2\text{NCN}$ . Geometrical parameters of the  $\text{NH}_2$  group were obtained using the spacing of the rotational structure of the three micron band, together with a non-critical estimate of the mean value of the two smallest rotational constants, and the mean value of the  $\text{NH}_2$  stretching frequencies. The HNH angle is approximately  $126^\circ$ , and the NH bond distance is  $1.002 \text{ \AA}$ . A vibrational assignment was made with the aid of Raman data obtained by Kahovec and Kohlrausch. A normal coordinate analysis of the vibrations primarily involving the NCN stretching and the HNH scissors deformations was made. This analysis gave values, depending parametrically on the HNH bending force constant, of the CN stretching and interaction force constants. The forms of the normal modes of the three lowest frequency  $\text{A}_1$  vibrations for a plausible set of force constants was calculated, and applied to a

discussion of the intensities of the absorptions of these vibrations. The high dispersion spectra of methylene chloride solutions of cyanamide showed no absorptions attributable to hydrogen-bonded polymers of cyanamide.

2. The spectra of  $\text{HCONH}_2$ ,  $\text{HCOND}_2$  and  $\text{HCONHCH}_3$  were obtained in the gas and in the liquid states. The three micron spectrum of  $\text{HCONH}_2$  gas was examined under high dispersion. These data together with the results obtained by Prof. R. M. Badger in a study of vibrating mechanical models, and by Dr. R. Newman in a study of the polarized spectrum of sodium formate have been the basis for an analysis of the vibrational spectra of the formamides. An explanation has been presented for the differences between the spectra of each substance in the gas and in the liquid states based on the effects of hydrogen-bonding. The spectral data have been used to support the hypothesis that formamide is a planar molecule, and an estimate of  $0.993 \overset{\text{O}}{\text{\AA}}$  for the NH bond distance based on the value of the mean frequency of the  $\text{NH}_2$  stretching vibrations has been made. The rotational structure of the three micron high dispersion band has been analyzed, and a value for the difference of the large rotational constant and the average of the two smallest rotational constants has been found which agrees, within experimental error, with the microwave value.

# TABLE OF CONTENTS

## PART I

### THE INFRARED SPECTRA AND STRUCTURE OF CYANAMIDE

	Page
Introduction . . . . .	1
Experimental . . . . .	5
Vibrational Spectrum of Cyanamide . . . . .	8
A. Cyanamide dissolved in methylene chloride . .	12
B. Crystalline cyanamide . . . . .	15
C. Gaseous cyanamide . . . . .	17
D. The Raman spectrum . . . . .	20
E. Discussion of the vibrational spectrum . . . .	22
1. The $\text{NH}_2$ vibrations . . . . .	22
2. The NCN stretching vibrations . . . . .	25
The Combination Band at Three Microns . . . . .	49
The Rotational Structure of the Three Micron Band .	51
A. Introduction . . . . .	51
B. Analysis of the rotational structure . . . . .	52
C. Discussion of the rotational structure . . . .	57
D. Molecular parameters . . . . .	66

## PART II

### THE INFRARED SPECTRA OF FORMAMIDE, N,N-DIDEUTEROFORMAMIDE, AND N-METHYLFORMAMIDE

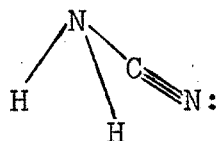
	Page
Introduction . . . . .	74
Experimental . . . . .	75
Vibrational Spectrum and Discussion . . . . .	78
A. Introductory discussion . . . . .	78
B. The hydrogen stretching vibrations . . . . .	96
C. The 1800 to 1250 $\text{cm}^{-1}$ A' vibrations . . . . .	99
D. The A' vibrations below 1250 $\text{cm}^{-1}$ . . . . .	101
E. The A" vibrations . . . . .	103
F. Remaining absorption bands . . . . .	105
G. Some summarizing comments . . . . .	106
H. The vibrational spectra of gaseous and liquid N-methylformamide . . . . .	108
1. The hydrogen stretching vibrations . . . . .	112
2. The 1800 to 1200 $\text{cm}^{-1}$ frequencies . . . . .	113
3. The vibrations below 1200 $\text{cm}^{-1}$ . . . . .	117
I. Concluding remarks . . . . .	118
Appendix 1 . . . . .	119
Appendix 2 . . . . .	120
Appendix 3 . . . . .	122
Appendix 4 . . . . .	125
References . . . . .	127
Propositions . . . . .	131

PART I

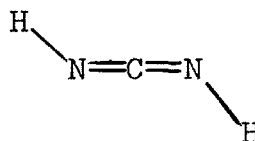
THE INFRARED SPECTRUM AND STRUCTURE OF CYANAMIDE

## Introduction

The structure of cyanamide has been a matter of interest and speculation for some time (1,2,3,4,5,6).



I



II

Figure 1. Possible structures for cyanamide.

The structures I and II have been generally proposed for the molecular configuration of this molecule. A search of the literature reveals that no definitive investigations employing the more powerful techniques of structural chemistry upon gaseous cyanamide have been published. In all probability, this lack of data arises from the instability of cyanamide at temperatures suitable for spectroscopic and electron diffraction experiments. However, investigations have been reported in which methods not subject to these limitations have been used. Measurements of the dipole moment (7), of the magnetic susceptibility (8), and of the Raman spectrum (2,9) of the molecule in various states have all indicated that the two hydrogens are bonded to one nitrogen atom, or if two species do exist in



tautomeric equilibrium, that  $\text{NH}_2\text{CN}$  is the predominant form. It should be noted that derivatives of both substances exist. Diisopropyl cyanamide,  $(\text{CH}_3\text{CHCH}_3)_2\text{NCN}$ , and diisopropyl carbodiimide,  $(\text{CH}_3\text{CHCH}_3)\text{NCN}(\text{CH}_3\text{CHCH}_3)$ , are well known; indeed, their properties have been used in earlier investigations as criteria for discussing the structure of cyanamide.

Evidence is presented below which proves that cyanamide is a planar molecule belonging to the symmetry point group  $\text{C}_{2v}$ , that the hydrogens are attached to the same nitrogen atom, and that the HNH angle is slightly larger than  $120^\circ$ . These facts make it convenient to discuss the structure of the molecule in terms of the resonating configurations I and II, presented in Figure 2.

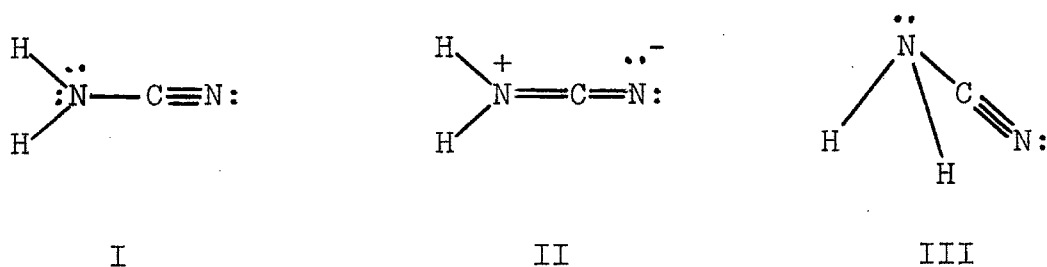


Figure 2. Resonating configurations for cyanamide.  
I and II are planar, III is non-planar.

Each configuration is planar, has an HNH angle of approximately  $120^\circ$ , and has  $\text{C}_{2v}$  symmetry. The main differences between I and II are the bond order of the CN bonds, the

charge distribution, and a slightly larger HNH angle in II. The positive charge on the inner nitrogen atom in structure II would induce positive charges on the hydrogen atoms greater than those in I, leading to the increase in the HNH angle. The particular structural parameters claimed for the resonating configurations can be explained by a trigonal hybridization,  $sp^2$ , of the inner nitrogen atom, and a linear,  $sp$ , hybridization of both the terminal nitrogen atom and of the carbon atom.

At first thought one might not consider using I as a resonating form, but instead one would rather use III, a more familiar form. III is like an ammonia molecule in which one hydrogen has been replaced by a CN group, i.e. the HNH angle is about  $107^\circ$ , and the configuration belongs to the point group  $C_s$ . The use of II and III would predict an HNH angle between  $107^\circ$  and  $120^\circ$ , CN bonds of an intermediate order, and a non-planar molecule. The use of I and II predicts an HNH angle somewhat greater than  $120^\circ$ , CN bonds of intermediate order, and a planar molecule. Since the use of resonating configurations in structural discussions is equivalent to expanding the molecular wave function in a linear combination of wave functions, each representing one of the resonating configurations, the usefulness of the particular forms chosen for the expansion depends, in part, on the completeness with which the contributing configurations include the properties (except

the energy) of the actual molecule. Thus the use of I and II is preferred to the use of II and III. The former choice is also better because there is little difference in the position of the hydrogens in the two resonating configurations.

### Experimental

E. K., practical grade, cyanamide was used in these experiments. It was purified by recrystallization from methylene chloride. After purification the cyanamide melted at  $46^{\circ}\text{C}$ . The listed melting point values range from  $42^{\circ}\text{C}$  to  $48^{\circ}\text{C}$ . The methylene chloride used was reagent grade material which was dried with  $\text{CaCl}_2$  or  $\text{CaSO}_4$ , then was treated with anhydrous  $\text{K}_2\text{CO}_3$  to remove traces of acid. The transfer and storage of these materials was made in a dry box to lessen the absorption of water by cyanamide.

The ease with which cyanamide polymerizes is an important source of experimental difficulty. Decomposition occurs when moist cyanamide is stored for extended periods of time. It has been stored satisfactorily by keeping it dry and refrigerated. The low vapor pressure of cyanamide, 19 mm Hg at  $140^{\circ}\text{C}$ , together with its instability at this temperature complicates the study of the gas. The products of pyrolysis are melam, melamine, and ammonia. The first two are heavy molecules formed with the evolution of ammonia. Thus the appearance of the absorption bands of ammonia present a way for following the decomposition of cyanamide during spectroscopic runs. An examination of cyanamide sealed in Pyrex tubes showed no decomposition in

periods of spectroscopic interest, i.e. 30 minutes, until temperatures higher than  $115^{\circ}\text{C}$  are reached. At  $120^{\circ}\text{C}$  the compound decomposes in a sudden manner. The molten liquid lies quiescent for periods generally less than five minutes, and then it abruptly begins to boil. Within 20 seconds the reaction is complete, and an opaque, white solid remains.

The absorption cells used for examining the gas spectrum were filled as follows: a saturated solution of cyanamide in methylene chloride was introduced into an evacuated cell from a special vessel that had been filled in the dry box. The cell was then connected to a vacuum system and the methylene chloride was removed under reduced pressure. Finally the side arm through which the cell was filled was sealed off and removed as near the cell as possible. Care had to be exercised to prevent cyanamide from adhering to the cell windows. A depression blown into the bottom of the cell was found to be helpful in this respect.

The spectra were obtained with a Beckman IR-2 spectrometer, adapted for automatic recording; with our vacuum grating spectrometer, using a  $\text{CO}_2(\text{s})/\text{MeOH}$  cooled PbS detector; and with a Perkin-Elmer Model 21C spectrometer. The gaseous spectra were obtained using a heated absorption cell. A 1.1 m glass cell with thin hemispherical Pyrex windows was used for the high dispersion spectra. An 0.5 m

cell with KBr windows was used for the prismatic spectrum. The cell was enclosed in a steel tube wrapped with asbestos, and heated electrically. The temperature of the windows was maintained at 5-10°C above the temperature of the tube. Copper-constantan thermocouples attached to the cell were used to measure temperatures.

Spectra of cyanamide dissolved in  $\text{CH}_2\text{Cl}_2$  were obtained using cells with rock salt windows.

The spectrum of the solid was obtained by allowing cyanamide to recrystallize (in a moisture free atmosphere) from  $\text{CH}_2\text{Cl}_2$  on a rock salt plate, which was then covered with another and placed in a special holder, employing "O" rings to exclude atmospheric moisture. Special care was taken to insure that the cyanamide did solidify since it tends to supercool.

Attempts to obtain a suitable spectrum of gaseous cyanamide in the rock salt region were not successful. Each attempt was vitiated by the absorption of liquid cyanamide condensed on the cell windows, or by decomposition of the cyanamide.

### Vibrational Spectra of Cyanamide

Cyanamide, a planar pentatomic molecule, has nine fundamental vibrations. The symmetry of the molecule causes these to be classed into four totally symmetric vibrations ( $A_1$ ), three in-plane vibrations antisymmetric with respect to the two-fold axis ( $B_1$ ), and two vibrations antisymmetric with respect to the plane of the molecule ( $B_2$ ). An approximate description of the form of these vibrations is shown in Figure 3.

The spectrum of cyanamide was examined from 2 to 15 microns. Table 1 lists the conditions under which the various spectra were obtained. The vibrational assignments are given in Table 2.

The Raman shifts observed by Kahovec and Kohlrausch (9) for crystalline cyanamide and for melted cyanamide have also been listed in Table 2. Assignments are made for the observed shifts in order to aid in the study of the infrared spectrum.

Table 1. Spectra of cyanamide obtained.

State	Range(microns)	Conditions
Gas	3	t=115°C, high dispersion spectrum
Gas	4	t=115°C, prismatic spectrum
Solution*	2-15	Sat'd sol'n, prismatic spectrum
Solution	3	Sat'd sol'n, high disp. spectrum
Solution	3	1/3.2 sat'd sol'n, high disp. spectrum
Solution	3	1/22.5 sat'd sol'n, high disp. spectrum
Crystal	3	High dispersion spectrum
Crystal	2-15	Prismatic spectrum

All temperatures, unless so noted, were approximately 25°C.

\*All solutions were in methylene chloride.





Figure 3. Schematic representation of the normal modes of cyanamide.

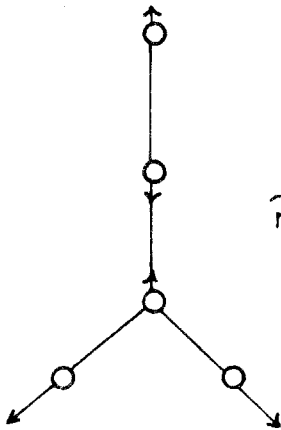
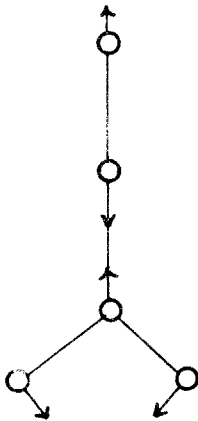
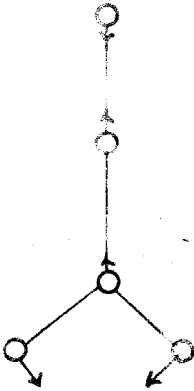
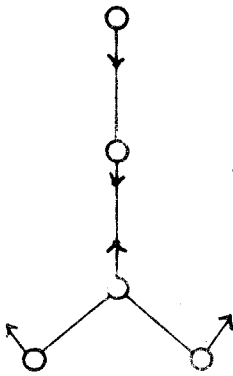
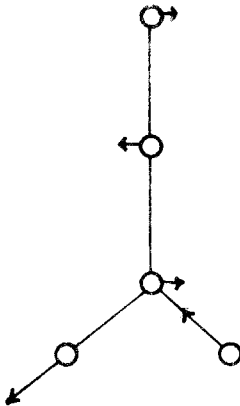
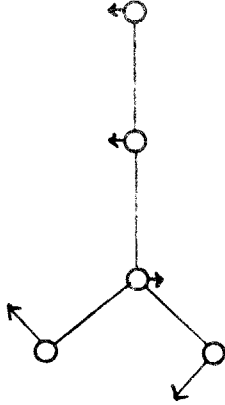
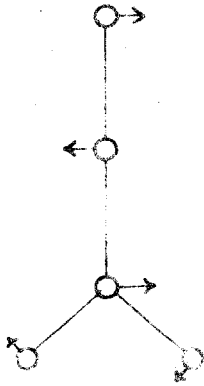
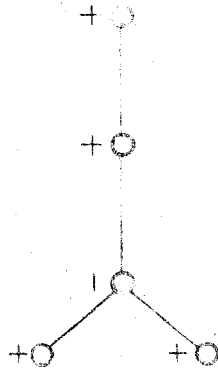
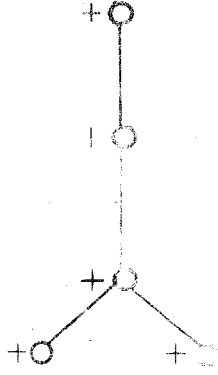
		
		
		

Table 2. Vibrational assignments for cyanamide.

Infrared				Raman (9)	
Assign't	Gas	Soln.	Crystal	Crystal	Melt
$\nu_5$ ( $b_1$ )*	3469.1(s)**	3443(s)	3327(s)	3326(3)	
$\nu_2 + \nu_4$ ( $A_1$ )	(?)***	3422(w)			
$\nu_1$ ( $a_1$ )	(3420)(m)	3363(s)	3248(w)	3232(6b)	
?		3269(w)			
?		3148(vw)			
$2\nu_3$ ( $A_1$ )			3105(w)	3108	
$2\nu_6 + \nu_8$ ( $B_2$ )			3058(w)		
$\nu_2 + \nu_7$ ( $B_1$ )		2732(w)	2730(w)		
$\nu_2$ ( $a_1$ )	2275(s)	2257(s)	2247(s)	2259(1)	2232(3b)
$2\nu_4$ ( $A_1$ )				2210(6)	
?				2115(1/2?)	
$\nu_3$ ( $a_1$ )		1590(s)	1587(s)	1556(2)	1580(2)
$\nu_8 + \nu_9$ ( $A_1$ )			1390(vw)		
$\nu_4 + 2\nu_c$ ****				1174(1?)	
$\nu_4 + \nu_c$ ****				1148(4)	
$\nu_4$ ( $a_1$ )			1122(w)	1119(1?)	1119(4b)
$\nu_6$ ( $b_1$ )		1080(w)			1048(1/2?)
$\nu_8$ ( $b_2$ )					1003(1/2)
$\nu_7 + \nu_9$ ( $A_2$ )					912(1)
$\nu_7$ ( $b_1$ )				obscured	513(0)
$\nu_9$ ( $b_2$ )					429(1/2)

Frequencies are in  $\text{cm}^{-1}$ .

\*Vibrational species designations probably do not apply to crystal vibrations.

\*\*Precise value depends on analysis of rotational structure. This value is correct to  $0.4 \text{ cm}^{-1}$ .

\*\*\*  $\nu_2 + \nu_4$  may constitute part of the complex structure of the  $3\mu$  band.

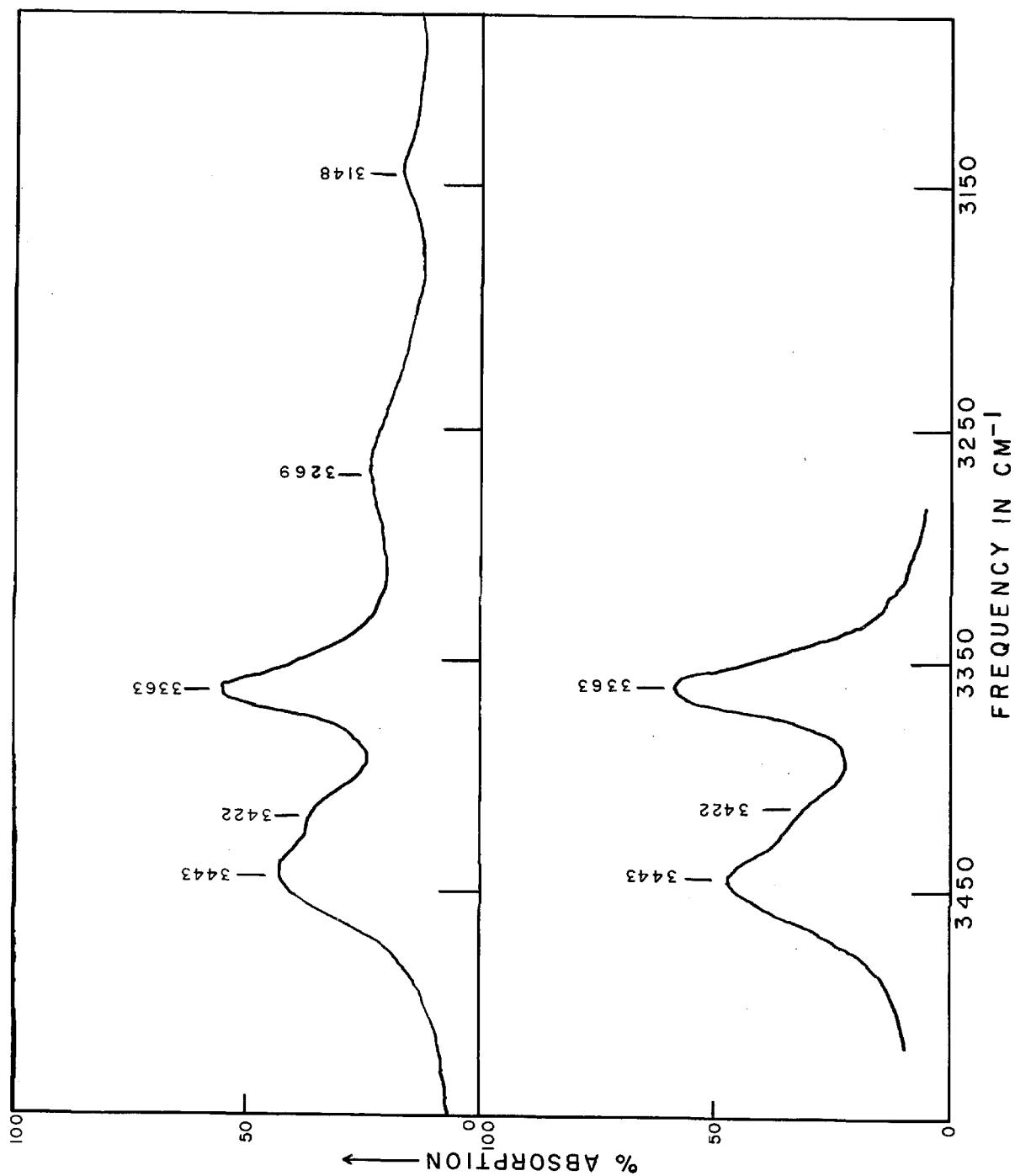
\*\*\*\* See p. 21 for discussion of  $\nu_c$ .

A. Cyanamide dissolved in methylene chloride.

Under high dispersion the spectrum of a saturated solution of cyanamide in methylene chloride shows five absorption maxima in the three micron region. This spectrum is shown in Figure 4. There are three clearly defined bands at 3443, 3422, and 3363  $\text{cm}^{-1}$ . These three bands show no significant change with respect to each other over a more than twenty-fold concentration range at constant concentration-length product. This indicates that these bands belong to vibrations of the cyanamide molecule, per se, and not to hydrogen-bonded species. The band at 3443  $\text{cm}^{-1}$  is assigned to  $\nu_5$ , the antisymmetric  $\text{NH}_2$  stretching vibration; the band at 3363  $\text{cm}^{-1}$  is assigned to  $\nu_1$ , the symmetric  $\text{NH}_2$  stretching vibration; and the band at 3422  $\text{cm}^{-1}$  is assigned to the combination band  $\nu_2 + \nu_4$ . This assignment is discussed on page 49. Two weak bands are also observed in the spectrum of the saturated solution at 3269 and 3148  $\text{cm}^{-1}$ . It may well be that these bands should be assigned to hydrogen-bonded species, since they are rather broad and seem to disappear with dilution. Unfortunately, observations in the spectral region of these two bands are rendered uncertain by solvent absorption and low instrumental sensitivity. The prismatic spectrum of a saturated solution of cyanamide in methylene chloride, presented in Figure 5, shows four additional ab-



Figure 4. 3 micron high dispersion spectra of methylene chloride solutions of cyanamide. Upper curve shows the spectrum of a saturated solution; path length is 0.20 mm. Lower curve shows the spectrum of a 1/22.5 saturated solution; path length is 4.5 mm.





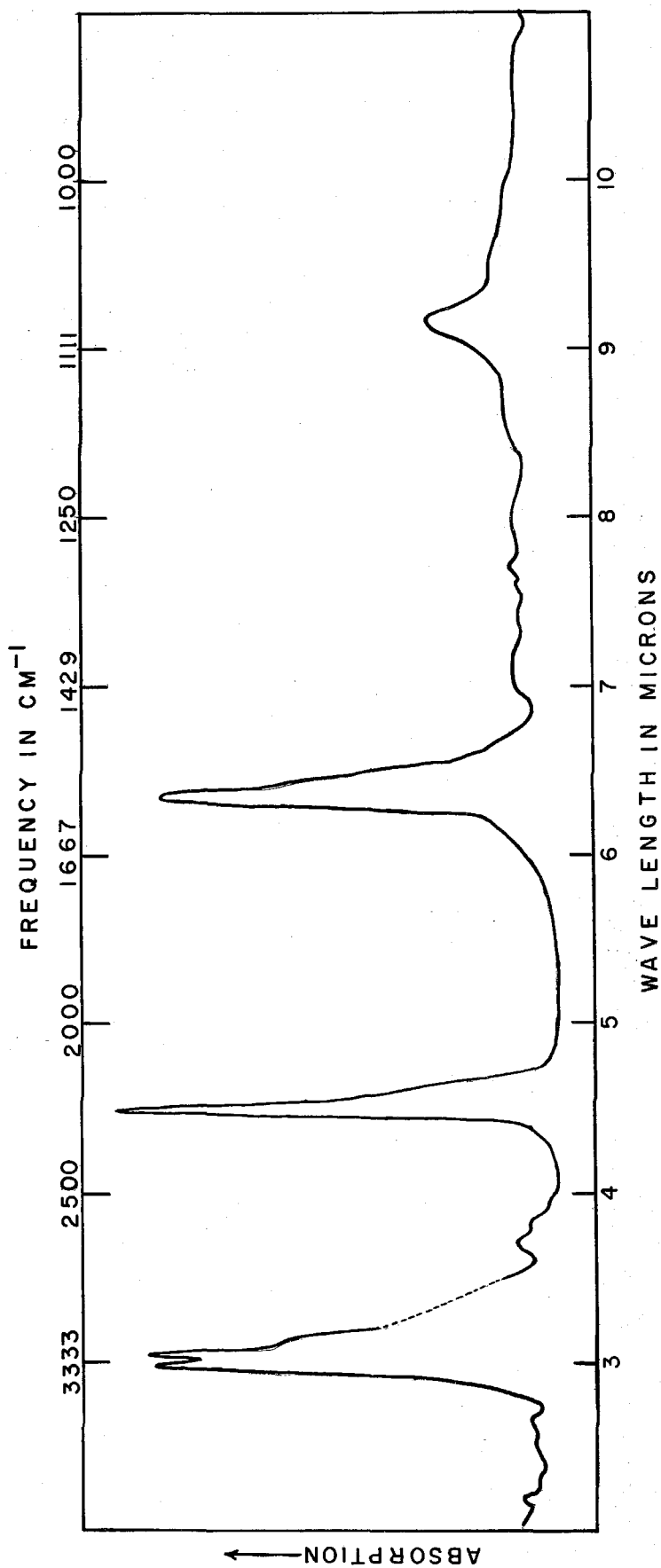


Figure 5. Spectrum of a saturated solution of cyanamide in methylene chloride; path length is 1 mm.

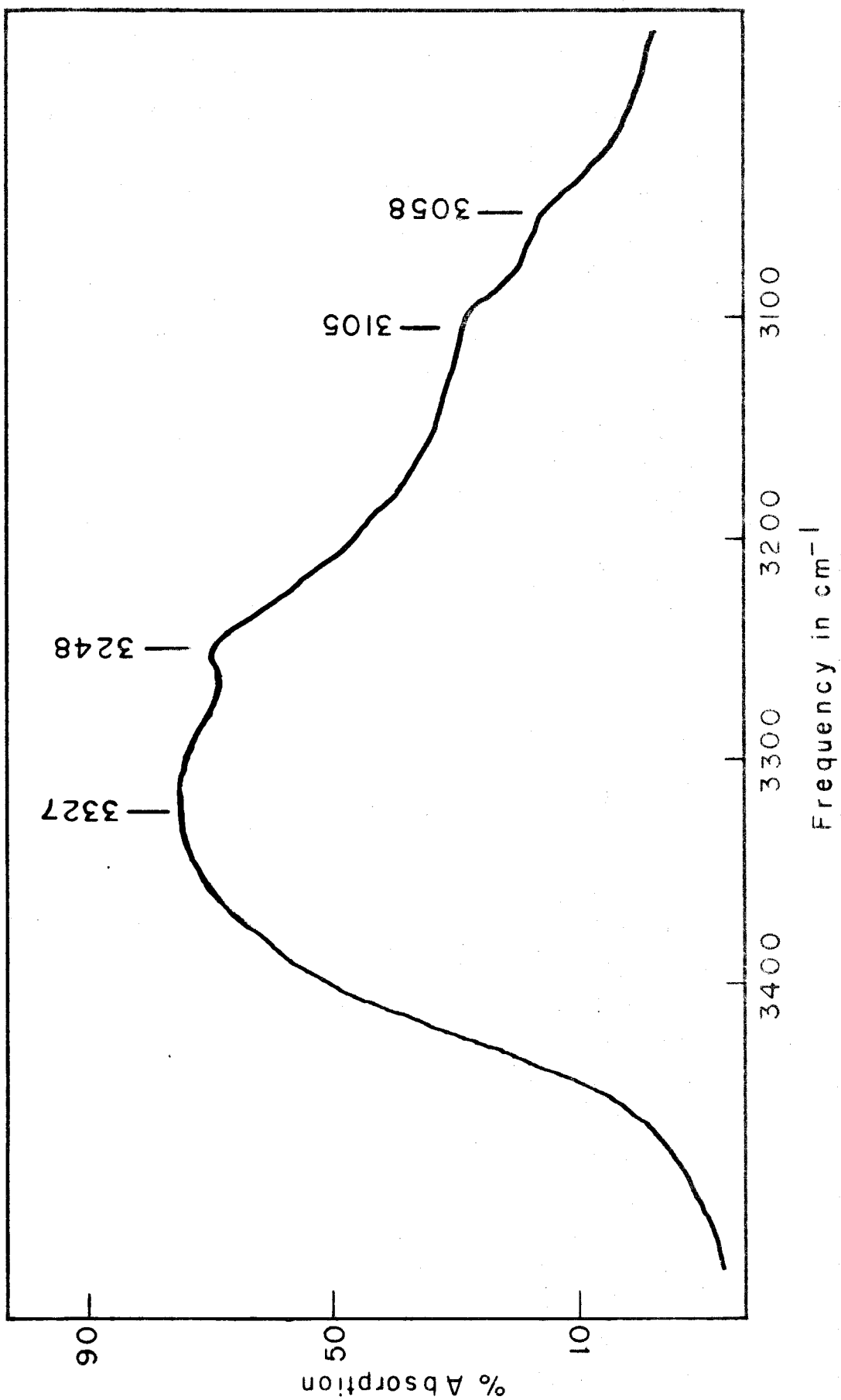
sorption bands. The bands at 2257 and 1590  $\text{cm}^{-1}$  are assigned to the  $\text{C}\equiv\text{N}$  stretching vibration and the symmetric  $\text{NH}_2$  bending vibration, respectively. The assignment of the band at 1080  $\text{cm}^{-1}$  is not clear from this spectrum alone, for it could be assigned to  $\nu_6$ , the antisymmetric in-plane bend, to  $\nu_8$ , the out-of-plane bend, or to  $\nu_4$ , the N-C stretching vibration. The assignments of  $\nu_4$  to a higher frequency, and of  $\nu_8$  to a lower frequency are discussed below. Hence, the absorption at 1080  $\text{cm}^{-1}$  is assigned to  $\nu_6$ . The weak band at 2732  $\text{cm}^{-1}$  fits the assignment  $\nu_2 + \nu_7$  ( $513 + 2257 = 2770 \text{ cm}^{-1}$ ). The Raman frequency of the melt is used for  $\nu_7$ , since no infrared datum is available.

#### B. Crystalline cyanamide.

The interpretation of the 3 micron spectrum of cyanamide obtained under high dispersion is not clear, because this substance is strongly hydrogen-bonded in the crystalline state. This condition may cause such complications as the marked lowering of the hydrogen stretching frequencies, intensification of combination bands, appearance of new bands, etc. Hence few positive conclusions can be drawn from this spectrum of crystalline cyanamide. The observed absorption maxima are listed in Table 2, and the spectrum is presented in Figure 6. The two maxima at 3327 and 3248  $\text{cm}^{-1}$  are separated by nearly the same amount as are  $\nu_5$  and  $\nu_1$  in the spectrum



Figure 6. 3 micron spectrum of crystalline cyanamide under high dispersion.

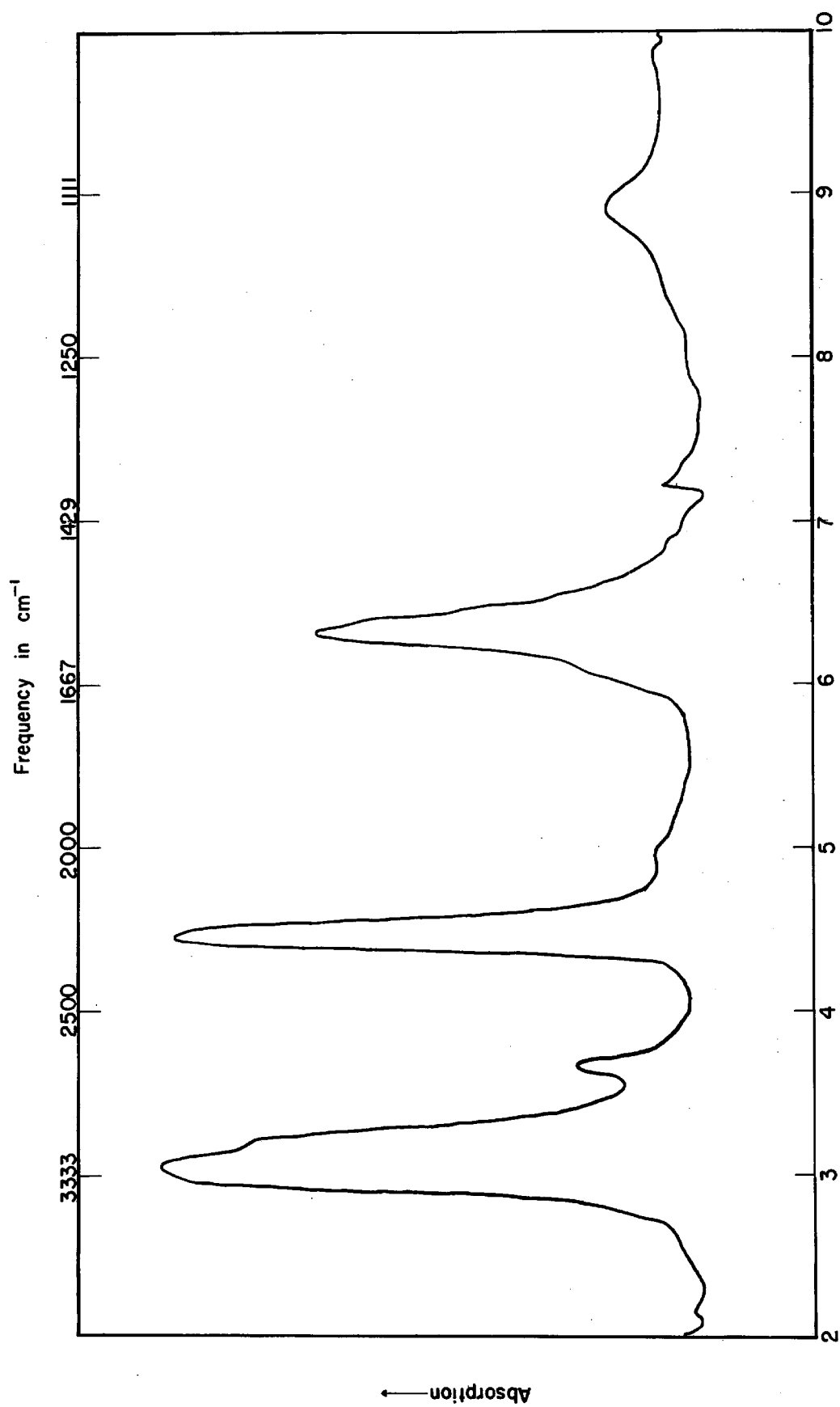


of the solution, thus these maxima are assigned to these vibrations in the crystalline substance (it must be remembered, however, that this may be a poor description of the absorbing vibrations, for the crystal symmetry may give rise to new normal modes of vibration). The band at  $3105 \text{ cm}^{-1}$  fits the assignment  $2 \nu_3$  ( $2 \times 1587 = 3174 \text{ cm}^{-1}$ ). The absorption at  $3058 \text{ cm}^{-1}$  can be fitted to  $2 \nu_6 + \nu_8$  ( $2 \times 1048 + 1003 = 3099 \text{ cm}^{-1}$ ).

The prismatic spectrum shows five additional absorption bands. Figure 7 presents this spectrum. The bands at  $2247$ ,  $1587$ , and  $1122 \text{ cm}^{-1}$  are assigned to  $\nu_2$ ,  $\nu_3$ , and  $\nu_4$ , respectively. The two weak bands at  $2730$  and  $1390 \text{ cm}^{-1}$  fit the assignments  $\nu_2 + \nu_7$  ( $2762 \text{ cm}^{-1}$ ), and  $\nu_8 + \nu_9$  ( $1433 \text{ cm}^{-1}$ ), respectively. The frequencies for  $\nu_7$  and  $\nu_9$  are taken from the Raman shifts for the melt.

### C. Gaseous cyanamide.

The 2-15 micron spectrum of the gas has not been obtained showing as much detail as was found for the condensed states. The frequency assigned to the band center of  $\nu_5$  depends on the particular analysis of the complex structure of the spectrum in this region, however, the value is  $3469.1 \pm 0.4 \text{ cm}^{-1}$ , regardless which of items 18, 19, or 20 is assigned to  $R_{Q_0}$  (see the discussion of the rotational structure of  $\nu_5$ ). A detailed discussion of



Wave Length in Microns  
Figure 7. Spectrum of crystalline cyanamide.

the three micron band is presented below, and the three micron-band is shown in Figure 12. The precise location of the band center of the parallel band,  $\nu_1$ , has not been determined. The gross appearance of the structure suggests that the Q branch of a parallel band falls near  $3420 \text{ cm}^{-1}$ . This frequency has been assigned to  $\nu_1$ . No lines are observed below  $3369 \text{ cm}^{-1}$  which can be assigned to the Q branch of a parallel band, hence if  $\nu_2 + \nu_4$  falls in this region, as it does in the spectrum of the solution, it occurs towards higher frequencies.  $\nu_2$  was observed in a prismatic spectrum of the gas as  $2275 \text{ cm}^{-1}$ . The absence of hydrogen bonding in the gas is presumably responsible for the higher value of  $\nu_2$  in this state than in the condensed states.  $\nu_2$  appears as a doublet with a separation of  $30 \text{ cm}^{-1}$  between the two maxima. Under low resolution parallel bands of a symmetric top molecule like cyanamide ( $I_A/I_B = 0.03$ ) should appear as doublets, because the Q branch of these bands has only 0.04 the intensity of the P or R branches (11). Using the method of Gerhard and Dennison (12) the calculated separation between the maxima of the P and R branches is  $28 \text{ cm}^{-1}$ , which agrees well with the observed  $30 \text{ cm}^{-1}$ . See Appendix 1 for details of the calculation.

The absorption band for the symmetric  $\text{NH}_2$  bending vibration has not been measured, although it has been observed. The absorption of the six micron water band interferes in



this region, and the experimental difficulties discussed above (see page 7 ), have prevented the satisfactory measurement of this portion of the spectrum.

The other bands of the gas are weak enough so that they were not observed under conditions suitable for measuring  $\nu_2$ .

#### D. The Raman spectrum.

The Raman data of Kahovec and Kohlrausch (9) on liquid and solid, listed in Table 2, have been employed to aid in the assignment of the absorption bands of the infrared spectra studied here. The two lowest frequency vibrations for the molecule are expected to be the two bending vibrations of the heavy atoms,  $\nu_7$  and  $\nu_9$ . The somewhat arbitrary assumption is made that the band at  $429\text{ cm}^{-1}$  is  $\nu_9$ . A priori it is not clear which of the two skeletal bending modes should occur at the lower frequency, however it seems that there might be more repulsion from the van der Waal's interaction of the hydrogen atoms and the terminal nitrogen atom in the  $B_1$  vibration, than in the  $B_2$  vibration, leading to the suggested assignment. The band at  $912\text{ cm}^{-1}$  is assigned to  $\nu_7 + \nu_9$ . The two lines at 1003 and 1048  $\text{cm}^{-1}$  have been assigned to the out-of-plane and the  $B_1$  in-plane hydrogen bending vibrations, respectively. The order of these two assignments is in agreement with other molecules of similar structure (see Table 4). The choice of

$1003\text{ cm}^{-1}$  rather than  $912\text{ cm}^{-1}$  for  $\nu_8$  is supported by the assignment of the combination bands found at 1390 and  $3058\text{ cm}^{-1}$  in the infrared spectrum of the crystal.

The interpretation and comparison of the infrared and Raman spectra of crystalline cyanamide presents some problems not encountered in the study of the liquid or gas spectra. Additional absorption bands (beyond the usual bands of an isolated molecule) will arise from the vibrations of the molecules in the unit cell of the crystal, and from combinations between molecular and lattice vibrations. Further complications may obtain if the crystal belongs to a space group of sufficiently high symmetry, for the relative intensities of the absorption bands may then be quite different in the infrared and the Raman spectra. Since the structure of cyanamide is not known, the discussion of these spectra will be of a rather speculative nature.

The three shifts in the 9 micron region may be an example of these complications. If the two lines at 1119 and  $1174\text{ cm}^{-1}$  are not spurious, the three shifts in this region might be assigned to combinations between  $\nu_4$  and a lattice mode,  $\nu_c$ . The sequence  $\nu_4 + n\nu_c$ ,  $n = 0, 1, 2$ , with  $\nu_c$  approximately equal to  $27\text{ cm}^{-1}$ , fits the observed shifts. Though the differences in intensities between the three absorptions seem rather high, this will tentatively be taken as the assignment. A problem also exists for the assignment of  $\nu_2$ . The shift at the more

reasonable frequency,  $2259\text{ cm}^{-1}$ , is less intense than the less reasonable shift at  $2210\text{ cm}^{-1}$ . The shift at  $2210\text{ cm}^{-1}$  will be assigned to  $2\nu_4$  ( $2238\text{ cm}^{-1}$ ) and the shift at  $2259\text{ cm}^{-1}$  will be assigned to  $\nu_2$ .

Two other discrepancies are found: a large frequency difference in  $\nu_3$  between the infrared absorption maximum at  $1587\text{ cm}^{-1}$ , and the Raman shift at  $1556\text{ cm}^{-1}$ ; and a smaller difference,  $16\text{ cm}^{-1}$ , for  $\nu_1$ . The shifts found at  $3326$ , and  $3108\text{ cm}^{-1}$  are in excellent agreement with the absorption maxima found at  $3327$  and  $3105\text{ cm}^{-1}$  in the infrared.

#### E. Discussion of the vibrational spectrum.

##### 1. The $\text{NH}_2$ vibrations.

The planar structure of cyanamide suggests that the vibrational frequency assignments made above should be compared not only with those of other  $\text{NH}_2\text{X}$  type molecules, but also with the frequency assignments for planar  $\text{H}_2\text{A-B-C}$  molecules in which a two-fold axis passes through the heavy atoms. The  $\text{NH}_2$  frequencies for several molecules are entered in Table 3. An examination of Table 3 shows a fair degree of constancy in the frequencies of similar vibrations of the  $\text{NH}_2$  group for the molecules listed, with the exception of the vibration described as the "rock." The bonding of the  $\pi$  orbitals perpendicular to the plane of the cyanamide molecule may give rise to an additional

Table 3. Frequencies, in  $\text{cm}^{-1}$ , of  $\text{NH}_2$  vibrations  
in  $\text{NH}_2\text{X}$  molecules.

Molecule	$\text{NH}_2\text{CH}_3$	$\text{NH}_2\text{Cl}$	$\text{NH}_2\text{OH}$	$\text{NH}_2\text{CHO}$	$\text{NH}_2\text{CN}$
asym. $\text{NH}_2$ st.	3470	3380	3350	3564	3469
sym. $\text{NH}_2$ st.	3360	--	3297	3440	(3420)
sym. $\text{NH}_2$ bend	1625	1553	1605	1585	1580 <sup>a</sup>
$\text{NH}_2$ rock <sup>*</sup>	783 <sup>**</sup>	--	765	1160	1080 <sup>b</sup>
$\text{NH}_2$ wag <sup>*</sup>	1127 <sup>**</sup>	1032	1120	820	1003 <sup>b</sup>

References:  $\text{NH}_3\text{CH}_3$ (13),  $\text{NH}_2\text{Cl}$ (14),  $\text{NH}_2\text{OH}$ (15),  $\text{NH}_2\text{CHO}$ (16).

\* In  $\text{C}_s$  molecules the rock belongs to species  $A''$ , and the wag to species  $A'$ . For species  $\text{C}_{2v}$  the rock is of species  $B_1$ , and the wag of species  $B_2$ . If formamide is planar the wag belongs to  $A''$  and the rock to  $A'$ . However, see discussion of formamide.

\*\* These assignments are suggested in reference (15).

<sup>a</sup> Approximate frequency, see p. 26.

<sup>b</sup> These frequencies are taken from the Raman spectrum of the melt (9) since they have not been observed in the gaseous spectrum.

resistance to the out-of-plane deformation which causes the  $\text{NH}_2$  rock to absorb at a frequency approximately  $200 \text{ cm}^{-1}$  higher in this planar molecule than in the pyramidal molecules.

The order of assignment of  $\nu_6(b_1)$  and  $\nu_8(b_2)$  made for cyanamide is the same for the similar vibrations of the molecules listed in Table 4. Some support for this assignment is found in the combination band at  $1390 \text{ cm}^{-1}$ , for if  $\nu_6$  were the lower frequency ( $1003 \text{ cm}^{-1}$ ) then the species of the line at  $1390 \text{ cm}^{-1}$  would be  $A_2$ , which is forbidden for dipole absorption. (If the Raman shift at  $439 \text{ cm}^{-1}$  is not  $\nu_9$ , but rather  $\nu_7$ ; then this argument is not valid.)

Table 4. Hydrogen bending frequencies in  $\text{cm}^{-1}$ ,  
of  $\text{H}_2\text{ABC}$  molecules.

Molecule	In-plane	Out-of-plane
$\text{H}_2\text{CCO}$ , ketene (10)	942 ( $b_1$ )	916 ( $b_2$ )
$\text{H}_2\text{CN}_2$ , diazomethane (17)	1147 ( $b_1$ )	920 ( $b_2$ )
$\text{H}_2\text{CCH}_2$ , ethylene (18)	$1050^* (b_{1g})$	$949^{**} (b_1)$
$\text{H}_2\text{NCN}$ , cyanamide	$1080^a (b_1)$	$1003^a (b_2)$

\*  $\nu_6$ , Raman shift

\*\*  $\nu_7$

<sup>a</sup> Approximate frequency, see p. 26.

## 2. The NCN stretching vibrations.

$\nu_2$  and  $\nu_4$  have been referred to as the  $C\equiv N$  and as the C-N stretching vibrations, respectively. This has been done for brevity, and because in the first approximation such vibrations might be expected. Compilations of group frequencies (for example, see Randall, et al. (20)) list  $C\equiv N$  and C-N stretching vibrations frequencies in neighborhoods which essentially includes the ranges of values for the various assignments of  $\nu_2$  and  $\nu_4$  given in Table 2. However, such a description is misleading, for the arrangement of the three heavy atoms in cyanamide is like that of a "not quite symmetric" linear triatomic molecule for which the stretching vibrations would not be localized in one bond. Indeed, a normal coordinate analysis will show that the names "antisymmetric NCN stretching vibration" and "symmetric stretching vibration" for  $\nu_2$  and  $\nu_4$ , respectively, are more descriptive. Thus in order to discuss these vibrations, it will be necessary to determine the normal modes of the three lowest frequency  $A_1$  vibrations.

### a. Normal coordinate analysis.

In this section a normal coordinate analysis is made for the three lowest frequency vibrations of the species  $A_1$ . The potential function that will be considered is

$$2V = F_5(\Delta r_{34})^2 + F_3(\Delta r_{45})^2 + 2f\Delta r_{45}\Delta r_{34} + F_4(\Delta \alpha)^2. \quad (1)$$

The methods used are those given by Wilson (19, 21).

The secular equation may be written in the form

$$|G'F' - \lambda'E| = 0, \quad (2)$$

in which  $G'$ ,  $F'$ , and  $\lambda'$  are matrices whose elements belong to the complete secular equation (the unprimed quantities will be used for the reduced secular equation). If the internal coordinates used in obtaining (1) are symmetry coordinates, then  $G'$  will factor into three factors, one for each of the three vibrational species of cyanamide. However, for brevity  $G'$  will be used below to refer to the  $A_1$  factor of the complete equation. This will not cause confusion because the other species,  $B_1$  and  $B_2$ , will not be discussed.

The highest frequency normal mode is factored out by letting the N-H stretching force constant approach an infinite value. In this treatment this is accomplished by changing the elements of the  $G'$  matrix to those of the  $G$  matrix, the reduced matrix, according to equation (3).

$$G_{nm} = G'_{nm} - \frac{G'_{2n}G'_{2m}}{G'_{22}} \quad (3)$$

The resulting  $G_{nm}$  are used with the  $F$  matrix in which only the force constants for the remaining deformations are included.

The frequencies used in this normal coordinate analysis

are meant to be gaseous frequencies.  $\nu_2$  is the measured frequency of the gaseous spectrum.  $\nu_3$  has not been measured in the gaseous spectrum (see p. 19), thus it is necessary to use an approximate value. Since hydrogen bending frequencies are generally less for free molecules than for hydrogen-bonded molecules,  $1580 \text{ cm}^{-1}$  has been used. This value is approximately  $10 \text{ cm}^{-1}$  less than the value for the solution or the crystal.  $\nu_4$  has not been observed in the gaseous or solution spectra, so that it has been necessary to take another approximate value. Since it is not clear how the frequency of  $\nu_4$  will change with state, the rounded value  $1120 \text{ cm}^{-1}$  of the observed non-gaseous spectra has been used.

The frequencies, formulas, symbols, and values for the pertinent molecular and spectral parameters used in this analysis are listed below

	$\lambda_i = (2\pi c \nu_i)^2$
$\nu_2 = 2275 \text{ cm}^{-1}$	$\lambda_2 = 18.45 \times 10^{28} \text{ sec}^{-2}$
$\nu_3 = 1580 \text{ cm}^{-1}$	$\lambda_3 = 8.86 \times 10^{28} \text{ sec}^{-2}$
$\nu_4 = 1120 \text{ cm}^{-1}$	$\lambda_4 = 4.46 \times 10^{28} \text{ sec}^{-2}$

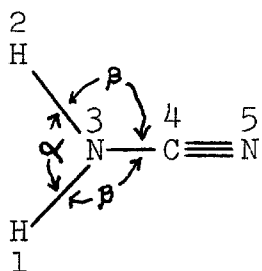


The  $G'$  matrix for the totally symmetric vibrations is

	$s_2$	$s_5$	$s_3$	$s_4$
$s_2$	$\frac{1}{m_1} + \frac{1 + \cos \alpha}{m_3}$	$\frac{\sqrt{2} \cos \beta}{m_3}$	0	$-\frac{\sqrt{2} \epsilon \sin \alpha}{m_3}$
$s_5$		$\frac{1}{m_3} + \frac{1}{m_4}$	$-\frac{1}{m_4}$	$-\frac{2\epsilon \tan \frac{\alpha}{2} \cos \beta}{m_3}$
$s_3$			$\frac{1}{m_4} + \frac{1}{m_5}$	0
$s_4$				$\frac{2\epsilon^2}{m_1} + \frac{2\epsilon^2(1 - \cos \alpha)}{m_3}$

Note that  $G'$  is symmetric, i.e.  $G'_{ij} = G'_{ji}$ .

Diagram of internal coordinates.



The symmetry coordinates are

$$\left. \begin{aligned} s_2 &= \sqrt{\frac{1}{2}} (\Delta r_1 + \Delta r_2) \\ s_3 &= \Delta r_{45} \\ s_4 &= \Delta \alpha \\ s_5 &= \Delta r_{34} \\ \alpha &= \beta = 120^\circ \end{aligned} \right\} \quad (4)$$

$$\epsilon = \frac{1}{r_{NH}} = (1.015 \times 10^{-8} \text{ cm})^{-1} = 0.985 \times 10^8 \text{ cm}^{-1};$$

The  $G_{nm}$  given by equation (3) are listed below.

$$G_{55} = \frac{1}{m_3} + \frac{1}{m_4} - \left( \frac{1}{m_1} + \frac{1+\cos\alpha}{m_3} \right)^{-1} \frac{(2\cos^2\beta)}{m_3^2}$$

$$G_{33} = \frac{1}{m_4} + \frac{1}{m_5}$$

$$G_{44} = \frac{2\xi^2}{m_1} + \frac{2\xi^2(1-\cos\alpha)}{m_3} - \left( \frac{1}{m_1} + \frac{1+\cos\alpha}{m_3} \right)^{-1} \frac{2\xi^2\sin^2\alpha}{m_3^2}$$

$$G_{53} = -\frac{1}{m_4}$$

$$G_{45} = -\frac{2\xi\tan\frac{\alpha}{2}\cos\beta}{m_3} + \left( \frac{1}{m_1} + \frac{1+\cos\alpha}{m_3} \right)^{-1} \frac{(2\xi\cos\beta\sin\alpha)}{m_3^2}$$

$$G_{34} = 0$$

The numerical values for these  $G_{nm}$  are listed below.

$$G_{55} = 9.17 \times 10^{22} \text{ gm}^{-1}$$

$$G_{33} = 9.32 \times 10^{22} \text{ gm}^{-1}$$

$$G_{44} = 12.90 \times 10^{39} \text{ gm}^{-1} \text{ cm}^{-2}$$

$$G_{35} = -5.02 \times 10^{22} \text{ gm}^{-1}$$

$$G_{45} = 7.09 \times 10^{30} \text{ gm}^{-1} \text{ cm}^{-1}$$

$$G_{34} = 0$$

Note that  $G_{nm} = G_{mn}$

The secular equation now takes the form

$$|GF - \lambda E| = \begin{vmatrix} G_{55} & G_{35} & G_{45} \\ G_{35} & G_{33} & 0 \\ G_{45} & 0 & G_{44} \end{vmatrix} \begin{vmatrix} F_5 & f & 0 \\ f & F_3 & 0 \\ 0 & 0 & F_4 \end{vmatrix} - \begin{vmatrix} \lambda & 0 & 0 \\ 0 & \lambda & 0 \\ 0 & 0 & \lambda \end{vmatrix} = 0. \quad (5)$$

In its expanded form this is written as

$$\begin{vmatrix} G_{55}F_5 + G_{35}f - \lambda & G_{55}f + G_{35}F_3 & G_{45}F_4 \\ G_{35}F_5 + G_{33}f & G_{35}f + G_{33}F_3 - \lambda & 0 \\ G_{45}F_5 & G_{45}f & G_{44}F_4 - \lambda \end{vmatrix} = 0. \quad (6)$$

Equation (6) is a cubic equation in  $\lambda$ . The coefficients of the powers of  $\lambda$  are functions of the  $G_{nm}$  and of the force constants. The dependence of the force constants on the  $G_{nm}$  and on the observed frequencies may now be obtained. For convenience (6) is rewritten as shown in equation (7)

$$\begin{vmatrix} A_1 - \lambda & A_2 & A_3 \\ B_1 & B_2 - \lambda & B_3 \\ C_1 & C_2 & C_3 - \lambda \end{vmatrix} = 0, \quad (7)$$

where  $A_1 = G_{55}F_5 + G_{35}f$ ,  $A_2 = G_{55}f + G_{35}F_3$ , etc.

The general cubic equation whose roots are  $\lambda_1$ ,  $\lambda_2$ , and  $\lambda_3$  may be written  $(\lambda_1 - \lambda)(\lambda_2 - \lambda)(\lambda_3 - \lambda) = 0$ . (8)

Expansion of equations (7) and (8), and a comparison of the coefficients of equal powers of  $\lambda$  yields the following relationships

$$\lambda_1 \lambda_2 \lambda_3 = A_1 B_2 C_3 + A_3 B_1 C_2 + A_2 B_3 C_1 - A_3 B_2 C_1 - A_2 B_1 C_3 - A_1 B_3 C_2 \quad (9)$$

$$\begin{aligned} \lambda_1 \lambda_2 + \lambda_1 \lambda_3 + \lambda_2 \lambda_3 = & A_1 B_2 + A_1 C_3 + B_2 C_3 - A_3 C_1 - A_2 B_1 \\ & - B_3 C_2 \end{aligned} \quad (10)$$

$$\lambda_1 + \lambda_2 + \lambda_3 = A_1 + B_2 + C_3 . \quad (11)$$

Substitution of the values for the A's, B's, and C's from equation (6) into equations (9), (10), and (11), and rearrangement of the resulting equations yields the following relationships among the force constants, the  $G_{nm}$ , and the observed frequencies:

$$G_{55}F_5 + G_{33}F_3 + 2G_{35}f = \lambda_1 + \lambda_2 + \lambda_3 - G_{44}F_4 \quad (12)$$

$$\begin{aligned} (G_{45}^2 - G_{44}G_{55})F_5 - G_{44}G_{33}F_3 + (G_{35}^2 - G_{55}G_{33})(F_5F_3 - f^2)/F_4 - 2G_{44}G_{35}f \\ = - (\lambda_1 \lambda_2 + \lambda_1 \lambda_3 + \lambda_2 \lambda_3)/F_4 \end{aligned} \quad (13)$$

$$[G_{44}(G_{55}G_{33} - G_{35}^2) - G_{33}G_{45}^2](F_3F_5 - f^2) = \lambda_1 \lambda_2 \lambda_3 / F_4 . \quad (14)$$

It should be noted that there are four force constants to be determined, and there are only three observed data. Consequently various values will be assumed for  $F_4$ , and the other three force constants will be expressed in terms of  $F_4$ .

Equations (12), (13), and (14) will now be solved for the three bond force constants. For convenience the coefficients and constants will be rewritten in the manner indicated below by equations (15).

$$\begin{aligned}
 A &= G_{55} \\
 B &= G_{33} \\
 C &= 2G_{35} \\
 D &= G_{45}^2 - G_{44}G_{55} \\
 E &= -G_{44}G_{33} \\
 F &= (G_{35}^2 - G_{55}G_{33})/F_4 \\
 G &= -2G_{44}G_{35} \\
 L &= \lambda_1 + \lambda_2 + \lambda_3 - G_{44}F_4 \\
 M &= -(\lambda_1\lambda_2 + \lambda_2\lambda_3 + \lambda_1\lambda_3)/F_4 \\
 N &= \frac{1}{F_4} \frac{\lambda_1\lambda_2\lambda_3}{G_{44}(G_{55}G_{33} - G_{35}^2) - G_{33}G_{45}^2} \\
 F_5 &= x \\
 F_3 &= y \\
 f &= z
 \end{aligned}
 \tag{15}$$

Equations (12), (13), and (14) may now be written as

$$Ax + By + Cz = L , \tag{16}$$

$$Dx + Ey + Fxy - Fz^2 + Gz = M , \tag{17}$$

$$xy - z^2 = N . \quad (18)$$

By substituting (18) into (17), and rewriting (16), the following two equations are obtained,

$$Ax + By = L - Cz \quad (19)$$

$$Dx + Ey = M - FN - Gz \quad (20)$$

These are readily solved for x and y as functions of z,

$$x = d_1 \quad (21)$$

$$\text{and} \quad y = d_2 + az . \quad (22)$$

$$\left. \begin{aligned} d_1 &= [EL - B(M - FN)] / (AE - BD) \\ d_2 &= [A(M - FN) - LD] / (AE - BD) \\ a &= (CD - AG) / (AE - BD) \end{aligned} \right\} \quad (23)$$

Then from equations (18), (19), and (20) is obtained

$$d_1 d_2 + ad_1 z - z^2 = N , \quad (24)$$

which yields for z

$$z = (ad_1)/2 \pm \frac{1}{2} \sqrt{a^2 d_1^2 - 4(N - d_1 d_2)} . \quad (25)$$

It is convenient to define the dimensionless quantity  $k$  according to the equation

$$k = F_4/10^{-11} \text{ ergs.} \quad (26)$$

$d_1$  and  $d_2$  may be evaluated from the relations

$$d_1 = -331.0k + 815.0 - \frac{567.6}{k} + \frac{119.6}{k^2} \quad (27)$$

$$d_2 = 311.9k - 768.0 + \frac{558.4}{k} - \frac{117.8}{k^2} \quad (28)$$

which follow from (15), (23), and (26).

With the two quantities (29), the three bond force

$$N = \frac{99.81}{k} \quad \text{and} \quad a = 1.078, \quad (29)$$

constants may be evaluated from (21), (22), and (25) as a function of  $k$ . The units will be  $10^5$  dynes/cm.

An examination of equations (27) and (28) shows that  $k$  has only two ranges of values in which solutions of physical interest can be obtained. Real values for  $f$  and  $F_3$  are found near  $F_4 = 0.65 \times 10^{-11}$  ergs ( $k = 0.65$ ), and near  $F_4 = 1.38 \times 10^{-11}$  ergs. Table 5 lists values for the force constants obtained by assuming successive values for  $k$  in the two regions of interest. For each value of  $k$  there is one value for  $F_5$ , and there are two values for  $F_3$  and two values for  $f$  corresponding to the two solutions, equation (25), of equation (24). All the values belonging to the

Table 5. Force constants to go with equation (1).

$F_4$ $\times 10^{11}$ ergs	$F_5$	$F_3$ $\times 10^{-5}$ dynes/cm	$f$
0.63	6.9	complex complex	complex complex
0.64	8.3	20.2 22.4	3.47 5.47
0.65	9.7	15.9 25.4	0.83 9.63
0.66	11.1	13.6 26.2	0.12 11.84
1.37	10.9	7.3 12.7	3.18 8.56
1.38	9.7	7.9 13.0	2.71 7.75
1.39	8.5	9.1 12.9	2.96 6.20
1.40	7.2	complex complex	complex complex

\* The upper value of these pairs of values corresponds to the lowest valued solution of equation (24), and vice versa.



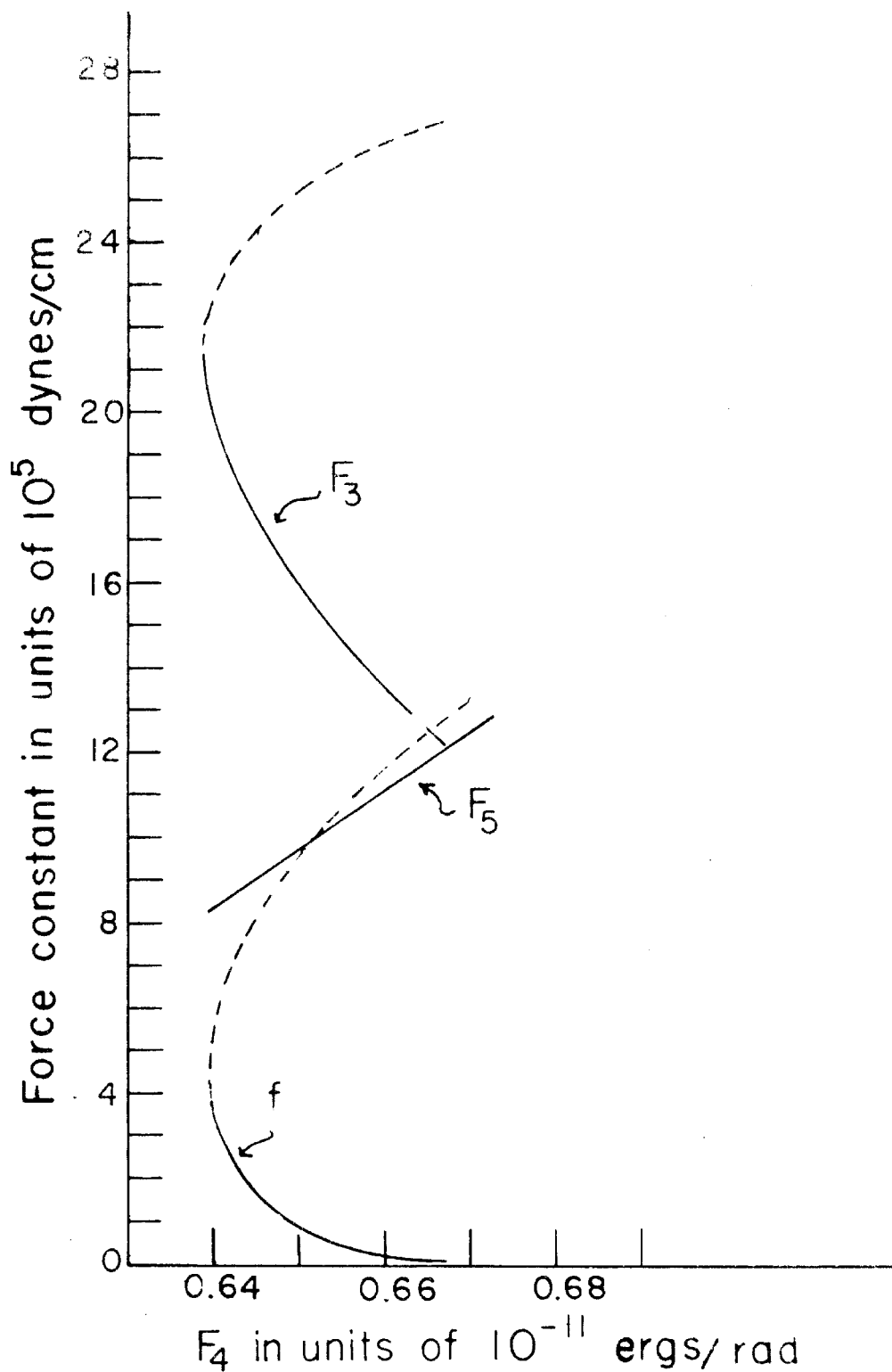


Figure 8. Graph of NCN stretching and interaction force constants vs. HNH bending force constant.

higher range of  $F_4$  have been discarded for several reasons. If the values with the more nearly reasonable values (smaller) for the interaction constant are chosen, then  $F_3$  is found to be smaller than  $F_5$ , implying that the inner CN bond is stronger than the terminal CN bond. This is very unlikely. Furthermore, this value for  $F_4$  (about  $1.38 \times 10^{-11}$  ergs) is considerably higher than listed values for this constant (see reference (21) p.176, where 0.4 to  $0.6 \times 10^{-11}$  ergs is given).

The other allowed range for  $F_4$  is much more satisfactory, for its value is approximately  $0.65 \times 10^{-11}$  ergs. The values of  $F_3$  and  $f$  are plausible if the smaller of the solutions of equation (24) is chosen. The values belonging to the other solution are not discussed because they seem too large. The discarded values for  $f$  are approximately two to eight times larger than values ordinarily expected for stretch-stretch interaction constants (see, for example, Coulson et al. (27)). Similarly, the discarded  $F_3$  values, ranging from about  $21 \times 10^5$  to about  $27 \times 10^5$  dynes/cm, are considerably larger than the expected maximum value for the  $C \equiv N$  stretching force constant of about  $18 \times 10^5$  dynes/cm.

The solid lines in Figure 8 give the values of  $F_5$ ,  $F_3$ , and  $f$  that seem most plausible. These constants vary, approximately, from 8.3 to 12.1, 21.0 to 12.1, and 4.0 to 0.0 (in units of  $10^5$  dynes/cm) for  $F_5$ ,  $F_3$ , and  $f$ , respectively. The dashed lines give the values which have been discarded.

It will be recalled that no interaction constant between  $S_4$  and  $S_5$  (HNN angle bend, and adjacent N-C bond stretch) has been included in the potential function given by equation (1). This may well be a rather serious omission because this constant may not be negligible. Coulson (22) has pointed out that for this particular case, the interaction between the symmetric bend of a trigonally hybridized atom and the stretch of the adjacent bond, there should be an appreciable interaction. However, the limited data available has not allowed this effect to be studied in the present investigation.

The present data are consistent with CN bonds having intermediate bond character. Neglecting the possible effects of the interaction between the bend and the stretch on the value of  $F_3$  and  $F_5$ , it will be noted that values for  $F_5$  less than  $8.2 \times 10^5$  dynes/cm are not possible, for smaller values correspond to complex values for  $F_3$ . This implies, roughly, a minimum bond order of 1.5 for the inner CN bond. Figure 9 which is a rough plot of force constant versus bond order for the CN bond is presented as an aid for estimating the bond order as a function of the stretching force constant. However, it must be noted that the force constant for a particular deformation in any molecule is, in general, unique, and that the calculated value for that constant may depend strongly on the assumed potential function; thus the curve shown in Figure 9 for the CN bond is only of a

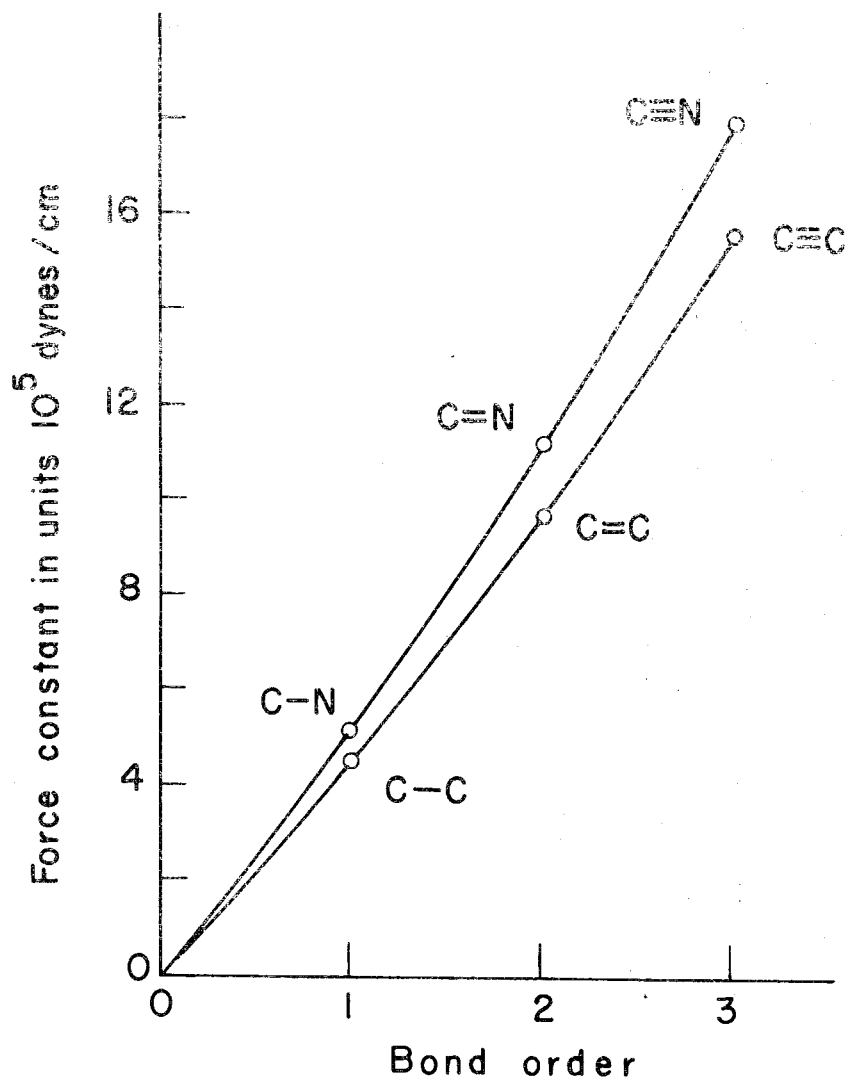


Figure 9. Graph of CN and CC stretching force constants vs. bond order.

semi-quantitative nature. The figure was obtained by assuming that the ratio of the CN to CC force constants for similar bonds is constant. The  $C\equiv N$  force constant was taken as  $18.0 \times 10^5$  dynes/cm, and the CC force constants were taken from Herzberg's compilation (see Ref. 11, p. 193). The CN force constant values are in reasonable agreement with the range of values given by Wilson (See Ref. 21, p. 175). The same plot for the CC bond has been drawn for comparison.

The normal modes for  $\nu_2$ ,  $\nu_3$ , and  $\nu_4$  will now be obtained for three sets of force constants taken from Figure 8. The contribution of  $S_2$ , the symmetric N-H stretch symmetry coordinate, to these normal modes is not included. However, this should not be a serious omission, because the high value of the N-H stretching force constant should allow only a small amount of mixing of  $S_2$  with the other three totally symmetric coordinates in the three lowest frequency normal modes.

The ratio of the amplitudes of the symmetry coordinates in the  $i$ th normal mode is given by equation (29)

$$s_5^i : s_3^i : s_4^i = M_5^i : M_3^i : M_4^i , \quad (29)$$

where the M's are the cofactors of the elements in the first row of equation (6) with the appropriate  $\lambda_1$  substituted for  $\lambda$ . The results are presented in Table 6.

Table 6.  $s_5^1:s_3^1:s_4^1$  for three sets of force constant values.

	Case 1	Case 2	Case 3
$F_4$	0.640	0.650	$0.661 \times 10^{-11}$ ergs/rad <sup>2</sup>
$F_5$	8.5	9.7	$11.2 \times 10^5$ dynes/cm
$F_3$	20.2	15.9	$13.4 \times 10^5$ dynes/cm
$f$	3.47	0.83	$0.0 \times 10^5$ dynes/cm
	$s_5^1:s_3^1:s_4^1*$	$s_5^1:s_3^1:s_4^1*$	$s_5^1:s_3^1:s_4^1*$
$\nu_2$	1:-0.759:0.331	1:-1.013:0.620	1:-0.945:0.804
$\nu_3$	1:0.125:10.4	1:0.741:15.3	1:1.54:23.2
$\nu_4$	1:0.0815:-1.64	1:0.403:-1.78	1:0.700:-1.95

\*The unit for the last member of each ratio is rad/Å

In order to represent a normal mode to scale, it is necessary to satisfy the following equations:

$$6 \delta_4 + 7 \delta_5 + \delta_H + 8 \delta_3 = 0 \quad (30)$$

$$(1+a) \delta_4 - a \delta_5 - \delta_3 = 0 \quad (31)$$

$$\delta_4 + b \delta_H - \delta_3 = 0 \quad (32)$$

$\delta_3$ ,  $\delta_4$ , and  $\delta_5$  are the displacements of the atoms (numbered as in the diagram of the symmetry coordinates, p. 28) parallel to the two-fold axis of the molecule; and they are measured from the equilibrium position of the respective atoms.  $\delta_H = \delta_1 = \delta_2$  gives the displacement of the hydrogens parallel to the two-fold axis for an angle change,  $\Delta\alpha$ , in the HNH angle.  $a$  is the ratio of the two bond stretches ( $S_5^1:S_3^1$ ), and  $b$  is given below.

$$b = -\frac{4}{\sqrt{3}} \frac{1}{r_{NH}} (S_5^1/S_4^1)$$

These equations are correct to the first order in the angular displacement,  $\Delta\alpha$ . Equation (30) is the condition for no change in the center of mass, and equations (31) and (32) are conditions on the ratios  $\Delta r_{34}/\Delta r_{45}$  and  $\Delta r_{34}/\Delta\alpha$ . Equations (33) are the solutions to equations (30), (31), and (32).

$$\left. \begin{aligned} \delta_4 &= \frac{a + 8ab - 7b}{a - 13ab - 7b} \delta_3 \\ \delta_5 &= \frac{a + 8ab + 14b}{a - 13ab - 7b} \delta_3 \\ \delta_H &= \frac{-21a}{a - 13ab - 7b} \delta_3 \end{aligned} \right\} \quad (33)$$

Table 7 presents the data from which Figure 10 is drawn.

Table 7. Atomic displacement factors\* for Case 2.

	$\delta_4$	$\delta_5$	$\delta_H$
$\nu_2$	-2.35	1.00	-0.898
$\nu_3$	0.152	-0.475	-5.62
$\nu_4$	-0.398	-0.955	1.08

\* The atomic displacement factors are the factors written to the left of  $\delta_3$  in equations (33).



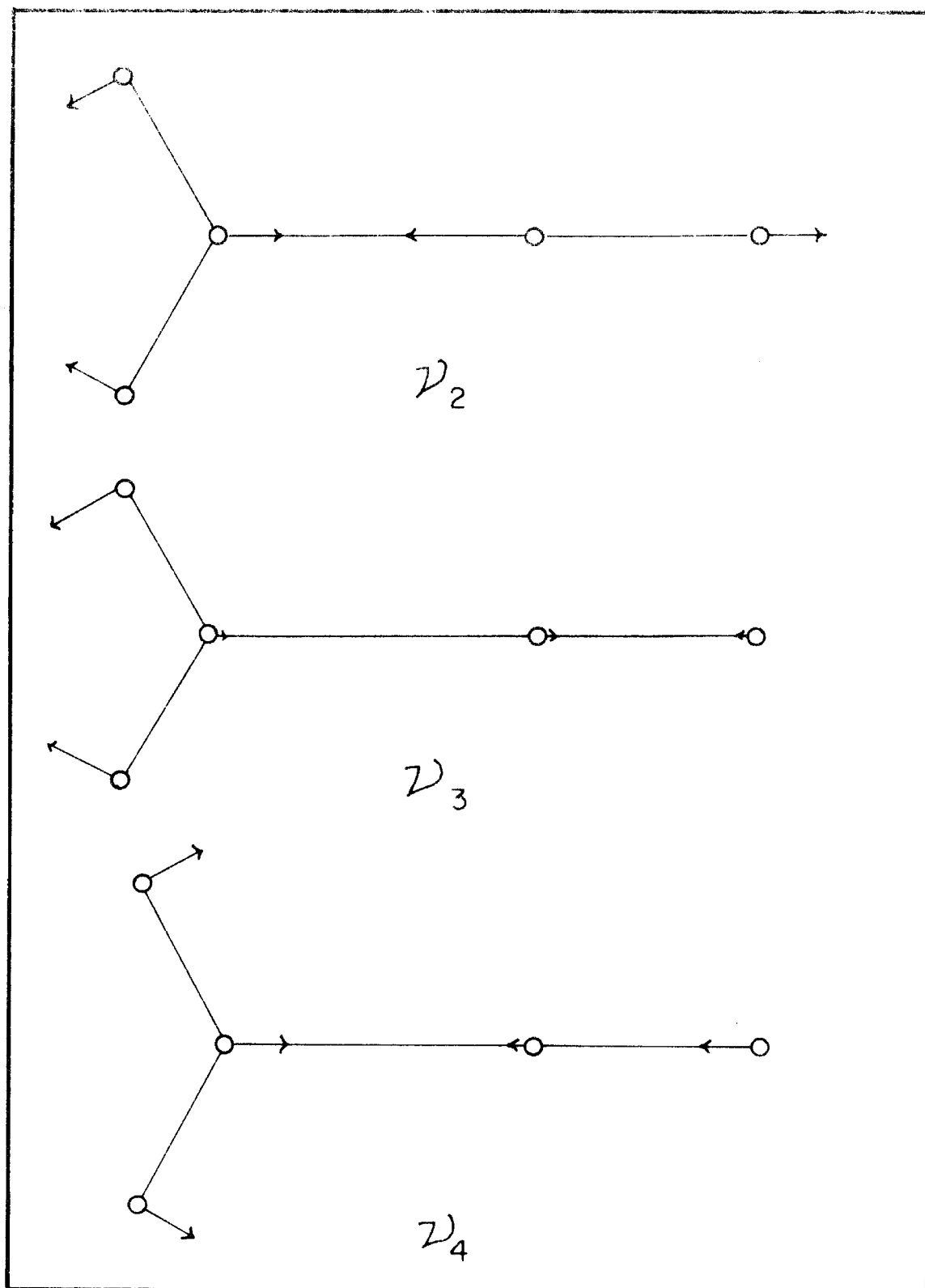


Figure 10. The three lowest frequency A' normal vibrations of cyanamide.

The form of the normal modes under Case 2 have been calculated and are presented in Figure 10. The appropriate changes for the other two cases may be visualized using the data in Table 6.

b. Intensities of  $\nu_2$  and  $\nu_4$ .

The planarity of the cyanamide molecule is evidence that considerable resonance exists between the configurations I and II.

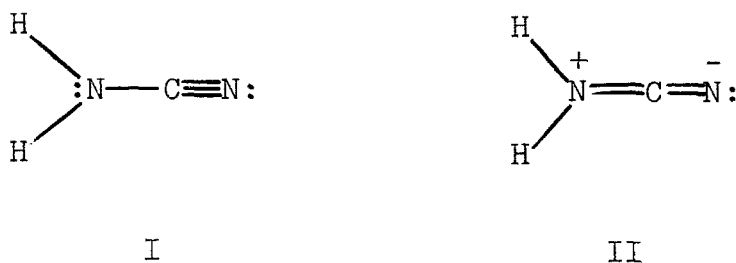


Figure 11. Resonating configurations of cyanamide.

This fact together with results of the normal coordinate analysis can be used to explain, in part, the intensities of the bands  $\nu_2$  and  $\nu_4$ . An examination of Figure 10 and Table 6 will show that for all sets of force constant values taken from Figure 8  $\nu_2$  and  $\nu_4$  are characterized, respectively, by antisymmetric and symmetric stretching of the heavy atoms.

In  $\nu_2$  a large contribution to the change in dipole moment arises from the large charge transfer as the contri-

bution of each of the two resonance forms changes during the course of the vibration. For example, in the phase of the normal mode of  $\nu_2$  shown in Figure 10 the contribution of II is increasing, and that of I is decreasing, because the decrease in  $r_{34}$  and the increase in  $r_{45}$  favor structure II. This causes a positive charge transfer towards the amino nitrogen. The movement of the positively charged hydrogens, as  $\alpha$  decreases, adds to the amount of positive charge movement towards the amino nitrogen. Hence a large change in dipole moment is expected, and an intensely absorbing vibration results. A different situation is found for  $\nu_4$ . Here two items must be considered: firstly, both bonds shorten or lengthen together, so that the ratio of the changes must be taken into account in order to predict changes in resonance; and secondly, this ratio is more strongly dependent on the particular set of values chosen for the force constants than is the corresponding ratio in  $\nu_2$ . In the case shown in Figure 10 for  $\nu_4$ , both bonds are compressing. This probably leads to less change in the respective contributions of I and II than in the antisymmetric vibration. However, there is approximately 2.5 times as much change in the inner CN bond as there is in the terminal CN bond, thus the contribution of II probably increases and that of I decreases; so that in the phase shown a transfer of positive charge towards the amino-nitrogen results (as is also true for  $\nu_2$ ). How-

ever, in this case ( $\nu_4$ ), the motion of the hydrogens, as  $\alpha$  increases, is away from the amino-nitrogen diminishing the change in dipole moment. Therefore,  $\nu_4$  should absorb less intensely than  $\nu_2$ .

It must be realized that these arguments are incomplete because they only consider the changes in dipole moment arising from changes in resonance, and from the motion of the hydrogen atoms. These considerations are probably adequate for discussing the differences in intensity of the bands in question, as can be seen from the following heuristic argument. The assumption is made that the total dipole moment of the molecule is the sum of the bond dipole moments

$$\mu_{\text{mol}} = \sum \mu_{\text{bond}}.$$

Then,

$$d\mu_{\text{mol}} = \sum d\mu_{\text{bond}}.$$

A bond dipole moment is given by

$$\mu = \epsilon r,$$

where  $\epsilon$  is the charge, and  $r$  is the distance between the charges of the dipole. Quite formally one may write

$$d\mu = \epsilon dr + r d\epsilon. \quad (1)$$

The first term of (1) gives the change in dipole moment for changes in internuclear distance, and the second term gives the change in dipole moment for redistribution of charge. The effects of the first term have been discussed for the motion of the hydrogen atoms, and the principal effects have been discussed for the second term. Thus there remains the effects of the first term for the motion of the heavy atoms. A plausible orientation of bond dipole moments for the heavy atoms is one in which the two dipole moments point from the nitrogen atoms towards the carbon atom (the convention of dipoles pointing from positive towards negative is used here). For such an arrangement the antisymmetric vibration would absorb more intensely than the symmetric vibration. Hence no change in the arguments given above would be necessary.

### The Combination Band at Three Microns

The assignment of the absorption maximum at  $3422\text{ cm}^{-1}$  in the spectrum of the solution is of particular importance because its species helps to determine the assignment of the  $\nu_4$ . The assumption is made that this band is to be assigned to a binary combination. An examination of the various possible binary combinations of fundamental frequencies giving an absorption in the vicinity of  $3420\text{ cm}^{-1}$  limits the choice to one,  $\nu_2 + \nu_n = 2257 + x = 3422$ ; i.e.  $x = 1165\text{ cm}^{-1}$ . The species of  $\nu_2$  is  $A_1$ , hence the species of the combination band will be the same as that of  $\nu_n$ . The high dispersion spectrum of the liquid shows that the absorption assigned to  $\nu_2 + \nu_n$  falls very near  $\nu_5$ . This suggests that  $\nu_2 + \nu_n$  is not of species  $B_1$ , i.e. the combination band belongs to  $A_1$  or  $B_2$ . Thus  $\nu_n$  is not  $\nu_6$ , for then the combination band would belong to species  $B_1$ . However, the arguments above concerning the relative magnitude of the frequencies of the hydrogen-bending vibrations imply that if  $\nu_n$  is  $\nu_8$ , then  $\nu_6$  occurs at a higher frequency than  $1165\text{ cm}^{-1}$ . No such assignment seems plausible, since no bands, except those whose assignment seems correct, occur above  $1165\text{ cm}^{-1}$ . Thus  $\nu_n$  is not  $\nu_8$ . Consequently  $\nu_n$  belongs to  $A_1$ , and is  $\nu_4$ .

An examination of the spectrum of the solution shows no absorption at  $1165\text{ cm}^{-1}$ . However, the infrared and Raman spectra of the crystal, and the Raman spectrum of the melt show a band occurring at approximately  $1120\text{ cm}^{-1}$ , which may well be  $\nu_4$ , and indeed it is assigned to  $\nu_4$  in the spectrum of the solution.  $\nu_4$  will not be expected at  $1165\text{ cm}^{-1}$  but at a lower frequency, since it is very likely that the band at  $3422\text{ cm}^{-1}$  has been pushed up by a Fermi interaction with  $\nu_1$ . The absence of  $\nu_4$  from the spectra of the gas and of the solution is attributed to its weak absorption. (This has been discussed above p. 45 et seq.) It may well be that this band is intensified by an increase in the contribution of the ionic resonance form in the hydrogen bonded state expected for the melt and the crystal.

## The Rotational Structure of the Three Micron Band

### A. Introduction.

The three micron high dispersion spectrum of cyanamide is of particular importance because it presents data of special value for structural considerations. The fundamental  $\text{NH}_2$  asymmetric stretching vibration absorbs in this region, and in the absence of serious perturbations or other complications may be expected to supply two items of information: first, the moments of inertia of the molecule may be obtained from the spacing of the rotational lines of this band; and second, the planarity of the molecule is proved by an intensity alternation of these lines. However, perturbations and other complications, which are discussed below, do exist, imposing limitations on the conclusions which can be drawn from these data. These same difficulties have also been encountered for the asymmetric hydrogen stretching vibration of ketene (23), diazomethane (17), and formaldehyde (24).

An examination of this spectrum (see Figure 12) reveals three principal features. The first is a series of lines of alternating intensity, with the approximate spacing expected for the Q heads of a perpendicular band of a molecule like cyanamide. A number of these lines appear



as doublets. The second feature is two rather broad absorption maxima about  $30 \text{ cm}^{-1}$  apart, which are very likely the P and R branches of a parallel band. The third feature is additional lines, perhaps attributable to the rotational structure of  $\nu_2 + \nu_4$ , to absorption of molecules in excited vibrational states, and to absorption by ammonia (formed by the pyrolysis of cyanamide). The large number of lines in this region has prevented unambiguous assignments to the various rotational transitions, though the general spectral pattern is quite clear, and an approximate value for the largest rotational constant in the ground state has been obtained.

#### B. Analysis of the rotational structure.

Cyanamide is very nearly a perfect symmetric top molecule, so that the methods given by Herzberg (Ref. 11, p. 400 et seq.) for the study of such molecules can be used here. The symbols employed in this analysis will have the meaning given by Herzberg, unless explicitly so stated.

The rotational selection rules for a vibration-rotation transition in which the change of dipole moment is perpendicular to the top axis are

$$\begin{aligned} \Delta K &= \pm 1 \\ \Delta J &= 0, \pm 1. \end{aligned} \tag{1}$$

The frequencies of the resulting Q branches of the subbands (hereafter called lines) of a perpendicular band are given by equation (2),

$$\nu_o^{\text{sub}} = \nu_o + (A_V' - B_V') \pm 2(A_V' - B_V')K + [(A_V' - B_V') - (A_V'' - B_V'')]K^2, \quad (2)$$

the plus sign referring to the  $R_{Q,K}$  lines ( $\Delta K = 1$ ), and the minus sign referring to the  $P_{Q,K}$  lines ( $\Delta K = -1$ ). Noting that the pairs of lines  $R_{Q,K-1}$  and  $P_{Q,K+1}$  have common upper levels leads to the combination relation (3),

$$\frac{R_{Q,K-1} - P_{Q,K+1}}{4K} = A_V'' - B_V''. \quad (3)$$

By plotting values of the left hand side of equation (3) versus  $K^2$  and extrapolating to  $K=0$ , values of  $A_V'' - B_V''$  for the rotationless state are obtained. The  $A_V''$  and  $B_V''$  are the average values of the rotational constants during a vibration and are related to the equilibrium value by

$$A_V'' = A_e'' - \sum \alpha_i^A (v_i + \frac{1}{2}) \quad (4)$$

$$B_V'' = B_e'' - \sum \alpha_i^B (v_i + \frac{1}{2}),$$

where

$$A_e'' = \frac{h}{8\pi^2 c I_A} \quad \text{and} \quad B_e'' = \frac{h}{8\pi^2 c I_B}. \quad (5)$$

$I_A$  and  $I_B$  are the equilibrium moments of inertia. The  $\alpha_i$  are not known. For a fundamental vibration, in the absence of perturbations, they are small. Since no means of evaluating the  $\alpha_i$  is available at this time, their contribution to the rotational constants will be assumed negligible. Thus the rotational constant for the vibrationless state will be taken equal to the rotational constant for the equilibrium configuration, e.g.  $A''_O = A''_e$ .  $B''_e$  will be taken as the average of the two smallest rotational constants, because cyanamide is not an exact symmetric top. (The two large moments of inertia differ by the amount of the smallest moment of inertia since the molecule is planar.) The value for  $A''_e$  is obtained from the extrapolated value of  $A''_O - B''_O$  by adding a calculated value for  $B''_e$  (see p. 71, and Appendix 2).

A perpendicular band of a nearly-symmetric top molecule will exhibit a central minimum, and two branches with a uniform (Boltzmann) intensity decrease away from the band center. In the case of a planar  $C_{2v}$  molecule with the smallest principal moment of inertia along the two-fold axis, an intensity alternation of 3:1 between adjacent lines (see Ref. 11, p. 479 et seq.) will be superposed on this gradual decrease. The band center will be located between the two strongest lines, midway between a weak and a strong line. Since the hydrogen nuclei follow Fermi statistics, the weak line,  $R_{Q_0}$ ,

will be the first line on the high frequency side of the band center. Such a pattern, if for the moment the finer details are neglected, is readily seen in the spectrum presented in Figure 12. However, as previously stated, a satisfactory assignment of the lines in this spectrum has not been made because of the large number of lines found. Thus it has been necessary to make several alternative trial assignments for the observed lines, using different methods of choice for each trial. Little question exists in making some of the assignments. For example,  $R_{Q_1}$  and  $P_{Q_1}$  are assigned the same way in every case. But uncertainties exist regarding other choices.

A certain amount of systematization was used in each trial assignment. In trial 2 the assumption was made that the lines of the band should be spaced according to a smooth function of the frequency. Hence the assignments of this trial were made by choosing lines in a manner which gave regularly changing frequency increments between adjacent lines. The methods for trials 3, 4, and 9 are self-explanatory (see listing in Table 10). The method used for trial 5, and for variations of trial 5 is discussed below.

For each trial assignment a value of  $A_e''$  was calculated from which further structural information was obtained in the manner indicated below.

Table 8 lists the frequencies of all the lines measured

Table 8. Frequencies\* in  $\text{cm}^{-1}$ , of maxima and certain minima in three micron spectrum.

Item	Frequency <sup>a</sup>	Item	Frequency <sup>a</sup>	Item	Frequency <sup>a</sup>
1.	3612.28	16.	3499.08	31.	[ 3418.10
2.	3588.49	17.	3490.17	32.	[ 3414.92
3.	[ 3575.70	18.	[ 3480.30	33.	3411.79
4.	[ 3571.08	19.	[ 3479.63**	34.	3407.98
5.	[ 3557.76	20.	[ 3478.58	35.	3405.75
6.	[ 3553.72	21.	3470.11***	36.	3402.62
7.	3549.98	22.	3464.83	37.	3397.46
8.	3545.12	23.	3458.68	38.	3390.89
9.	[ 3539.10	24.	3452.81	39.	3387.02
10.	[ 3536.07	25.	3446.29	40.	[ 3378.53
11.	[ 3520.57	26.	3438.58	41.	[ 3375.44
12.	[ 3517.74	27.	3437.75**	42.	3369.01
13.	3511.04	28.	3437.05	43.	[ 3357.58***
14.	3510.46**	29.	3432.88***	44.	[ 3355.35***
15.	3509.62	30.	3427.22	45.	3336.05***

\* Frequencies corrected to vacuum.

\*\* Frequency of minimum between two lines.

\*\*\* Ammonia lines, or lines coinciding with ammonia lines.

<sup>a</sup> Frequencies of apparent doublets are joined by brackets.

in the spectrum shown in Figure 12, and an identifying item number. Table 9 presents the assignments and combination relations for the particular assignment that seems most plausible for reasons given below (see p. 62 et seq.). Table 10 is a summary of the trial assignments, and of the method used in assigning the lines in each trial.

C. Discussion of the rotational structure.

Clearly complications do exist in the rotational spectrum since an unambiguous assignment of the observed structure in this region has not been possible. Possible explanations of the complexity of this spectrum include Coriolis perturbations, splitting of the rotational levels because the molecule is not a perfect symmetric top rotator, absorption by excited molecules, Fermi perturbations, and overlapping of lines from several closely adjacent absorption bands.

In cyanamide, according to Jahn's rule (Ref. 11, p. 376), Coriolis perturbations are possible, between all pairs of vibrational levels whose product species is  $A_2$ ,  $B_1$ , or  $B_2$ ; thus such perturbations may be expected between  $\nu_1$  and  $\nu_5$ , and between these and combination levels of appropriate symmetry occurring in this region. However, the interaction between  $\nu_1$  and  $\nu_5$  should be small. Since both vibrations are in the plane of the molecule, the coupling will be greatest when the molecule is rotating

Table 9. Assignment of rotational transitions in  $\nu_5$ ,  
and combination relations for trial 5.

Item	Assign't	Frequency	Diff
2.	$R_{Q6}$	3588.49	17.41
4.	$R_{Q5}$	3571.08	17.36
6.	$R_{Q4}$	3553.72	17.65
10.	$R_{Q3}$	3536.07	18.33
12.	$R_{Q2}$	3517.74	18.66
16.	$R_{Q1}$	3499.08	18.78
18.	$R_{Q0}$	3480.30	21.62
23.	$P_{Q1}$	3458.68	21.63
28.	$P_{Q2}$	3437.05	18.95
31.	$P_{Q3}$	3418.10	20.64
37.	$P_{Q4}$	3397.46	22.02
41.	$P_{Q5}$	3375.44	20.09
44.	$P_{Q6}$	3355.35	

K	1	2	3	4	5
$R_{Q_{K-1}}$	3480.30	3499.08	3517.74	3536.07	3553.72
$P_{Q_{K+1}}$	3437.05	3418.10	3397.46	3375.44	3355.35
$R_{Q_{K-1}} - P_{Q_{K-1}}$	43.25	80.98	120.28	160.63	198.37
A"-B"	10.81	10.12	10.02	10.04	9.92

Extrapolated value: A"-B" = 10.18 cm<sup>-1</sup>

Table 10. Summary of rotational assignments\* for  $\nu_5$ ,  
and method of assignment.

Assign't	Trial									
	2	3	4	5	6	7	8	9	10	11
$R_{Q_5}$	4	3	4	4	4	4	3	3,4	4	4
$R_{Q_4}$	6	5	6	6	6	6	5	5,6	6	6
$R_{Q_3}$	10	9	10	10	10	10	10	9,10	10	10
$R_{Q_2}$	12	11	12	12	12	12	12	11,12	12	12
$R_{Q_1}$	16	16	16	16	16	16	16	16	16	16
$R_{Q_0}$	19	18	20	18	19	19	19	18,20	20	20
$P_{Q_1}$	23	23	23	23	23	23	23	23	23	23
$P_{Q_2}$	26	26	28	28	27	27	27	26,28	28	28
$P_{Q_3}$	31	31	32	31	31	31	31	31,32	32	31
$P_{Q_4}$	37	37	38	37	37	37	37	37	37	37
$P_{Q_5}$	41	40	42	41	40	41	40	40,41	41	41
$P_{Q_6}$	44	43		44	43	44	43	43,44	44	44

Trial	Method
2	$\Delta \nu$ (between adjacent lines) kept smooth.
3	High frequency components of doublets chosen.
4	Low frequency components of doublets chosen.
5	See text p.63 <u>et seq.</u>
6	Variation of trial 5.
7	Variation of trial 5.
8	Variation of trial 5.
9	Average frequency of indicated doublets taken.
10	Variation of trial 5.
11	Variation of trial 5.

\* The numbers entered in the body of the table are the "items" from Table 8.



about an axis perpendicular to the molecular plane. The resultant Coriolis forces arising from the above rotation and the motion of the hydrogen atoms in  $\nu_1$  tend to excite the hydrogen atoms in the motion of  $\nu_6$ , not that of  $\nu_5$ ; similarly, the forces arising from the interaction of this rotation and  $\nu_5$  tend to excite  $\nu_3$ , and not  $\nu_1$ . Consequently the Coriolis perturbations between  $\nu_1$  and  $\nu_5$  should be weak. Parenthetically, strong Coriolis perturbations between the in-plane and out-of-plane bending vibrations should be expected (as has been found for formaldehyde (28)).

K-type doubling of the rotational energy levels of the molecule, arising from the asymmetry of the molecule, should be of negligible importance. This assertion finds support in the following two facts. Cyanamide is more nearly a symmetric top rotator than chloramine (14), for example, which does not show significant doubling; and, as shown in Table 11 the amount of splitting of the apparent doublets changes little with K, whereas the amount of the splitting should decrease markedly as K increases.

The present data cannot be said to offer strong support for the suggestion that the apparent doublets listed in Table 11 arise from split energy levels in the upper state of  $\nu_5$ . Indeed, it may well be that the components of the apparent doublets actually belong to two different series of lines. Assuming that the Raman shifts at 429 and

Table 11. Apparent doublets of the three micron band

Items	Assign't	$\Delta\nu$ , $\text{cm}^{-1}$
18,20	$R_{Q_0}$	1.72
16	$R_{Q_1}$	- *
11,12	$R_{Q_2}$	2.83
9,10	$R_{Q_3}$	3.03
5,6	$R_{Q_4}$	(4.04) **
3,4	$R_{Q_5}$	(4.62) **
23	$P_{Q_1}$	-
26,28	$P_{Q_2}$	1.53
31,32	$P_{Q_3}$	3.18
37	$P_{Q_4}$	-
40,41	$P_{Q_5}$	3.09
43,44	$P_{Q_6}$	(2.23) **

\* This line has a broad base.

\*\* The numbers in parentheses indicate dubious parings.

513  $\text{cm}^{-1}$  are  $\nu_9$  and  $\nu_7$ , respectively, and that these values are not too different from the corresponding frequencies in the gas, one can calculate that approximately 16% of the molecules are in the excited state  $\nu_9 = 1$  and that approximately 14% of the molecules are in the state  $\nu_7 = 1$ , at 117°C. Consequently there will be nearly half as many molecules with  $\nu_7 = 1$  or  $\nu_9 = 1$  as there are in the ground vibrational state. Therefore if the differences of the rotational constants in these excited states are sufficiently different from the difference in the ground state, two series of lines will be found. One series will belong to vibration-rotation transitions from the ground vibrational state to  $\nu_5 = 1$ , and the other set will belong to vibration-rotation transitions from  $\nu_7$  (or  $\nu_9$ ) = 1,  $\nu_5 = 0$  to  $\nu_7$  (or  $\nu_9$ ) = 1,  $\nu_5 = 1$ . In an excited skeletal bending state the mean square displacements of the heavy atoms from the two-fold axis of the molecule will be larger than in the ground vibrational state, so that the effective large rotational constant will be smaller, and the effective small rotational constant may be somewhat larger than the corresponding constants in non-excited molecules. Since the approximate spacing of the lines of a perpendicular band is 2 ( $A''-B''$ ), the rotational structure of a band of molecules absorbing from these excited skeletal bending states will be more closely spaced than the structure of an absorption band of molecules absorbing from the ground vibrational state.

The application of this analysis to the three micron spectrum has been considered. A series of lines, listed in Table 12, with a spacing of approximately  $12\text{ cm}^{-1}$  is found. This spacing yields a value for  $A''-B''$  of  $6\text{ cm}^{-1}$  for the excited molecules in the lower vibrational state. There are at least two unsatisfactory features which should be considered. The lines listed in Table 12 show rather little change in intensity over the breadth of the band, and there is no obvious intensity variation between adjacent lines. These objections may not be too serious because the general complexity of the spectrum makes estimates of the intensity of individual weak absorptions unreliable. However, this analysis does supply an explanation for the apparent doubling found in this spectrum. It is on this basis that trial assignment 5 has been made.

Figure 12 presents a graphical summary of the data listed in Tables 8, 9 and 12. The lower curve shows the complete high dispersion spectrum in the three micron region, the middle curve represents the perpendicular band for trial 5, and the upper curve shows the absorption lines thought to belong to vibrationally excited molecules. No effort has been made to distribute the intensity of the lines of the lower curve correctly between the two upper curves in the cases where apparent doublets have been separated. The dashed lines are drawn to aid in picturing the continuity of the curves.

Table 12. Lines possibly arising from excited molecule  
absorption.

Item	Frequency	$\Delta \nu$ , cm <sup>-1</sup>
5	3557.76	
8	3545.12	12.64
11	3520.57	24.55
*		---
17	3490.17	
20	3478.58	11.59
22	3464.83	13.75
24	3452.81	12.02
26	3438.58	14.23
30	3427.22	11.36
32	3414.92	12.30
36	3402.62	12.30
38	3390.89	11.73
40	3378.53	12.46

\* An absorption could lie underneath the wings of  
item 16.

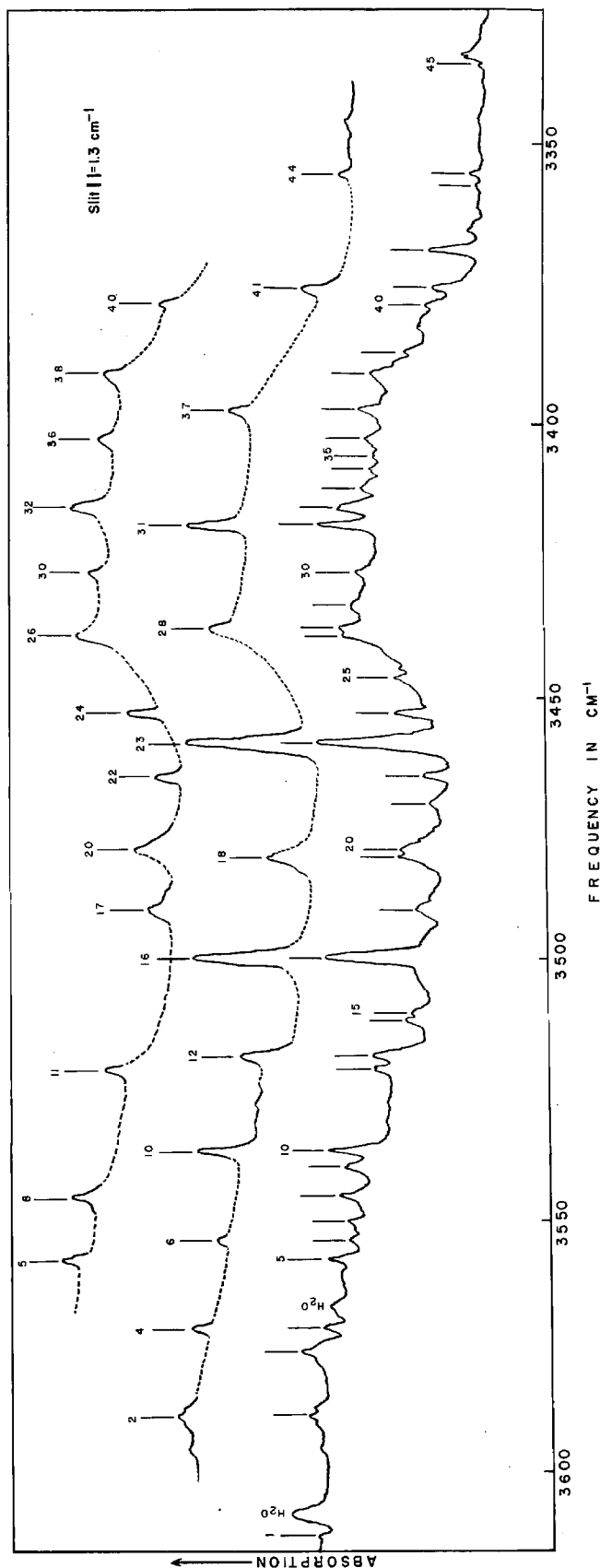


Figure 12. Three micron spectrum of gaseous cyanamide under high dispersion. Path length 1.1 m. Temperature 1150°C. Lower curve shows the complete spectrum; middle curve shows the rotational structure assigned to  $J_5$  transitions from the ground vibrational state; upper curve shows structure possibly arising from  $J_5$  transitions from excited vibrational states.

The possibility of Fermi perturbations in the three micron region is restricted to perturbations between  $A_1$  vibrational levels if only fundamental and binary vibrational transitions are considered (see p.49 et seq.). Thus  $\nu_1$  and  $\nu_2 + \nu_4$  may interact giving rise to a larger number of strong lines in this region than in the absence of such a perturbation. For the sake of completeness it should be noted that there might possibly be a Fermi perturbation between  $\nu_5$  and  $\nu_8 + \nu_9 + \nu_6$  ( $1080 + 1003 + 429 = 3512 \text{ cm}^{-1*}$ ). However, several assumptions must be verified before the position and species of this level are accepted as proved.

#### D. Molecular parameters.

The equilibrium value for the smallest moment of inertia,  $I_A$ , depends on two molecular parameters, the N-H bond distance,  $r_{N-H}$  and the HNH angle,  $\alpha$ . Equation (1) gives this relationship

$$I_A = 2m_H(r_{N-H}\sin \alpha/2)^2 . \quad (1)$$

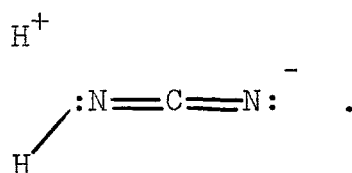
$m_H$  is the mass of a hydrogen atom. This expression may be rearranged in terms of the rotational constant  $A_e''$  to the following

---

\* Gaseous frequencies are not available. The quoted frequencies are taken from the states given in Table 2.

$$r_{\text{N-H}} = \frac{2.91}{\sqrt{A_e''} \sin \alpha/2} \quad (2)$$

In equation (2)  $A_e''$  is in  $\text{cm}^{-1}$ , and  $r_{\text{N-H}}$  in Angstroms. Figure 13 is a graph of equation (2) for various values of  $A_e''$ . For a given value of  $A_e''$ , and of  $r_{\text{N-H}}$ , the allowed value of  $\alpha$  is given by the ordinate of the intersection of the line of given  $A_e''$  with the abscissa of the given value of  $r_{\text{N-H}}$ . The N-H bond length in cyanamide may be expected to be shorter than that in ammonia, since bond lengths shorten as the amount of s character of the bond increases (22). On the other hand, some tendency towards lengthening of this bond may result from a repulsion between the amino-nitrogen and the hydrogen or from the contributions of resonating configurations such as



Despite these uncertainties  $r_{\text{N-H}}$  may be estimated from an assumed functional dependence of  $\nu_{\text{N-H}}$  on  $r_{\text{N-H}}$ . A graph of  $\nu_{\text{N-H}}$  versus  $r_{\text{N-H}}$  for molecules for which these data are known is a straight line.\* If a molecule has more than

---

\* The simple plot is made because bond distances can be read directly for a given frequency. However, the data do fit Badger's Rule relationship of the form

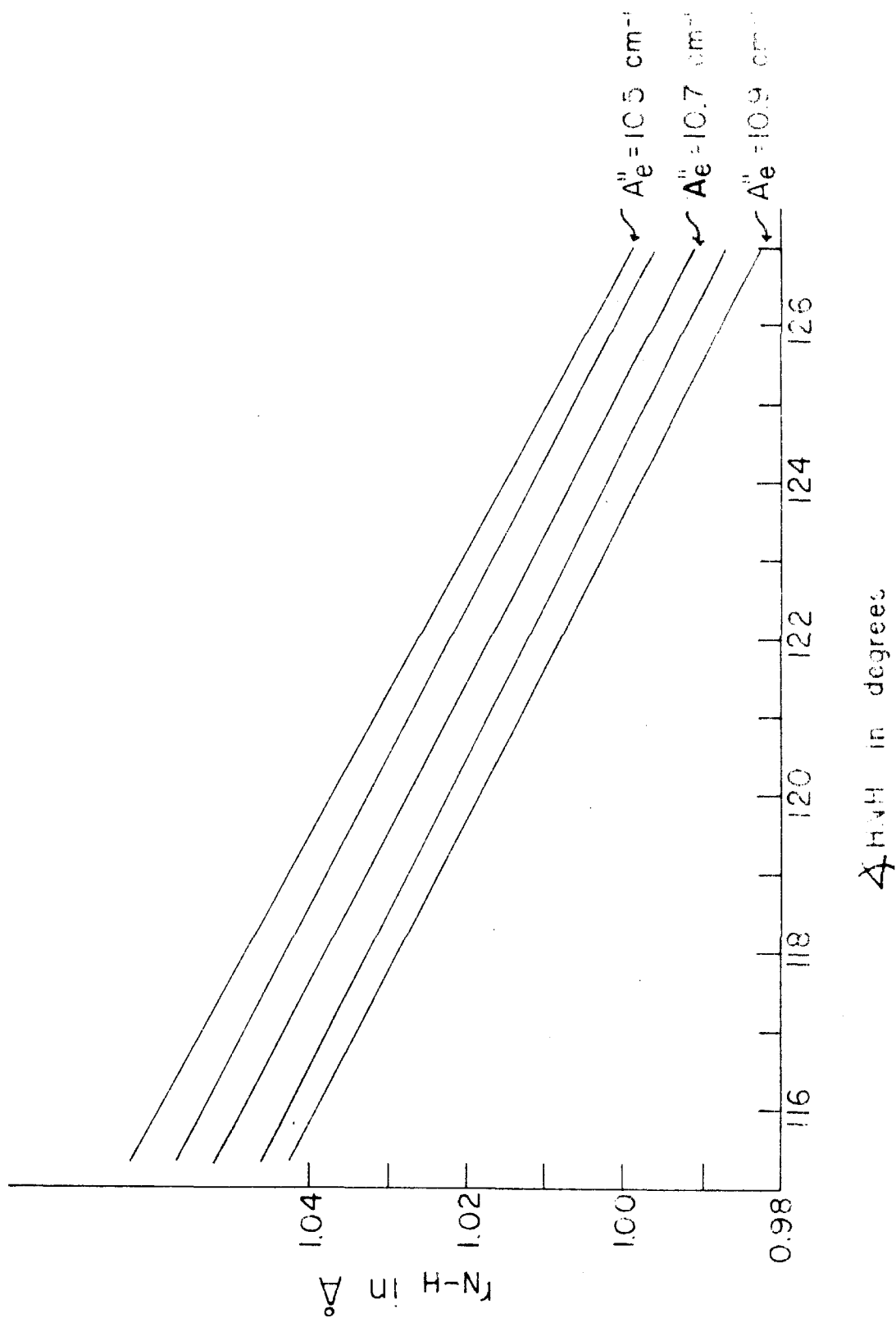
$$\nu_{\text{N-H}} = c(r_{\text{N-H}} - 0.34)^{-3/2}$$

extremely well.  $c$  is a constant, and  $r_{\text{N-H}}$  is in Angstroms.





Figure 13. Graph of  $r_{\text{N-H}}$  vs. HNH for given values of the large rotational constant.



one NH vibration, the mean frequency of these vibrations is used. Table 13 presents the available data. The graph is shown in Figure 14. The value of  $r_{\text{N-H}}$  corresponding to the mean of  $\nu_1$  and  $\nu_5$  in cyanamide,  $3445 \text{ cm}^{-1}$ , is  $1.002 \text{ \AA}$ . It should be noted that strong Fermi perturbations may lead to deviations from the simple relation found for the data in Table 13. However, even a perturbation of  $50 \text{ cm}^{-1}$  in  $\nu_1$  of cyanamide would lead to an error of just  $0.005 \text{ \AA}$ , since only half the frequency shift would be used in determining the value of  $\nu_{\text{N-H}}$  to be used for the estimation of the bond distance.

Table 13. NH stretching frequencies for known NH bond distances.

Molecule	$\nu, \text{cm}^{-1}$	$r_{\text{N-H}}$	Method	Reference
$\text{HN}_3$	3336	$1.021 \text{ \AA}$	a,b	(29)
$\text{NH}_3$	$3335^*$	$1.014 \text{ \AA}$	a	(30)
$\text{HNCO}$	3534	$0.987 \text{ \AA}$	a,b	(31)

a Infrared.

b Microwave

\* Mean value of  $\nu_1(a_1)$  and  $\nu_3(e)$ .

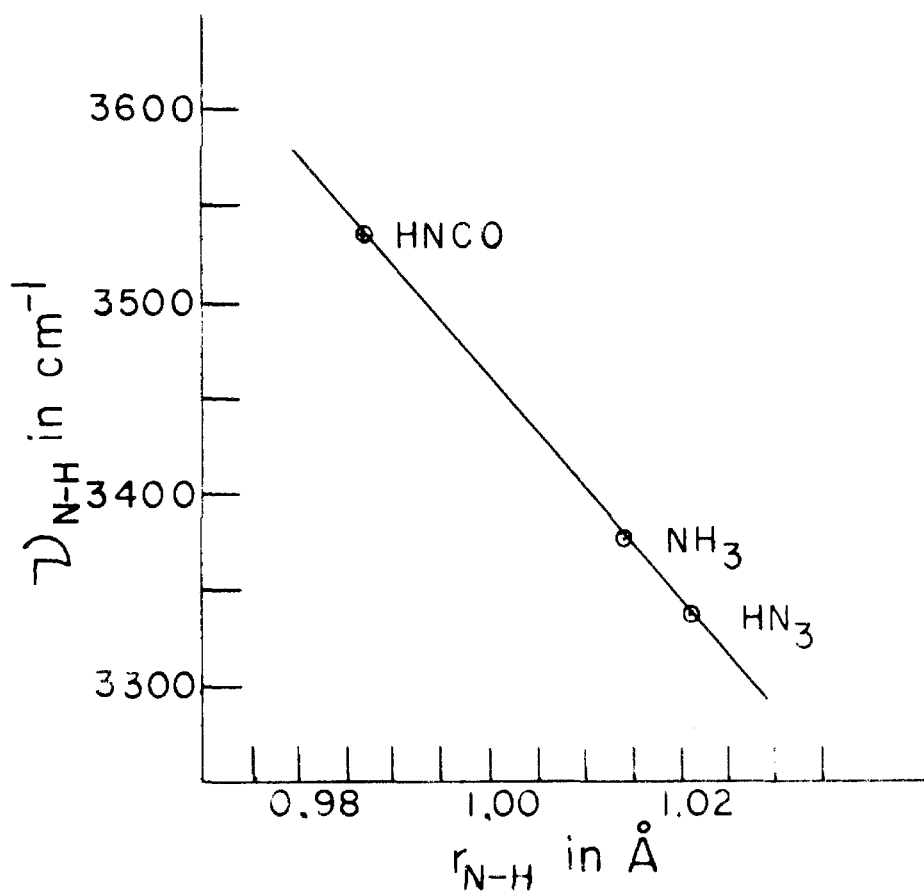


Figure 14. Graph of  $\nu_{N-H}$  vs.  $r_{N-H}$ . See Table 13.

Table 14 lists the values of  $A_e''$  and of  $\alpha$  for the various trial assignments.  $A_e''$  has been obtained from the extrapolated value of  $A''-B''$  by adding to it  $0.32 \text{ cm}^{-1}$ . This latter number is the average of the two smaller rotational constants for a particular model of cyanamide. The details of the calculation of these values are given in Appendix 2. Since slight changes in the CN bond distances will give rise to negligible changes in the values of  $A''-B''$ , the value of  $A_e''$  is rather insensitive to the NCN distances (if the heavy atom configuration is linear).

An examination of Table 14 will show that a value of  $\alpha$  between  $122^\circ 50'$  and  $127^\circ 25'$  (a maximum error of  $0.005 \text{ \AA}$  in  $r_{\text{N-H}}$  is assumed) is consistent with any of the trial assignments. This range of large values for  $\alpha$  lends support to the assertion that the molecule has trigonal hybridization about the amino-nitrogen atom, and that the HNH angle is greater than  $120^\circ$  because of coulombic repulsion between the hydrogen atoms.

Table 14. Values of  $A_e''$  and of  $\alpha$ , the HNH angle, for various trial assignments.

Trial	$A_e''$ , $\text{cm}^{-1}$	*
7	10.48	$126^{\circ}35'$
5	10.50	$126^{\circ}20'$
10	10.50	$126^{\circ}20'$
11	10.52	$126^{\circ}15'$
2	10.54	$126^{\circ}10'$
6	10.54	$126^{\circ}10'$
8	10.55	$126^{\circ}10'$
9	10.62	$125^{\circ}40'$
3	10.72	$124^{\circ}40'$
4	10.82	$123^{\circ}50'$

\*  $\alpha$  is given for  $r_{\text{N-H}} = 1.002 \text{ \AA}$ ,  $\alpha$  increases or decreases by one degree for a decrease or an increase of  $0.005 \text{ \AA}$ , respectively.

PART II

THE INFRARED SPECTRA OF FORMAMIDE, N,N-DIDEUTEROFORMAMIDE,  
AND N-METHYLFORMAMIDE



### Introduction

The general interest in the proteins and related substances has led to the utilization of every experimental method which gives information about the crystal and molecular structure of these vital substances. Infrared spectroscopy can be a powerful technique in these studies. However, to make an effective attack on this complex problem it is desirable first to secure an understanding of the origin of the predominant absorption bands characteristic of the polypeptide chain by studying the simplest substances which contain the groupings found in this chain. For this purpose the two simplest amides formamide,  $\text{HCONH}_2$ , and N-methylformamide,  $\text{HCONHCH}_3$  are particularly suitable. Since these substances exhibit the minimum interference from absorptions arising from the bending vibrations of the methyl, methylene, and other groups attention can be focused on the vibrational spectra of the  $-\text{CONH}-$  and the  $-\text{CONH}_2$  groups. Thus a study of the infrared spectra of these substances has been undertaken in order to obtain information applicable to the study of the proteins.

The vibrational spectra of liquid and gaseous  $\text{HCONH}_2$ ,  $\text{HCOND}_2$ , and  $\text{HCONHCH}_3$  will be discussed below. The high dispersion three micron spectrum of gaseous  $\text{HCONH}_2$  will be discussed in appendix 3.

### Experimental

The formamide used in these experiments was Eastman Kodak White Label Formamide. In the earlier work no special effort was made to dry the amide, however, the spectra obtained in earlier experiments were identical to those obtained when the amide was dried under a reduced pressure of about 0.1 mm Hg.

The N-methylformamide was prepared in these laboratories by Dr. H. Rinderknecht. He measured the following properties:

vapor press. = 90 mm Hg at 134°C

melting pt. = -6°C

$n_D^{21}$  = 1.4309.

The listed (45) melting point of N-methylformamide is -5.4°C.

The deuteration of formamide was accomplished by mixing excess heavy water and formamide in the absorption cell, and allowing them to remain in contact for approximately one minute, and then removing the excess light and heavy water under reduced pressure. An examination of the spectrum indicated that a mixture of  $\text{HCONH}_2$ ,  $\text{HCONHD}$ , and  $\text{HCOND}_2$  was obtained.

A vacuum grating spectrometer employing a  $\text{CO}_2/\text{MeOH}$  cooled PbS cell was used for high dispersion spectra in the 1-3.5 micron region.

The gaseous spectra were taken in an 80 cm glass cell equipped with either silver chloride, or potassium bromide windows, sealed onto the cell with glyptal. The silver chloride windows used initially were quite unsatisfactory, since they rapidly became increasingly opaque, thus increasing the experimental difficulties. Thin KBr plates (about 3 mm thickness) were used subsequently with very satisfactory results.

The high boiling point of formamide and N-methylformamide (ca. 200°C) made it necessary to heat the absorption cell to obtain a suitable vapor pressure, and also to take some pains to insure that the spectrum being obtained was that of the vapor, and not that of liquid condensed on the windows of the absorption cell. This was done by placing the cell within a metal tube wrapped with resistance wire, and by using independently controlled auxiliary heaters for the cell windows. Generally it was found necessary to heat the windows first, and then gradually to increase both the cell and window heater currents until a desirable pressure was obtained.

Satisfactory tracings of the three micron spectrum of formamide were obtained by enclosing as much of the light path as possible within glass tubes through which a slow stream of dry nitrogen was passed. This served to decrease the intensity of the 2.8 micron water band, and to make an examination of the high dispersion spectrum in this region

easier.

The decomposition of formamide was detected through the appearance of the 10 micron bands of  $\text{NH}_3$  when the amide was heated excessively.

The liquid spectra were taken on samples of the amides pressed between two rocksalt plates to a thickness that gave the desired absorption.

## Vibrational Spectrum and Discussion

### A. Introductory discussion

The presentation and discussion of the vibrational spectra of the formamides will be prefaced by a discussion of the difficulties encountered in making the vibrational assignments of the observed absorption maxima in the various spectra.

The complete molecular structure of formamide has not been determined.\* However the assumption will be made in this discussion that the molecule is planar. Several good reasons exist which lend strong support to this assumption. Kurland (32) has measured several rotational transitions in formamide using microwave techniques, and from these data he has calculated the following moments of inertia for formamide:

$$\begin{array}{rcll} I_A & = & 6.952 & \text{atomic mass units } \text{\AA}^2 \\ I_B & = & 44.448 & \text{ " " " " } \\ I_C & = & 51.407 & \text{ " " " " } \end{array}$$

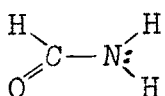
---

\*Ladell and Post (46) have published a crystal structure determination of formamide. They find that the CO and CN bond distances are 1.25<sub>5</sub> and 1.30<sub>0</sub> Å, respectively, and that the OCN bond angle is 121.5°. Unfortunately, the author was not aware of these data at the time the discussion above was written. However, these data do support the hypothesis that the molecule is planar, and in no way affect adversely the arguments that are presented.

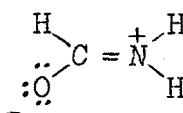
Since  $I_C = I_A + I_B$  for a planar molecule, neglecting the effect of the zero-point vibrations, he concludes from this data that formamide is a planar molecule. The small difference, 0.007 a.m.u. Å<sup>2</sup>, between the largest moment of inertia and the sum of the two smallest moments may well be due to the effect of the zero-point out-of-plane (A'') vibrations.

Another datum suggesting the planarity of the formamide molecule is the relatively high frequency of the NH<sub>2</sub> stretching vibrations. The mean frequency of the two NH<sub>2</sub> stretching vibrations is 3502 cm<sup>-1</sup> (see below), consequently according to the arguments presented above, see page 67 et seq., the NH bond distance in formamide is 0.993 Å. Compared with the NH bond distance in ammonia, 1.014 Å, this bond is quite short. Coulson (33) has discussed the shortening of bond distances with increase in s character of the bond. If the formamide molecule is planar, an sp<sup>2</sup> hybridization of the nitrogen atom is expected, and these NH bonds would have more s character than the NH bonds of ammonia which probably has sp<sup>3</sup> hybridization of the N atom.

A third reason for expecting that formamide may be planar is the resonance energy of the aliphatic amides. The most important configurations which contribute to the structure of formamide are shown in Figure 15.



I



II

Figure 15. Resonating configurations for formamide.

Pauling (34) gives the value for the resonance energy, with respect to I, as 21 kcal/mole. The planarity of a special amide, urea ( $\text{NH}_2\text{CONH}_2$ ), has been demonstrated by Waldron (35). However, the conclusion that the  $\text{CONH}_2$  part of other amide molecules is also planar may not necessarily follow since urea is a particularly favorable case for planarity because identical resonance configurations contribute to the structure of the molecule.\*

Thus since formamide is presumably a planar hexatomic molecule, it has twelve fundamental vibrations of which nine are totally symmetric and belong to the species A', and three are antisymmetric with respect to the plane of the molecule and belong to the species A". These will be discussed at greater length below.

A simplification in the description of the normal modes of vibration of a molecule is the assumption that each fundamental absorption band corresponds to a vibration of the molecule in which the motion is largely localized in a particular

---

\*The resonance energy of urea is 37 kcal/mole (34).

set of atoms. This idea of the localization of motion in a normal mode in some particular set of atoms is a very attractive idea, for it offers a convenient visualization of the motion of the atoms, and supplies a simple basis for spectral correlations between different molecules having the same groups. In particular, one might argue that the molecules of the series  $RCONH_2$  would have rather similar spectra (aside from the effects of the R group). Furthermore, one would expect vibrations that would be well described as the CO stretching, the CN stretching, and the  $NH_2$  scissors vibrations, and that the frequency of the same vibrations in other molecules containing these groups would be approximately the same as in the amides. However these simplifications must be examined carefully for they apply only in a limited manner to the amides.

A persistence of several vibrational frequencies is found in the amides. The frequencies assigned to the  $NH_2$  and CH stretching vibrations are in all probability well described as such, but the vibrations involving the skeletal stretchings, and the  $NH_2$  scissors deformation are not simple to describe. Randall, et al. (36) list several vibration frequencies characteristic of the amide group. However, studies of the spectra of deuterated amides, and dichroic studies have led to the suggestion by Price and Fraser (38) that the vibrations naively referred to as the CO stretch, CN stretch, and  $NH_2$  scissors vibrations are more complex



than this simple nomenclature implies. They suggested further, that the actual form of the vibrations would be well described as combinations of symmetric and asymmetric stretchings of the OCN part of the molecules with the scissors bend of the  $\text{NH}_2$  group. Badger (37) using a vibrating mechanical model has shown that such descriptions are indeed applicable to acetamide and that the older nomenclature of CO stretching, etc., is not really descriptive.

The application of Badger's results with the acetamide model to the formamides is seriously complicated by the difference in mass of the methyl group and of the hydrogen atom bound to the amide carbon atom. In some of the amide vibrations of acetamide there is a considerable contribution of the C-C stretching to the normal modes; while for formamide the light mass of the hydrogen atom should lead to a negligible contribution of the H-C stretching to the corresponding normal modes. The contribution of the C-C-O and the H-C-O bending deformations to the particular vibrations of these amides will also be quite different, i.e., the H-C-O bend should contribute appreciably to normal modes absorbing in the  $1500$  to  $1200\text{ cm}^{-1}$  range of formamide, while the C-C-O bend contributes to a smaller extent in the corresponding modes of acetamide.

A particularly difficult task is the correlation of the observed absorption bands in the spectra of  $\text{HCONH}_2$  and  $\text{HCOND}_2$ . Badger's (37) results with the vibrating

mechanical model of acetamide demonstrate that upon deuteration gross changes occur in the form of the normal modes. A striking example is the change in the nature of the vibration he calls Amide IIa. The contribution of the  $\text{NH}_2$  group to this vibration is primarily in the form of the scissors deformation, while in  $\text{CH}_3\text{COND}_2$  the contribution of the  $\text{ND}_2$  group is in the rocking deformation. Other marked changes also occur in the other modes. Indeed the changes in the character of modes are so pronounced that for the most part the only possible correlation which can be made between the vibrations of the two molecules is the purely arbitrary one made on the basis of frequencies. In this connection it may be mentioned that though the amplitudes of vibration may be considerably altered even by small changes in the potential function, steric arrangement, etc., the frequencies of certain vibrations may be rather insensitive to rather large changes of the sort mentioned. Some measure of the plausibility of the assigned frequencies (at least within a symmetry class) can be obtained by applying the Teller-Redlich product rule. This test has been applied to vibrational assignments made for formamide and will be discussed below after the various assignments have been made.

In view of the difficulties mentioned, the assignment of the vibrational bands to particular vibrations in formamide is weakened by the absence of a normal coordinate

analysis. Such an analysis would be quite difficult because of the large number of force constants and interaction constants needed for an adequate description of the potential function of the molecule. Many of these constants would be extremely difficult to estimate reliably, so that the results of such an analysis would not be entirely free of uncertainty. However, the results of the vibrating mechanical model analysis and other considerations, which are discussed below, do offer a reasonable, although limited, basis for a discussion of the spectra of the formamides.

In discussing the spectrum of formamide it is convenient to divide the normal modes into the four following classes:

- i. The hydrogen stretching vibrations,
- ii. The 1800 to 1250  $\text{cm}^{-1}$  A' vibrations,
- iii. The remaining A' vibrations,
- iv. The A" vibrations.

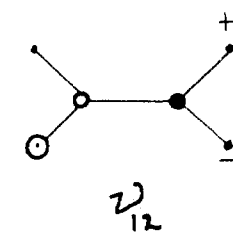
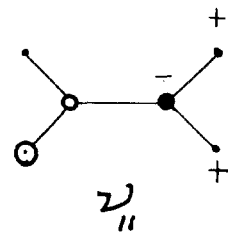
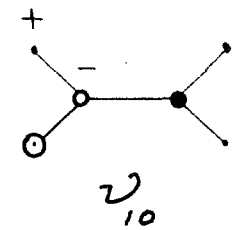
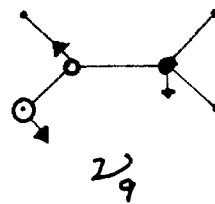
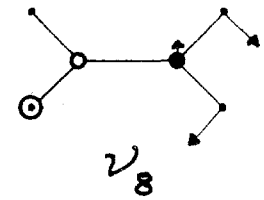
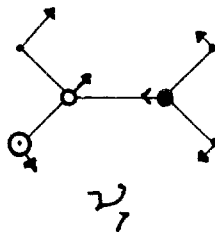
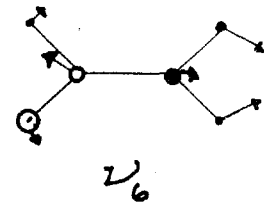
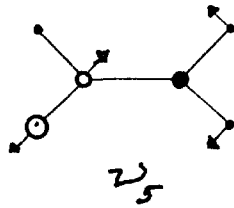
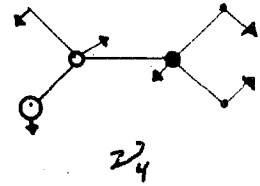
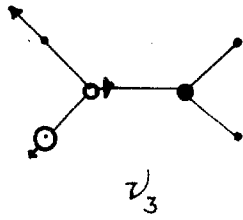
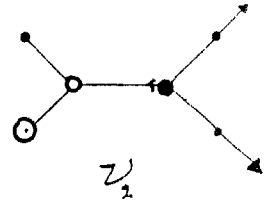
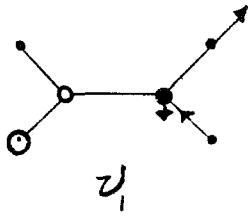
The above grouping separates the vibrational modes of the molecule into fairly well defined sets between which there is little or no interaction. However, some question may arise concerning the vibrations of iii and the lower frequency vibrations of ii. The lowest frequency A' vibration is, very likely, primarily a bending of the OCN angle with a small amount of the  $\text{NH}_2$  rock contributing. The next higher frequency vibration is essentially the  $\text{NH}_2$  rocking vibration. Now, Badger's (37) results with the

vibrating model of acetamide show that the  $\text{NH}_2$  scissors is the only  $\text{NH}_2$  bending deformation contributing to the modes of ii, thus the interaction between the modes of ii and iii should be quite small because of the near-orthogonality of the scissors and the rocking deformations. The extension of these arguments to the case of  $\text{HCOND}_2$  is open to question. It will be recalled that Badger (37) found that in the vibration IIa the scissors deformation of the  $\text{NH}_2$  group in the normal molecule model goes over into the rocking deformation of the  $\text{ND}_2$  group in the deuterated molecule model. Thus the near-orthogonality of the  $\text{NH}_2$  scissors and rocking deformations is destroyed and a geometrical exclusion for interaction between the two modes no longer exists. However, these two vibrations, IIa and the  $\text{ND}_2$  rocking vibration, probably differ by about  $800 \text{ cm}^{-1}$  so that little interaction between them may be expected. The fundamental vibrations of formamide will be named in the conventional manner: the nine in-plane vibrations ( $A'$ ) will be numbered in the order of decreasing frequency from  $\nu'_1$  to  $\nu'_9$ , and the three out-of-plane vibrations from  $\nu'_{10}$  to  $\nu'_{12}$ , also ordered according to decreasing frequency. Figure 16 shows a schematic representation of the normal modes.

The three highest frequency fundamental vibrations are probably well described as the asymmetric  $\text{NH}_2$  stretching vibration, the symmetric  $\text{NH}_2$  stretching vibration, and



Figure 16. Schematic representation of the normal modes of formamide. Small solid circles represent hydrogen atoms.



the CH stretching vibration, respectively. The remaining vibrations must be considered carefully.

$\nu_4$ ,  $\nu_5$ , and  $\nu_7$  are named according to Badger's nomenclature as amide I, IIa, and IIb, respectively. The description of these three frequencies is best made graphically (see Figure 16), however, they are approximately asymmetric and symmetric stretchings of the three heavy atoms (as if they formed a bent triatomic molecule) coupled in different ways with the symmetric (scissors) bending of the  $\text{NH}_2$  group.  $\nu_4$  and  $\nu_5$  are asymmetric stretchings of the heavy atoms with the HNH angle decreasing (or increasing) as the CO distance increases (or decreases) in the mode; and with the HNH angle increasing (or decreasing) as the CO distance increases (or decreases) in the latter mode.  $\nu_7$  is a symmetric stretching of the heavy atoms with the HNH angle decreasing (or increasing) as the CO distance increases (or decreases). The contribution of the bending of the OCH angle has not been determined (37), however it seems that it may contribute appreciably to  $\nu_7$ . If  $\nu_6$  is a localized vibration, then it is primarily an in-plane bending of the tertiary hydrogen atom.  $\nu_6$ , which in the naive assumption of localized vibrations would involve the CH in-plane bend, but which undoubtedly involves the motion of all the atoms of the molecule in some complex manner, will be named amide IIab. The remaining two  $A'$  vibrations are the  $\text{NH}_2$  rock, and the heavy atom bending mode.



The three  $A''$  vibrations are probably well described as the  $\text{NH}_2$  out-of-plane bend, the C-H out-of-plane bend, and the  $\text{NH}_2$  twist.

Figures 17, 18, 19, and 20 present the spectra of gaseous formamide, liquid formamide, gaseous dideuteroformamide, and liquid dideuteroformamide, respectively. Figure 21 is a schematic representation of the 1800 to  $600\text{ cm}^{-1}$  spectra of formamide, and of the spectra of gaseous and liquid N-methylformamide, which will be discussed below. Table 15 lists the observed absorption frequencies for the formamide spectra and the assignments made in the discussion to follow.

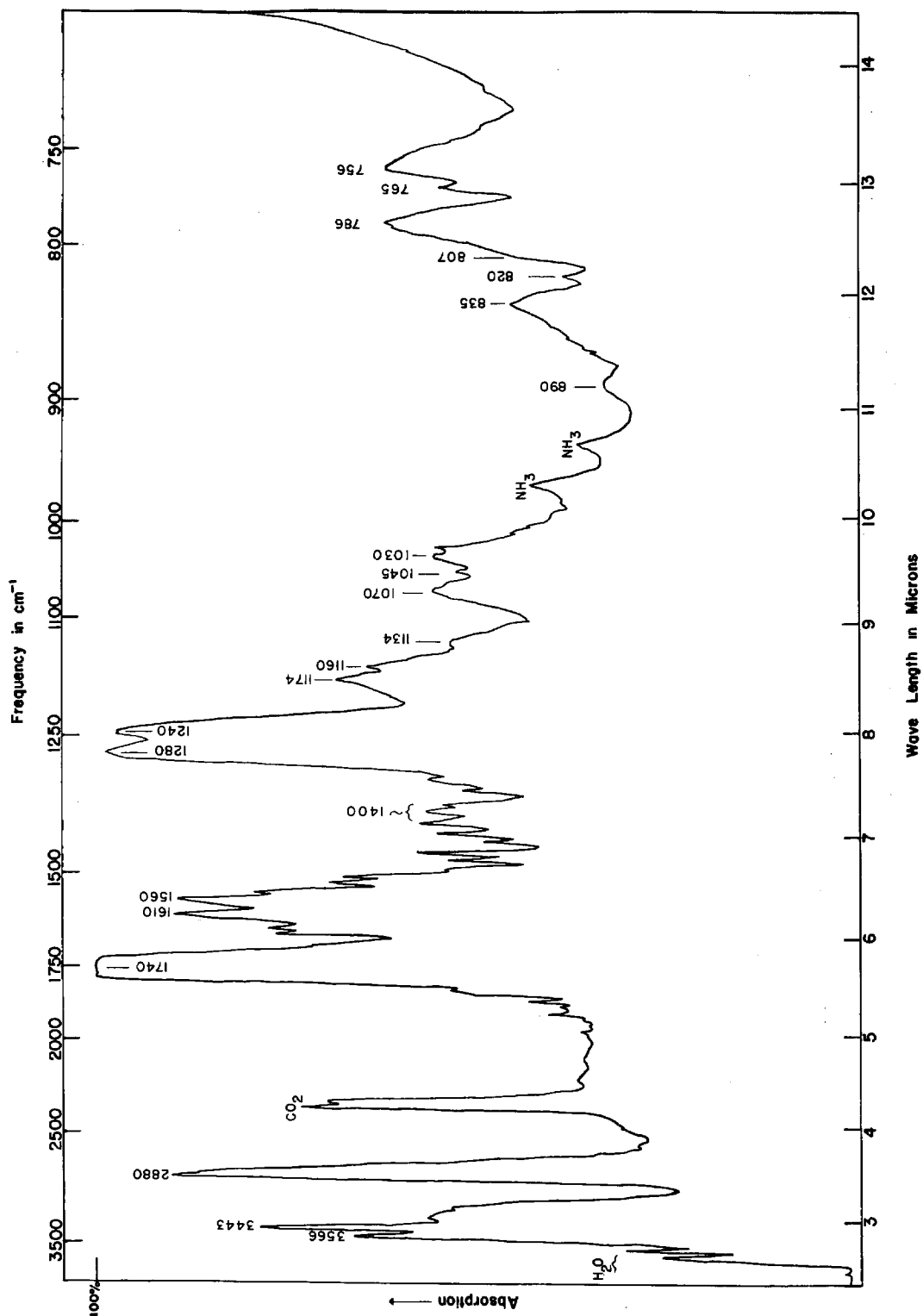


Figure 17. Spectrum of gaseous  $\text{HCONH}_2$ . Path length 80 cm. Temperature approximately  $120^\circ \text{C}$ .

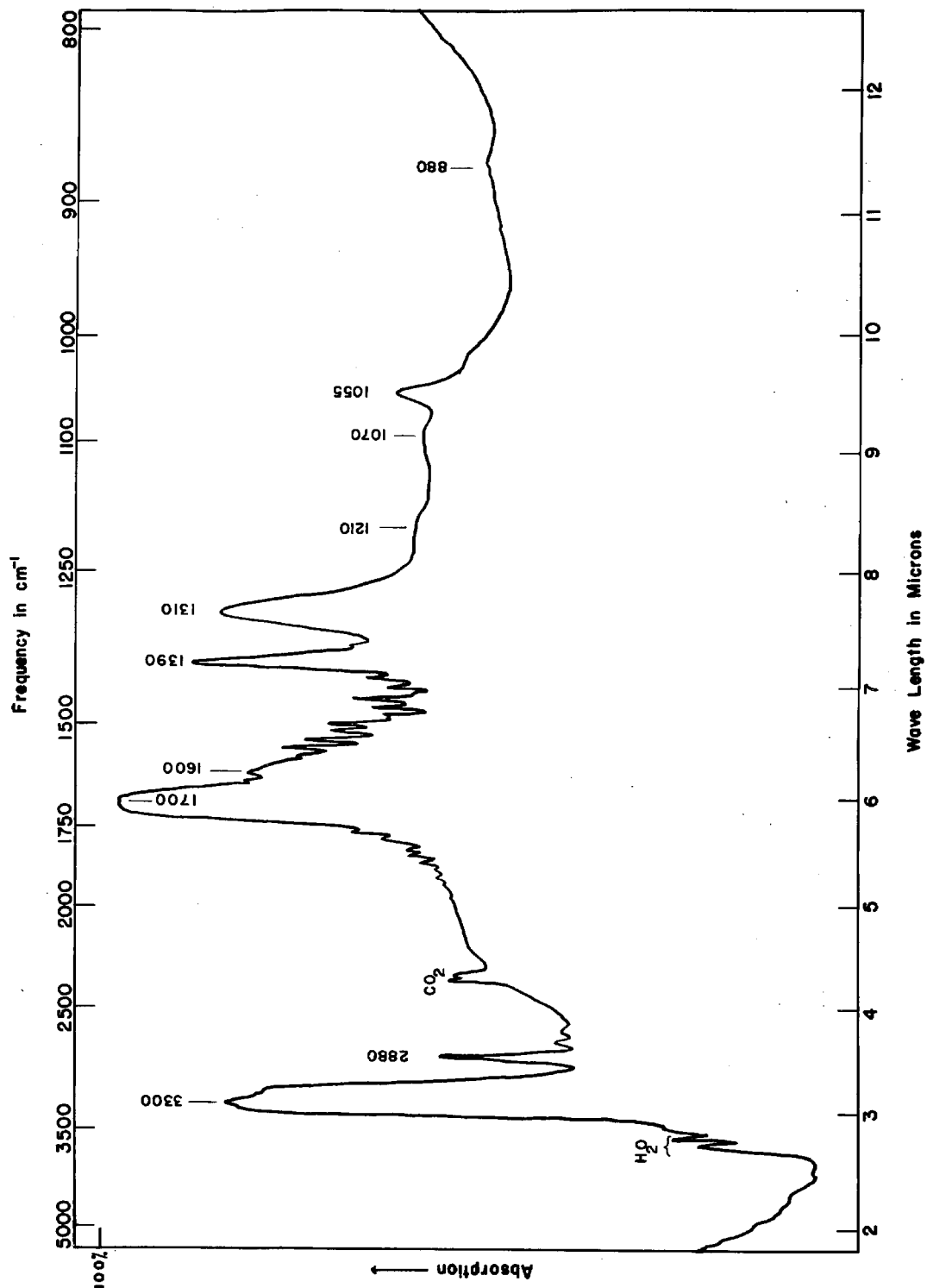


Figure 18. Spectrum of liquid  $\text{HCONH}_2$ .

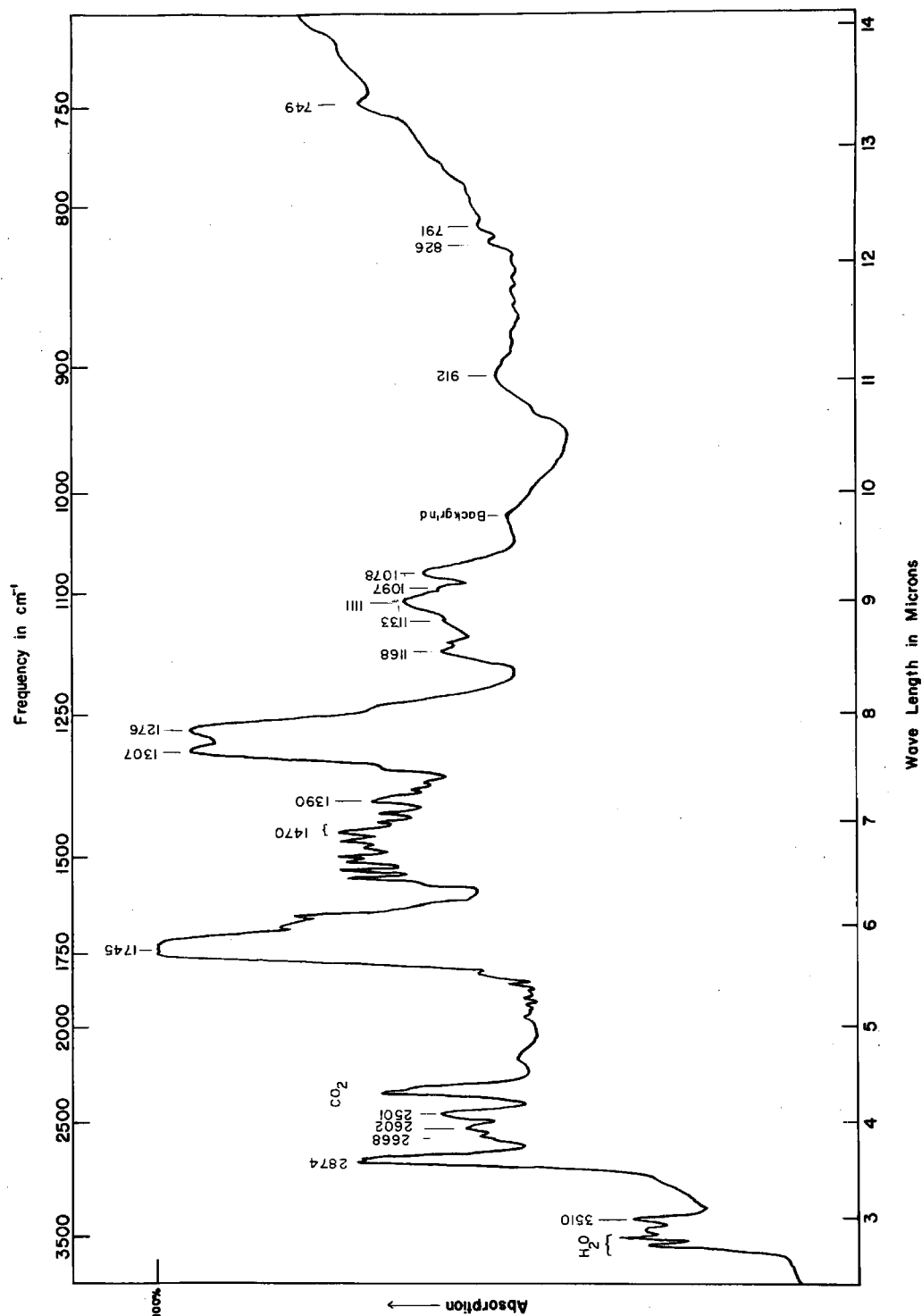


Figure 19. Spectrum of gaseous  $\text{HCOND}_2$ . Path length 80 cm. Temperature approximately  $120^\circ\text{C}$ .

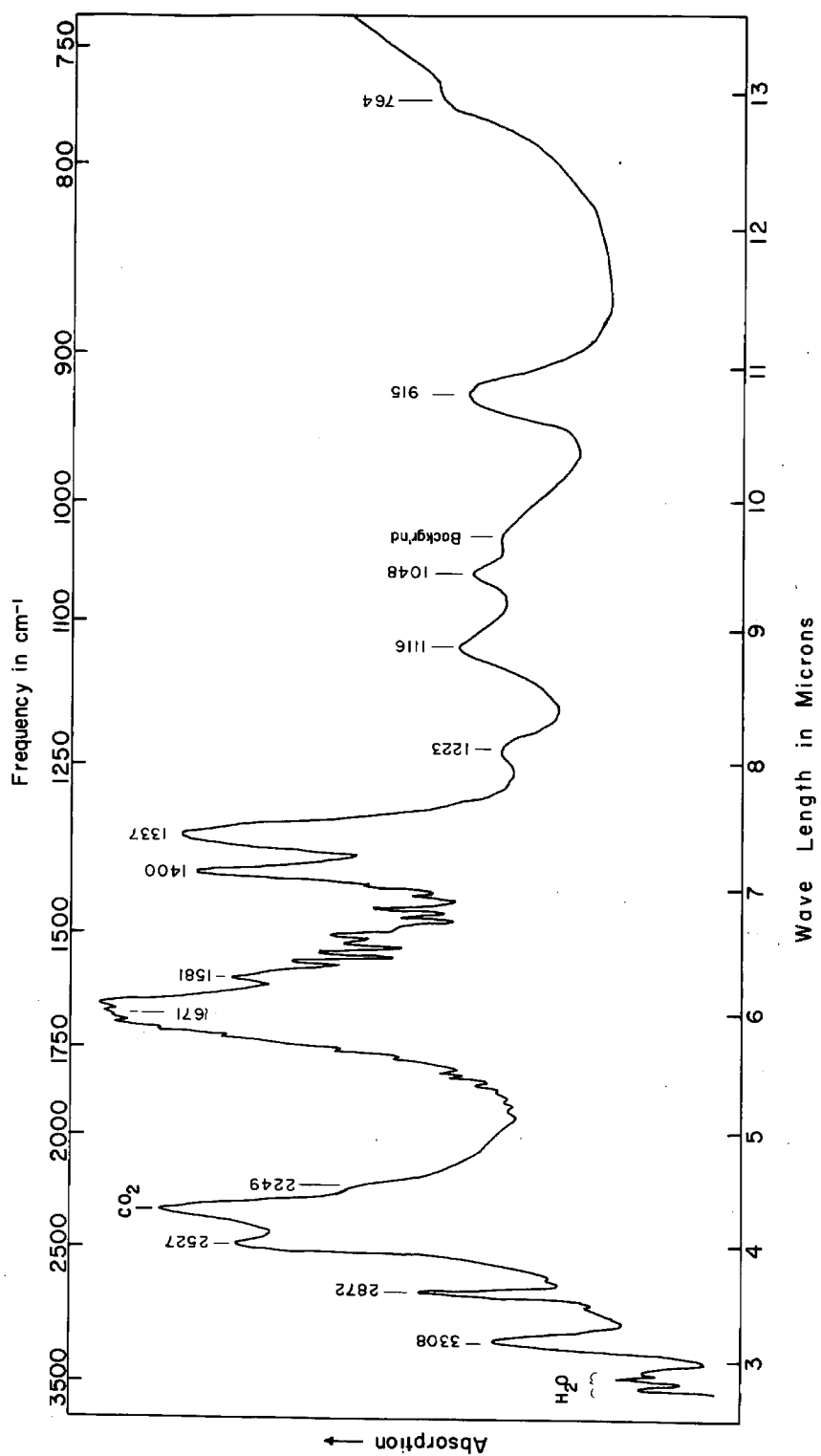


Figure 20. Spectrum of liquid  $\text{HCND}_2$ .



Figure 21. Schematic representation of the spectra of the indicated substances.  
Dashed lines show absorptions that are assigned to the same normal vibration.

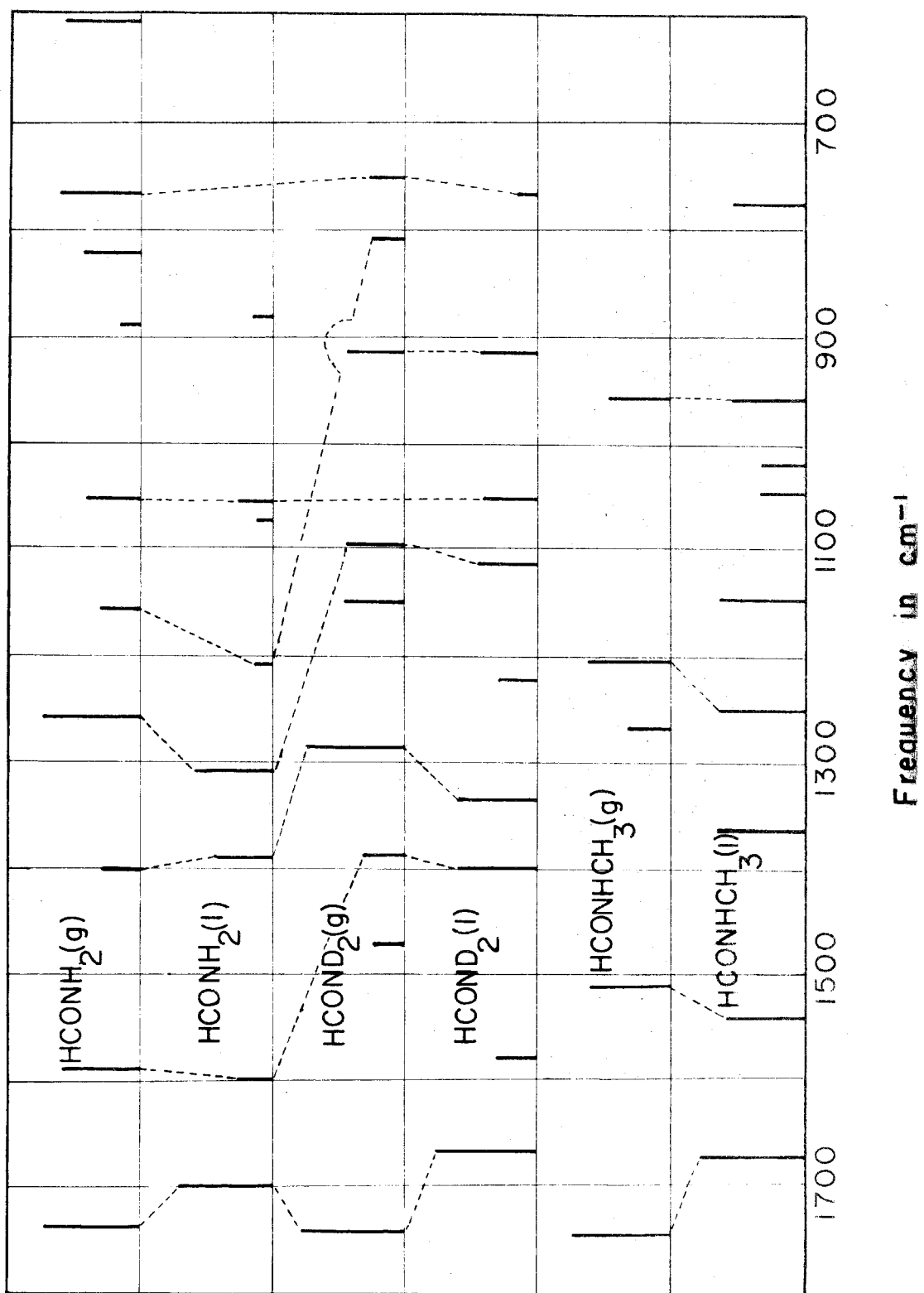




Table 15. Vibrational frequencies ( $\text{cm}^{-1}$ ) of the  
formamides

Assign't	$\text{HCONH}_2(\text{g})$	$\text{HCONH}_2(\text{l})^{\text{c}}$	$\text{HCOND}_2(\text{g})^*$	$\text{HCOND}_2(\text{l})^{*\text{c}}$
A' fundamentals				
$\nu_1$	3566.2 m	3300 <sup>a</sup>	2602 w	2348 <sup>a</sup> s
$\nu_2$	3442.8 m		2501 m	
$\nu_3$	2880 s	2880 w	2874 w	2872 w
$\nu_{4,\text{I}}$	1740 vs	1700 vs	1745 vs	1671 vs
$\nu_{5,\text{IIa}}$	$\left. \begin{matrix} 1610 \\ (1585) \\ 1560 \end{matrix} \right\}^{\text{b}} \text{s}$	1600 w	1390 w	1400 s
$\nu_{6,\text{IIab}}$	1400 w	1390 m	$\left. \begin{matrix} 1307 \\ (1292) \\ 1276 \end{matrix} \right\}^{\text{b}} \text{vs}$	1337 s
$\nu_{7,\text{IIb}}$	$\left. \begin{matrix} 1280 \\ (1260) \\ 1240 \end{matrix} \right\}^{\text{b}} \text{vs}$	1310 s	$\left. \begin{matrix} 1111 \\ 1097 \\ 1078 \end{matrix} \right\}^{\text{b}} \text{m}$	1116 m
$\nu_8$	$\left. \begin{matrix} 1174 \\ 1160 \\ 1134 \end{matrix} \right\}^{\text{b}} \text{m}$	1210 vw ?	$\left. \begin{matrix} 862 \\ (808) \\ 791 \end{matrix} \right\}^{\text{b}} \text{vw}$	---
$\nu_9$	$\left. \begin{matrix} 786 \\ 765 \\ 756 \end{matrix} \right\}^{\text{b}} \text{s}$	---	749 vw	764 vw
A'' fundamentals				
$\nu_{10}$	$\left. \begin{matrix} 1070 \\ 1045 \\ 1030 \end{matrix} \right\}^{\text{b}} \text{m}$	1055 w	---	1048 m
$\nu_{11}$	$\left. \begin{matrix} 835 \\ 820 \\ 807 \end{matrix} \right\}^{\text{b}} \text{m}$	---	590 <sup>**</sup>	---
$\nu_{12}$	$\left. \begin{matrix} 637 \\ 603 \\ 580 \end{matrix} \right\}^{\text{b}} \text{s}$	---	460 <sup>**</sup>	460 <sup>**</sup>

Table 15.--Continued

Assign't	HCONH <sub>2</sub> (g)	HCONH <sub>2</sub> (l) <sup>c</sup>	HCOND <sub>2</sub> (g)*	HCOND <sub>2</sub> (l)* <sup>c</sup>
other absorptions				
$\nu_{7+} \nu_5$	---	---	---	2527 m
$2\nu_7$	---	---	---	2249 w
$2\nu_8$	---	---	---	1581 w
$2\nu_9$	---	---	1470	---
$\nu_{9+} \nu_{12}$	---	---	$\left. \begin{array}{l} 1168 \\ (1150) \\ 1133 \end{array} \right\}^b$	1223 w
?	---	1070 vw	---	---
$2\nu_{12}$	---	---	912 m	915 m
?	890 vw	880 vw	---	---

<sup>a</sup>Maxima of unresolved NH<sub>2</sub>, and ND<sub>2</sub> stretching vibration absorptions are given for the liquid spectra.

<sup>b</sup>Brackets enclose P, Q, R branches of the bands. If no Q branch is observed, the average frequency is presented within parentheses.

\*HCONDH absorption bands assigned were  $\nu_{\text{NH}} = 3510 \text{ cm}^{-1}$  (w),  $\nu_{\text{ND}} = 2668 \text{ cm}^{-1}$  (m).

\*\*Estimated.

<sup>c</sup>The symmetry designations are probably incorrect for the molecular species found in the liquid. The correct designation is quite likely B<sub>u</sub> for the frequencies listed under A'; A<sub>u</sub> for those listed under A"; and overtones are actually combinations of nearly degenerate levels which for the isolated molecules would have the designation listed in the table. These assumptions are based on the evidence found by Badger and Rubalcava (39) which indicated that acetamide, propionamide, and butyramide formed cyclic dimers in CCl<sub>4</sub> solution.

## B. The hydrogen stretching vibrations.

Two well defined absorption maxima are found at 3566.2 and 3442.8  $\text{cm}^{-1}$  in the spectrum of gaseous formamide (see Figures 17 and 25). These two bands exhibit hybrid structure under high dispersion. They have been assigned to  $\nu_1$  and  $\nu_2$ , respectively. This is the frequency range where the  $\text{NH}_2$  stretching vibrations are expected, provided that the NH bond is short.  $\nu_3$ , the CH stretching vibration, falls at the reasonable frequency of 2880  $\text{cm}^{-1}$  in the gas.

In the spectrum of the deuterated gaseous compound (see Figure 19), a mixture of  $\text{HCONH}_2$ ,  $\text{HCONHD}$ , and  $\text{HCOND}_2$ , four new bands appear at 2602, 2501, 3510, and 2668  $\text{cm}^{-1}$ . These have been assigned, respectively, to  $\nu_1$  and  $\nu_2$  in  $\text{HCOND}_2$ , and to  $\nu_{\text{N-H}}$  and  $\nu_{\text{N-D}}$ , the N-H and N-D stretching vibrations in  $\text{HCONHD}$ .  $\nu_3$  undergoes little change in the spectrum of the gaseous deuterated molecule, for it falls at 2874  $\text{cm}^{-1}$ .

The spectrum of liquid formamide shown in Figure 18, shows the expected features that accompany hydrogen bonding. The N-H stretching vibration absorptions form a strong, broad band centered approximately at three microns.

$\nu_3$  remains at 2880  $\text{cm}^{-1}$ .

The spectrum of liquid deuterioformamide, presented in Figure 20, shows five bands above 2000  $\text{cm}^{-1}$ . A weak band at 3308  $\text{cm}^{-1}$  is assigned to an absorption by a small

amount of  $\text{HCONH}_2$  and  $\text{HCONHD}$ . The CH stretching vibration remains at essentially the same frequency as in the spectrum of gaseous  $\text{HCOND}_2$ , for it falls at  $2872 \text{ cm}^{-1}$ . A third band is a strong absorption centered at  $2348 \text{ cm}^{-1}$ . Although this frequency very nearly coincides with the frequency of the  $2349 \text{ cm}^{-1}$  band of  $\text{CO}_2$ , it is quite certain that a strong  $\text{HCOND}_2$  absorption falls very near this frequency, for an examination of the background in this region shows that the observed band is too intense and too wide to be solely attributable to the  $\text{CO}_2$  absorption. The overlapping of the  $\text{CO}_2$  band renders the measurement of the maximum of the absorption band of the  $\text{HCOND}_2$  uncertain by about  $\pm 10 \text{ cm}^{-1}$ . The frequency difference between the maximum of this band the average of the  $\text{ND}_2$  stretching vibration frequencies is within experimental error, the same as the corresponding difference for  $\text{HCONH}_2$ , approximately  $200 \text{ cm}^{-1}$ .

The two remaining bands, at  $2527$  and  $2249 \text{ cm}^{-1}$ , may be assigned to combination levels. They will be discussed below.

The ratio of the  $\text{NH}_2$  to the corresponding  $\text{ND}_2$  stretching frequencies in the gaseous spectra is 1.37. The ratio of the maxima of the absorptions for the corresponding vibrations in the liquid spectra is 1.41.  $\nu_{\text{N-H}}$ , at  $3510 \text{ cm}^{-1}$ , falls almost at the mean frequency of  $\nu_1$  and  $\nu_2$  in gaseous  $\text{HCONH}_2$ ,  $3502 \text{ cm}^{-1}$ . The ratio of  $\nu_{\text{N-H}}$

to  $\nu_{\text{N-D}}$  is 1.32. The nearness of these ratios to the value corresponding to the change upon deuteration of an unperturbed harmonic oscillator, 1.41, may perhaps be taken as evidence that the hydrogen stretching vibrations are nearly localized in the NH bonds, and are very nearly pure stretchings. The smallness of the change in the CH stretching vibration frequency may also be taken as evidence of its simple character.

C. The 1800 to 1250  $\text{cm}^{-1}$   $A'$  vibrations.

The spectral range from 1800 to 1250  $\text{cm}^{-1}$  is very interesting for vibrations of importance in the molecular study of the proteins occurring in this region.

The most striking feature of the spectra of  $\text{HCONH}_2$  and  $\text{HCOND}_2$  is their similarity in appearance in the states studied. Were it not for the weakness of the  $\text{NH}_2$  stretching absorption, and the shifts in frequency one would almost be led to conclude that no deuteration had been made. The four bands in the spectrum of gaseous  $\text{HCONH}_2$  at 1740, 1585, 1400, and 1260  $\text{cm}^{-1}$  have been assigned to Amide I, IIa, IIab, and IIb ( $\nu_4$ ,  $\nu_5$ ,  $\nu_6$ , and  $\nu_7$ ), respectively. Figure 21 indicates the correlation of these absorption maxima with those of the other three formamide spectra.

The overlapping of the 6 micron water band causes an uncertainty in the measurement of the band at 1400  $\text{cm}^{-1}$  in the spectrum of gaseous  $\text{HCONH}_2$ , and in the measurement of the bands at 1470 and 1390 in the spectrum of gaseous  $\text{HCOND}_2$ .

The assignment of the band found at 1400  $\text{cm}^{-1}$  in the spectrum of gaseous  $\text{HCONH}_2$ , and at 1390  $\text{cm}^{-1}$  in the spectrum of the liquid to Amide IIab finds support in the following facts. Kohlrausch and Köppl (40) found a band at approximately 1390  $\text{cm}^{-1}$  in the spectra of several aldehydes, and not in the spectra of several ketones. They

assigned this band to the HCO bending vibration of the aldehydes. Newman (41), examining the spectrum of crystalline sodium formate,  $\text{NaHCO}_2$ , with polarized radiation found a band at  $1365\text{ cm}^{-1}$ , which he assigned to the CH in-plane bending vibration of the formate ion.

The scissors deformation of the  $\text{NH}_2$ , and of the  $\text{ND}_2$  probably contribute appreciably to normal mode IIab for both the normal and the deuterated molecules, thus the frequency of this vibration would be expected to change upon deuteration. The absorptions at  $1292\text{ cm}^{-1}$  in the spectrum of gaseous  $\text{HCOND}_2$ , and at  $1337\text{ cm}^{-1}$  in the spectrum of liquid  $\text{HCOND}_2$  have been assigned to Amide IIab.

D. The A' vibrations below  $1250\text{ cm}^{-1}$ .

Two A' vibrations have not been accounted for in the above discussion. These vibrations,  $\nu'_8$  and  $\nu'_9$ , are probably well described as the  $\text{NH}_2$  rocking vibration, and as the OCN bending vibration. The bands at  $1160$ ,  $1210$  and  $808\text{ cm}^{-1}$  in the spectra of gaseous  $\text{HCONH}_2$ , of liquid  $\text{HCONH}_2$ , and of gaseous  $\text{HCOND}_2$ , respectively, have been assigned to  $\nu'_8$ . The higher frequency of this band in liquid  $\text{HCONH}_2$  than in gaseous  $\text{HCONH}_2$  is consistent with its assignment to a bending mode of the  $\text{NH}_2$  group, since hydrogen-bending generally causes an increase in the frequency of modes involving a bending motion of the hydrogen atoms. The shift in frequency of this vibration on deuteration to  $808\text{ cm}^{-1}$  is consistent with the idea that this vibration is primarily an  $\text{NH}_2$  rocking motion. The higher intensity of  $\nu'_8$  in the spectrum of gaseous  $\text{HCONH}_2$  than in the spectrum of liquid  $\text{HCONH}_2$  suggests that the intensity of this band should be very low in the spectrum of liquid  $\text{HCOND}_2$ , since the intensity of  $\nu'_8$  in the spectrum of gaseous  $\text{HCOND}_2$  is quite low. The deuterium atoms very probably have a smaller amplitude of vibration than the hydrogen atoms in this mode, thus it is not surprising that  $\nu'_8$  is less intense in the spectra of  $\text{HCOND}_2$  than in the spectra of  $\text{HCONH}_2$ .

The bands at  $765$ ,  $749$  and  $764\text{ cm}^{-1}$  in the spectra of gaseous  $\text{HCONH}_2$ , of gaseous  $\text{HCOND}_2$  and of liquid  $\text{HCOND}_2$ ,



respectively, have been assigned to  $\nu_9$ . The relatively small change in frequency of this vibration upon deuteration indicates little contribution of the motion of the hydrogen or deuterium atoms to the form of the normal mode.

E. The A" vibrations.

The bands at 1045, 1055, and 1048  $\text{cm}^{-1}$  in the spectra of gaseous  $\text{HCONH}_2$ , of liquid  $\text{HCONH}_2$ , and of liquid  $\text{HCOND}_2$ , respectively, have been assigned to  $\nu'_{10}$ , the CH out-of-plane bending vibration. This assignment finds support in the relative constancy of the bands, and in Newman's (41) observations on crystalline sodium formate. He made the corresponding assignment to a band appearing at 1070  $\text{cm}^{-1}$ . The difference between this latter frequency and the frequencies of this vibration in the various formamide spectra is not large if account is taken of the difference in state and in nature of the substances in question.

The band centered at 820  $\text{cm}^{-1}$  in the spectrum of gaseous  $\text{HCONH}_2$  has been assigned to  $\nu'_{11}$ , the out-of-plane  $\text{NH}_2$  bending vibration (wag). The frequency of this vibration probably shifts to about 590  $\text{cm}^{-1}$  ( $820/\sqrt{2} = 582 \text{ cm}^{-1}$ ) upon deuteration, if, as expected, the vibration is primarily a motion of the amino hydrogen or deuterium atoms.

The band observed at 603  $\text{cm}^{-1}$  in the spectrum of gaseous  $\text{HCONH}_2$  has been assigned to  $\nu'_{12}$ , the  $\text{NH}_2$  twisting mode. Although considerable difficulty was experienced in obtaining this 15 to 25 micron spectrum, the presence of a band at 603  $\text{cm}^{-1}$  is probably real, since it finds support in the work of Saksena (42). He mentions a shift at 603  $\text{cm}^{-1}$  in the Raman spectrum of liquid formamide. The twisting modes in ethane and ethylene (Ref. 11, p. 343, and p. 328)

are given as falling at 275 and 825  $\text{cm}^{-1}$ , respectively. The intermediate value of the frequency in formamide may well be an indication of the partial double bond character of the CN bond in the molecule.

F. Remaining absorption bands.

A number of absorption bands in the spectra of the formamides have yet to be discussed. The spectra of gaseous, and of liquid  $\text{HCONH}_2$  show only two sets of bands for which no assignment has been made. The two bands at 1070 and 880  $\text{cm}^{-1}$  in the spectrum of the liquid, and the band at 890  $\text{cm}^{-1}$  in the spectrum of the gas do not seem to fit any simple assignment pattern.

The spectra of liquid, and of gaseous  $\text{HCOND}_2$  show several bands which fit binary combinations as shown in Table 15. The two bands at 2527 and 2249  $\text{cm}^{-1}$  in the spectrum of the liquid have been assigned  $\nu_7 + \nu_5$  (2516  $\text{cm}^{-1}$ ), and to 2  $\nu_7$  (2232  $\text{cm}^{-1}$ ), respectively. Badger and Rubalcava (43) made similar assignments in a study of the three micron, high dispersion spectrum of propionamide in carbon tetrachloride solution.

G. Some summarizing comments.

The assignments made above have been examined with the aid of the Teller-Redlich product rule (Ref. 11, p. 232), as applied to the A' vibrations of  $\text{HCONH}_2$  and  $\text{HCOND}_2$ .

$$\prod_{i=1}^9 \frac{\omega_i'}{\omega_i} = \sqrt{\left(\frac{m_H}{m_D}\right)^4 \left(\frac{47}{45}\right)^2 \left(\frac{I_z'}{I_z}\right)} = 0.278 \quad (1)$$

Equation (1) expresses the Teller-Redlich product rule. The primed quantities refer to  $\text{HCOND}_2$ , and the unprimed quantities to  $\text{HCONH}_2$ . 47/45 is the ratio of the mass of  $\text{HCOND}_2$  to the mass of  $\text{HCONH}_2$ . The other symbols have their usual significance. The pertinent details of the calculation of the moments of inertia are given in Appendix 4. Since the zero order frequencies,  $\omega_i$ , are not known, the observed frequencies,  $\nu_i$ , have been used.

The value of  $\prod_{i=1}^9 \frac{\nu_i'}{\nu_i}$  using the assignments shown in Table 15 for the gases is 0.255. Compared with the value 0.278, the former value seems acceptable, particularly since approximations are present in replacing the  $\omega_i$  with the  $\nu_i$ , and in the values of the moments of inertia. The Teller-Redlich product rule does not help distinguish, in this case, among the various assignments within a symmetry species, i.e. two assignments can be interchanged without affecting the value of the product of the ratios of the

vibrations of that species. However, it does help find gross inconsistencies which may be present in a given set of vibrational assignments. The correlations shown in Figure 21 for  $\nu'_5$  and for  $\nu'_8$  (1097 and 808  $\text{cm}^{-1}$  in the spectrum of gaseous  $\text{HCOND}_2$ ) were obtained in this manner from a previous assignment scheme.

The separation of the maxima of the P and R branches of the absorption bands of gaseous  $\text{HCONH}_2$  was calculated according to the method given in Appendix 1, and found to be 40  $\text{cm}^{-1}$ . The observed values, see Table 15, are not seriously different from the calculated value. The spacing was an aid in finding the centers of overlapping absorption bands in the spectra of the gases.

H. The vibrational spectra of gaseous and liquid  
N-methylformamide.

N-methylformamide,  $\text{HCONCH}_3$ , has 21 fundamental vibrations. The molecule, neglecting the methyl hydrogens, very likely possesses a plane of symmetry coinciding with the  $\text{HCONH}$  group. If the assumption is made that the methyl hydrogens are symmetrically disposed about this plane of symmetry, then the molecule will belong to the symmetry point group  $C_s$ , and 14 fundamental vibrations will be totally symmetric (species  $A'$ ), and 7 vibrations will be antisymmetric with respect to the plane of the molecule (species  $A''$ ).

The following discussion of the vibrations and their implications will be divided into three sections: 1) the hydrogen stretching vibrations, 2) the fundamental vibrations absorbing in the region from  $1800$  to  $1200\text{ cm}^{-1}$ , and 3) the vibrations absorbing below  $1200\text{ cm}^{-1}$ . Combination levels will be discussed along with the fundamentals near which they absorb.

The spectra of gaseous and liquid N-methylformamide have been observed in the rock salt region, and are presented in Figures 22 and 23. (A summary of the spectra between  $1800$  and  $600\text{ cm}^{-1}$  has been presented in Figure 21.) Table 16 lists the observed absorption maxima, and their assignments.

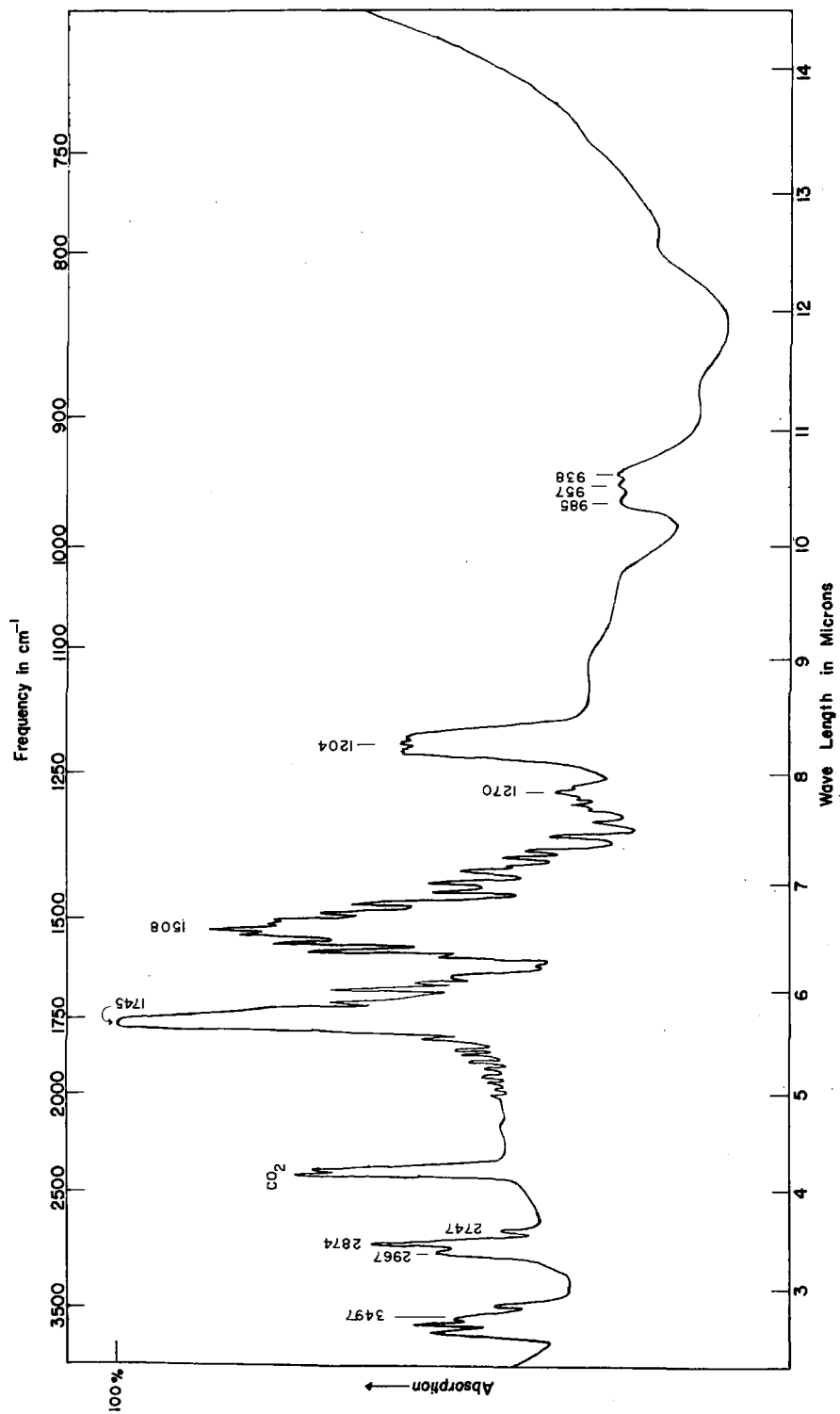


Figure 22. Spectrum of gaseous  $\text{HCONHCH}_3$ . Path length 80 cm. Temperature approximately 120° C.



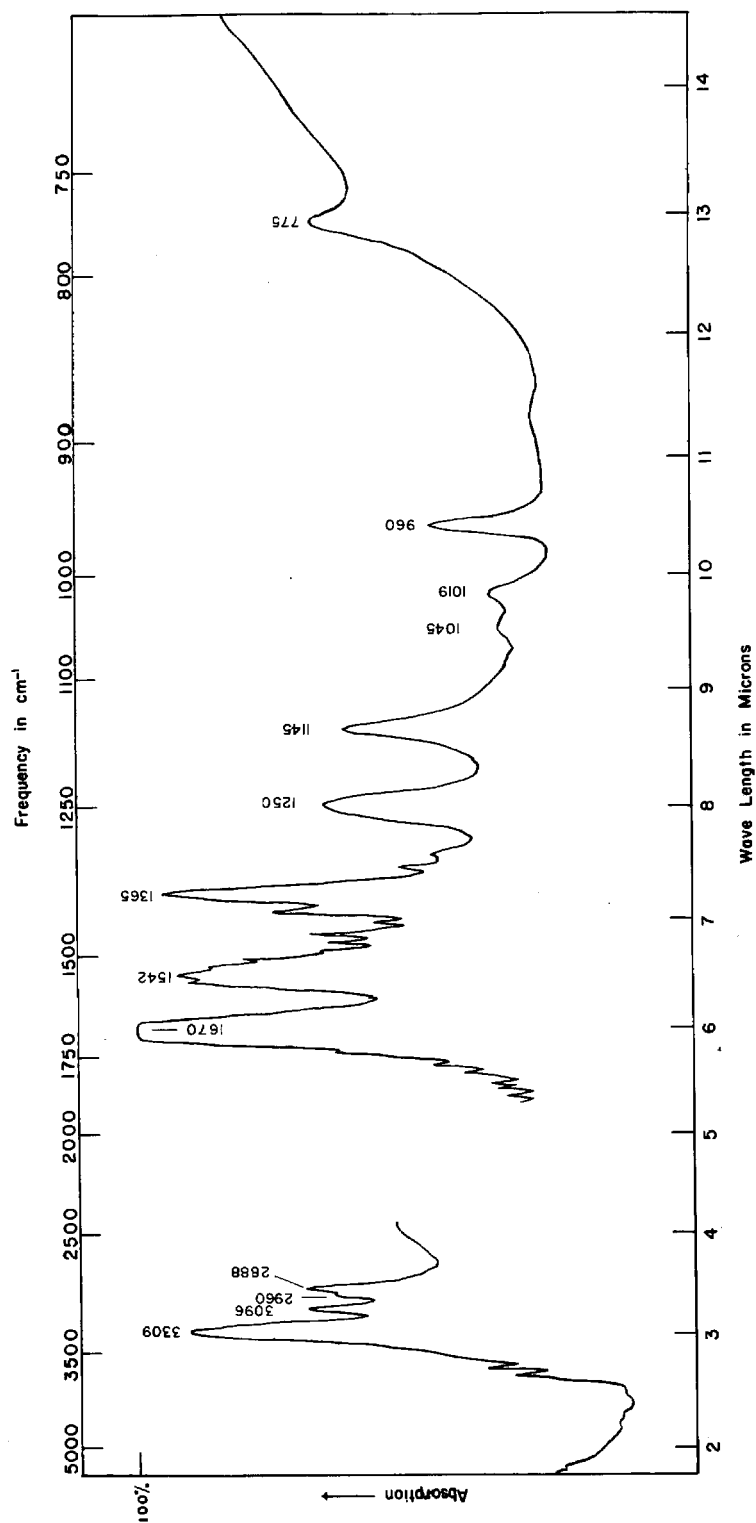


Figure 23. Spectrum of liquid  $\text{HCONHCH}_3$ .

Table 16. Frequencies, in  $\text{cm}^{-1}$ , of absorption bands in gas and liquid N-methylformamide.

Assign't.	Gas	Liq.	Comments
$\nu_{\text{N-H}}$ ( $a'$ )	3497 (w)	3309* (s)	
$2\nu_{\text{IIa}}$ ( $A'$ )	---	3096 (m)	
$\nu_{\text{CH}_3}$	2967 (w)	2960 (w)	$a'$ or $a''$ ?
$\nu_{\text{C-H}}$ ( $a'$ )	2874 (m)	2888 (m)	
?	2747 (vw)	---	$1508 + 1270 = 2778$ ?
Amide I ( $a'$ )	1745 (vs)	1670 (vs)	
Amide IIa ( $a'$ )	1508 (s)	1540 (s)	
$\nu_{\text{CH}}$ ( $a'$ )	---	1365 (s)	CH in-plane bend.
$\nu_{\text{CH}_3}$ ( $a'$ )	1270 (w)	---	$\text{CH}_3$ bending mode?
Amide IIb ( $a'$ )	1204 (s)	1250 (s)	
?	---	1145 (s)	$\text{CH}_3$ mode
$\nu_{\text{CH}}$ ( $a''$ )	---	1045 (w)	CH out-of-plane bend.
?	---	1019 (w)	
	(985 )		
$\nu_{\text{N-CH}_3}$ ( $a'$ )	(957 ) (m) (938 )	960 (m)	
$\nu_{\text{NH}}$ ( $a''$ )	---	775 (m)	NH out-of-plane bend.

\* Several different transitions contribute to this unresolved band.

1. The hydrogen stretching vibrations.

The bands at 3497, 2967, and 2874  $\text{cm}^{-1}$  in the spectrum of the gas are assigned to fundamental hydrogen stretching vibrations. The band at 2747  $\text{cm}^{-1}$  is assigned to a combination band.  $\nu_{\text{N-H}}$  at 3497  $\text{cm}^{-1}$  nearly falls at the mean frequency, 3502  $\text{cm}^{-1}$ , of the two  $\text{NH}_2$  vibrations in formamide. This suggests that the NH bond in N-methylformamide is like the NH bonds in formamide, and that the former molecule is planar about the amide nitrogen atom. In this connection it is interesting to note that the difference between the NH stretching frequency in the gas and the frequency of the maximum of the band assigned to the NH stretching vibration in the spectrum of the liquid is nearly the same for both formamide and N-methylformamide. This similarity suggests a similarity in the O-N-H...O-N-H part of the hydrogen bonded structure of the two molecules. In particular, one might expect that the NH stretching force constants are approximately equal for the two molecules in corresponding states. This may imply, though not necessarily, that the N...O distance is the same in both cases.

The two bands at 2967 and 2874  $\text{cm}^{-1}$  are assigned to a  $\text{CH}_3$  and to the CH stretching vibrations, respectively. On the basis of the methyl halide spectra (Ref. 11, p. 315) the assignment of the 2967  $\text{cm}^{-1}$  band might well be made to the  $\text{A}' \text{CH}_3$  vibration. However an examination of other  $\text{CH}_3\text{X}$  vibrational assignments (Ref. 11, p. 333 and 335, for

example) indicates that it might also be an A" CH<sub>3</sub> absorption band. The band at 2874 cm<sup>-1</sup> lies at nearly the same frequency as in the spectrum of gaseous formamide (2880 cm<sup>-1</sup>). The band at 2247 cm<sup>-1</sup> most likely arises from a combination level. The binary combination 1508 + 1270 = 2778 cm<sup>-1</sup> fits nicely.

The spectrum of the liquid shows four bands at 3309, 3096, 2960, and 2888 cm<sup>-1</sup>. The highest frequency band has been assigned to the NH stretching mode in the hydrogen bonded liquid. The 2960 and 2888 cm<sup>-1</sup> bands are assigned to the CH<sub>3</sub> A' stretching vibration, and the CH stretching vibration. The band at 3096 cm<sup>-1</sup> seems at too high a frequency to be a CH<sub>3</sub> vibration. A plausible assignment is as the first overtone of the band at 1540 cm<sup>-1</sup>. This assignment is in agreement with the similar suggestion made by Badger and Rubalcava (43).

## 2. The 1800 to 1200 cm<sup>-1</sup> frequencies.

Professor Badger has studied the vibrational modes of N-methylformamide in this region with the aid of his mechanical vibrating model (37).<sup>\*</sup> A reproduction of his results is shown in Figure 24. Again, as with the amides, the vibrations involving the amide atoms have no simple description. The CO stretching vibration does not exist

---

<sup>\*</sup>This model does not show CH<sub>3</sub> vibrations.

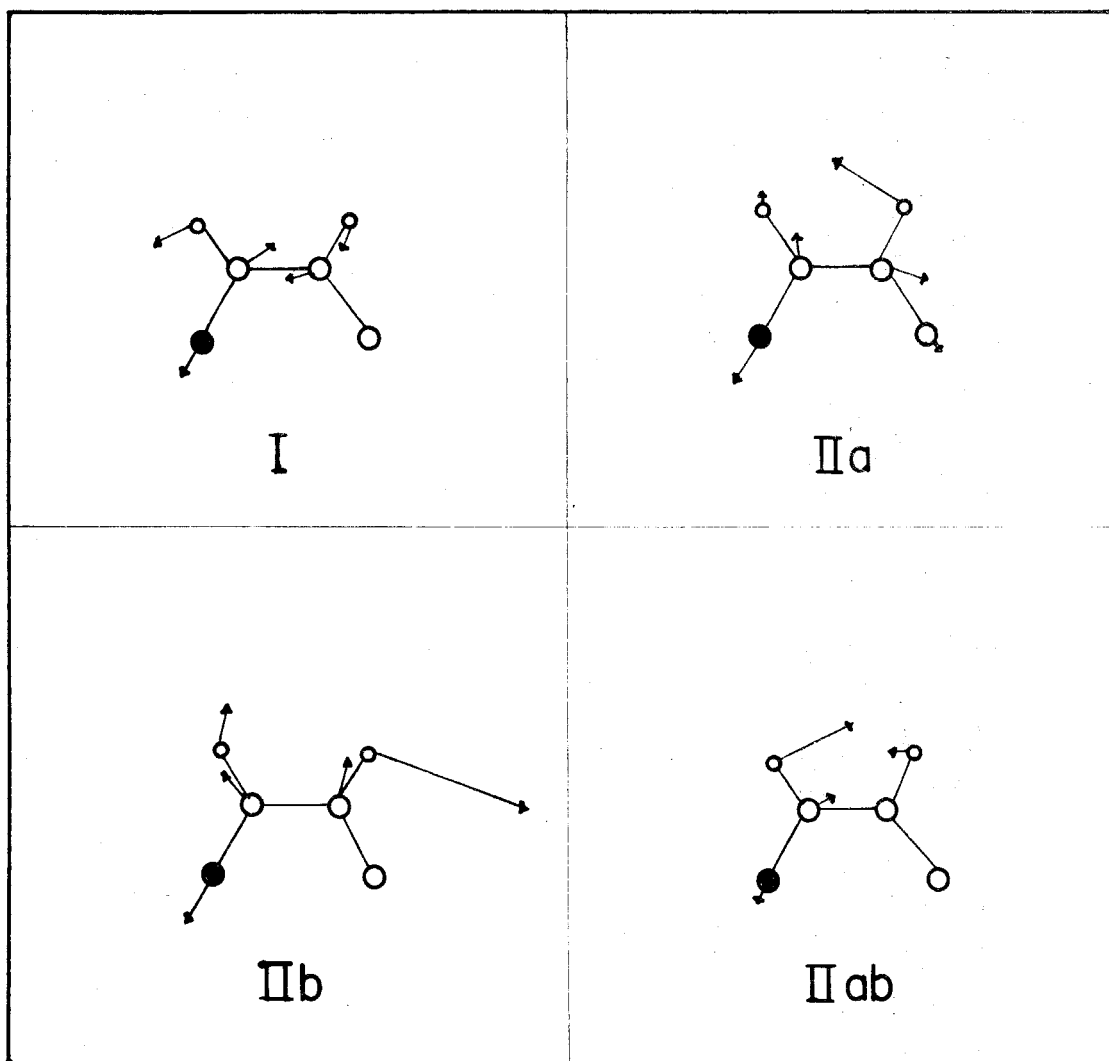


Figure 24. Form of indicated normal vibrations of  $\text{HCONHCH}_3$  (taken from reference (37)). Vibration labeled IIab is the CH in-plane bend. Large solid circle represents the oxygen atom.

as such, but rather it is an asymmetric stretch of the OCN group coupled with an NH bend and a CH bend. Similarly involved descriptions apply to the other amide frequencies in this spectral region.

A comparison of the liquid and gaseous spectra is of particular value in making vibrational assignments for a substance such as N-methylformamide, since the effects of hydrogen bonding will lead to certain frequency shifts which may be qualitatively predicted with a fair degree of reliability. It seems very reasonable to assume that the contribution of the ionic resonance configuration of an amide (see I of Figure 15) will be greater in the liquid than in the gas. Hydrogen-bonding will bring the molecules together in such a way that there can be an electrostatic interaction between the negative charge on the oxygen atom, and the induced positive charge on the hydrogen (or hydrogens) adjacent to the nitrogen atom. This interaction will lead to the stabilization of the resonance configuration. Thus the effects of hydrogen-bonding will weaken the CO and the NH stretching force constants, and strengthen the amide CN stretching force constant and the NH bending force constants. The CH force constants should remain essentially unchanged. The overall effect of hydrogen bonding on any frequency is thus complicated, and difficult to predict or explain unless the results of a normal coordinate treatment are available, because the frequency of any vibration is, in

general, dependent on all the force constants of the molecule. Predictions can be made with some success for those vibrations in which the motion is well localized in some particular set of atoms.

The bands at 1745, 1508, and  $1204\text{ cm}^{-1}$  in the spectrum of the gas are assigned to Amide I, IIa, and IIb, respectively. These bands are shifted, respectively to 1670, 1540, and  $1250\text{ cm}^{-1}$  in the spectrum of the liquid. The band at  $1365\text{ cm}^{-1}$  in spectrum of the liquid is assigned to the CH in plane bending vibration.

The observed differences in frequency between the gaseous and liquid spectra of Amide I, IIa, and IIb are consistent with the above discussion of the effects of hydrogen-bonding. The band at  $1365\text{ cm}^{-1}$  in the spectrum of the liquid behaves like the corresponding absorption in  $\text{HCONH}_2$ , i.e. it is very weak or absent in the spectrum of the gas, and of medium strength in the liquid spectrum. The increase in intensity may well arise from the increased contribution of the ionic resonance configuration and the contribution of the motion of the heavy atoms to this vibration (see Figure 24). The motion of the heavy atoms is not unlike an asymmetric stretch, so that a large charge transfer may be expected. This effect would be more pronounced in the liquid than in the gas because of the increased contribution of the ionic configuration to the equilibrium structure of the molecule.

The band at  $1204\text{ cm}^{-1}$ , in the spectrum of the gas, rather than the band at  $1270\text{ cm}^{-1}$ , is assigned to Amide IIb on the basis of the relative intensities of the two absorptions, and on the reasonable assumption that Amide IIb will be found at a higher frequency in the spectrum of the liquid than in the spectrum of the gas. The band at  $1270\text{ cm}^{-1}$  may possibly be assigned to a  $\text{CH}_3$  deformation mode.

3. The vibrations below  $1200\text{ cm}^{-1}$ .

The band at  $957\text{ cm}^{-1}$ , with P and R branch maxima at  $985$  and  $938\text{ cm}^{-1}$ , has been assigned to a mode which is largely a stretching of the non-amide CN bond. This band apparently remains essentially unshifted in the liquid spectrum, where it falls at  $960\text{ cm}^{-1}$ .

Four bands remain in the spectrum of the liquid. These are found at  $1145$ ,  $1045$ ,  $1020$ , and  $775\text{ cm}^{-1}$ . The last of these may be assigned to the  $\text{A}''$  NH bend, which Sutherland has found to lie in this region in a number of molecules (44). The band at  $1045\text{ cm}^{-1}$  is assigned to the  $\text{A}''$  CH bend, in essential agreement with the assignment made for the formamides. No assignment is proposed for the bands at  $1145$  and  $1020\text{ cm}^{-1}$  although they may possibly correspond to  $\text{CH}_3$  bending vibrations.



I. Concluding remarks.

The above presentation and discussion of the several formamide spectra have shown a reasonably consistent scheme of vibrational assignments. Spectral evidence, based on the NH stretching vibration frequencies, has been presented as additional support for the hypothesis of the planarity of the amide group. The data of this study, together with Professor Badger's (37) experiments with vibrating mechanical models of acetamide and N-methylformamide, and Dr. R. Newman's (41) excellent investigation of the spectrum of crystalline sodium formate have formed a basis for a straightforward interpretation of the spectra of these simple amides. The possible effects of the motions of the formyl hydrogen have been discussed. These are important, for an understanding of their contribution to the normal vibrations of these "simple" molecules is necessary, if the amide vibrations themselves are to be understood. Such an understanding is of prime importance in the study of the proteins.

The differences between the spectra of the gas and of the liquid for each substance have been discussed with relation to the effects of hydrogen-bonding in the liquid.

## Appendix 1

Calculation of the separation of the maxima of the P and R branches of a parallel band in cyanamide. The method used is that given by Gerhard and Dennison (12). Equation (1) gives the separation,

$$\Delta \nu = \frac{S(\beta)}{\pi} \left( \frac{kT}{I_C} \right)^{\frac{1}{2}} . \quad (1)$$

The various quantities are defined below

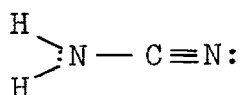
$$\begin{aligned} \log S &= \frac{0.721}{(\beta + 4)^{1.13}} , \\ &= \frac{I_C - I_A}{I_A} . \end{aligned}$$

$I_C$  and  $I_A$  are the largest and the smallest moments of inertia of the molecule, respectively.  $k$  is Boltzmann's constant. The temperature,  $T$ , is taken as  $390^\circ\text{K}$  ( $117^\circ\text{C}$ ). Using the values of Appendix 2 for the moments of inertia, and evaluating equation (1),  $28 \text{ cm}^{-1}$  is obtained for  $\Delta \nu$ .

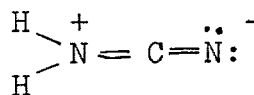
## Appendix 2

Moments of inertia for a model of cyanamide.

The two resonating configurations I and II are considered.



I



II

The following molecular parameters are used:

$$r(\text{C} - \text{N}) = 1.51 \text{ \AA}$$

$$r(\text{C} = \text{N}^-) = 1.31 \text{ \AA}$$

$$r(\text{N}^+ = \text{C}) = 1.26 \text{ \AA}$$

$$r(\text{C} \equiv \text{N}) = 1.15 \text{ \AA}$$

$$r(\text{N} - \text{H}) = 1.015 \text{ \AA}$$

$$\alpha = 123^\circ$$

The CN bond distances are taken from Schomaker and Stevenson's compilation (25); and the formal charge correction is made according to Pauling (26). The ammonia N-H bond distance has been used. The resultant bond distances are calculated by the method given by Pauling (Ref. 26, p. 197). An approximate wave function for the molecule will be given by equation (1)

$$\Psi = a \Psi_{\text{I}} + b \Psi_{\text{II}} \quad (1)$$

Rather arbitrarily, the values  $a = \sqrt{2/3}$ , and  $b = \sqrt{1/3}$  are assigned to  $a$  and  $b$ . It may well be that  $a = b = 1/2$  is better, however, this will have little effect on the average value of the two small rotational constants, which is needed in order to obtain  $A_e''$ , from the analysis of the spacing of the rotational lines in  $\nu_5$ . The resultant bond length is given by equation (2)

$$R = \frac{\sum x_i k_i R_i}{\sum x_i k_i} \quad (2)$$

$x_1 = a^2$ , and  $x_2 = b^2$ . The  $K$ 's are taken in the ratio  $k_1 : k_2 : k_3 = 1:3:6$ .

Using the above relations the following are obtained:

$$R_{NC} = \frac{2/3(1.51) + 1/3(3)(1.26)}{2/3(1) + 1/3(3)} = 1.36 \text{ \AA}$$

$$R_{CN} = \frac{2/3(6)(1.15) + 1/3(3)(1.31)}{2/3(6) + 1/3(3)} = 1.18 \text{ \AA}$$

These values lead to the following moments of inertia and rotational constants

$$\begin{aligned} I_A &= 2.63 \times 10^{-40} \text{ gm cm}^2 & A_e'' &= 10.66 \text{ cm}^{-1} \\ I_A &= 85.16 \times 10^{-40} \text{ gm cm}^2 & B_e'' &= 0.329 \text{ cm}^{-1} \\ I_C &= 87.79 \times 10^{-40} \text{ gm cm}^2 & C_e'' &= 0.319 \text{ cm}^{-1} \\ & & \frac{B_e'' + C_e''}{2} &= 0.324 \text{ cm}^{-1} \end{aligned}$$

### Appendix 3

The three micron band of formamide under high dispersion.

The three micron band of formamide has been examined under high dispersion, and is presented in Figure 25. The band shows two major features, each corresponding to vibrational-rotational transitions of the antisymmetric and the symmetric  $\text{NH}_2$  stretching vibrations. The band for the antisymmetric vibration is centered at  $3566.20 \text{ cm}^{-1}$ , and the band for the symmetric vibration is centered at  $3442.83 \text{ cm}^{-1}$ . Both bands, as expected, show hybrid structure.

The rotational structure of the high frequency band has been measured. The assignments and combination relations are presented in Table 17. An extrapolation of the combination relations to  $K^2 = 0$  gives a value of  $A'' - \bar{B}'' = 2.076 \text{ cm}^{-1}$ . However, there is considerable uncertainty in this value because the values of  $A'' - \bar{B}''$  scatter rather seriously when plotted against  $K^2$ . It is interesting to note that the mean value of  $A'' - \bar{B}''$  averaged over its values from  $K = 4$  to  $K = 11$  is  $2.07_{15} \text{ cm}^{-1}$ , while Kurland's (32) measurements in the microwave region gave a result  $A''_e - \bar{B}''_e = 2.072_4 \text{ cm}^{-1}$ .

The large number of structural parameters in formamide limits the application of the above data to structural considerations.

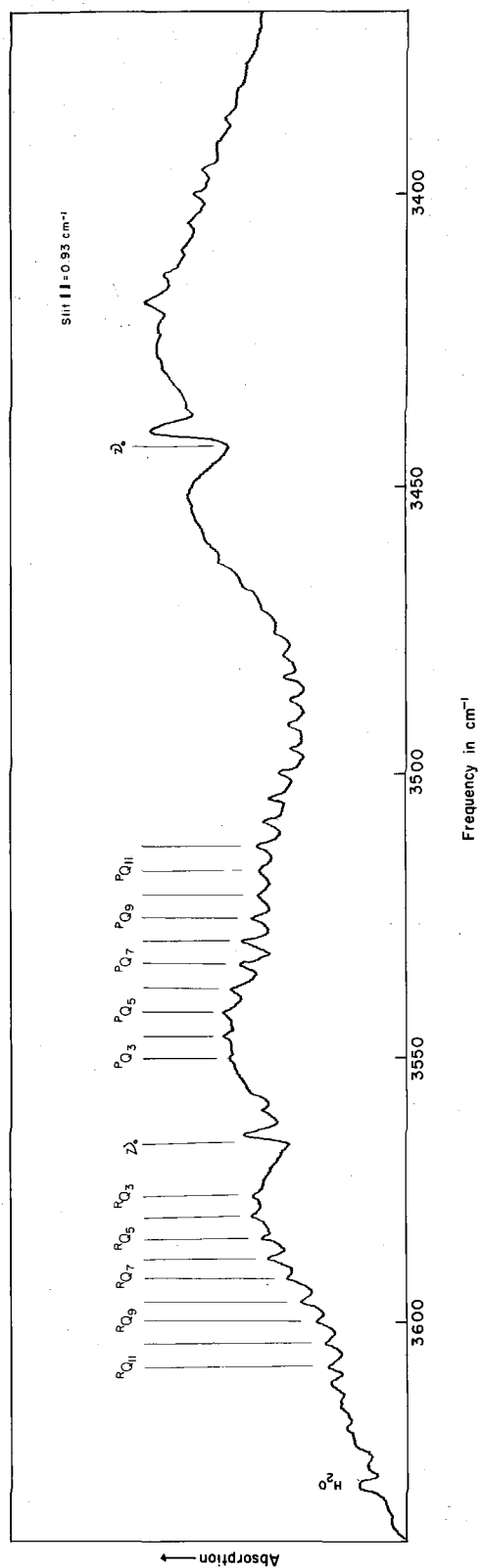


Figure 25. Rotational structure of  $\nu_1$  and  $\nu_2$  of gaseous  $\text{HCONH}_2$ .

Table 17. Rotational assignments,\* and combination relations for  $\nu_1$ .

K	$R_{Q_{K-1}}$	$P_{Q_{K+1}}$	$\Delta^{**}$	$\Delta/4K^{***}$
4	3575.53	3541.98	33.55	2.097
5	3579.15	3537.91	41.24	2.062
6	3583.19	3533.59	49.60	2.067
7	3587.10	3529.48	57.62	2.058
8	3591.13	3525.19	65.94	2.061
9	3595.30	3520.56	74.74	2.076
10	3599.22	3516.22	83.00	2.075
11	3603.37	3512.10	91.27	2.074

\*Frequencies in  $\text{cm}^{-1}$  (vacuum).

\*\*  $\Delta = R_{Q_{K-1}} - P_{Q_{K+1}}$

\*\*\*  $\Delta/4K = A'' - B''$

Appendix 4

The molecular parameters used for calculating the moments of inertia of formamide for the Teller-Redlich product rule application, and some additional comments are given here. Figure 26 gives the molecular parameters.

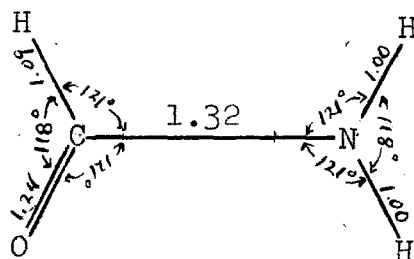


Figure 26. Molecular parameters of formamide used in the calculation of the moments of inertia for the Teller-Redlich product rule application. Lengths in Angstroms.

The moments of inertia were calculated for the model shown for both HCONH<sub>2</sub> and HCOND<sub>2</sub>. The particular parameters shown may not represent the best estimates possible. However, the best set would not change appreciably the value of the right-hand member of equation (1), p. 106. The values for the moments of inertia are listed in Table 18.



Table 18. Moments of inertia\* of  $\text{HCONH}_2$  and  $\text{HCOND}_2$  corresponding to Figure 10.

	$\text{HCONH}_2$	$\text{HCOND}_2$
$I_x$	7.28	8.29
$I_y$	42.48	47.99
$I_z$	49.76	56.28

\* Units are a.m.u.  $\text{\AA}^2$

## References

1. A. Franssen, Bull. soc. chim., 43, 177 (1928).
2. L. Kahovec and K. W. F. Kohlrausch, Z. physik Chem., B, 37, 421 (1937).
3. L. Hunter and H. A. Rees, Nature, 153, 284 (1944).
4. S. Imanishi and T. Tochi, J. Chem. Soc. Japan, 63, 492 (1942).
5. Y. Otagari, J. Chem. Soc. Japan, Pure Chem. Sect., 70, 263 (1949).
6. Colson, J. Chem. Soc., 554 (1917).
7. W. C. Schneider, J. Am. Chem. Soc., 72, 761 (1950).
8. J. Ploquin and C. Vergneau-Souvray, Compt. Rend., 234, 97 (1952).
9. L. Kahovec and K. W. F. Kohlrausch, Z. physik Chem., 193, 188 (1944).
10. B. Bak and F. A. Andersen, J. Chem. Phys., 22, 1050 (1954).
11. G. Herzberg, Infrared and Raman Spectra of Polyatomic Molecules, D. van Nostrand Company, Inc., New York (1945), p. 421.
12. S. L. Gerhard and D. M. Dennison, Phys. Rev., 43, 197 (1933).
13. A. P. Cleaves and E. K. Plyler, J. Chem. Phys. 7, 563 (1939).
14. G. E. Moore and R. M. Badger, J. Am. Chem. Soc., 74, 6076 (1952).

15. P. H. Giguere and I. D. Liu, Can. J. of Chem., 30, 948 (1952).
16. This thesis.
17. B. L. Crawford, Jr., and W. H. Fletcher, J. Chem. Phys., 19, 406 (1951).
18. Ref. 11, p. 326.
19. E. B. Wilson, Jr., J. Chem. Phys., 9, 76 (1941).
20. H. M. Randall, R. G. Fowler, N. Fuson, and J. R. Dangle, Infrared Determination of Organic Structures, D. van Nostrand Company, Inc., New York (1949), p. 46 et seq.
21. E. B. Wilson, Jr., J. C. Decius and P. C. Cross, Molecular Vibrations, McGraw-Hill Book Company, Inc., New York (1955).
22. C. A. Coulson, Vol. Commemoratif Victor Henri (1947-1948), p. 15.
23. F. Halverson and V. Z. Williams, J. Chem. Phys., 15, 552 (1947).
24. H. H. Nielsen, Phys. Rev., 46, 117 (1937).
25. V. Schomaker and D. P. Stevenson, J. Am. Chem. Soc., 63, 37 (1941).
26. L. Pauling, The Nature of the Chemical Bond, Cornell Univ. Press, Ithaca, N. Y. (1948), p. 169.
27. C. A. Coulson, J. Duchesne, and C. Manneback, Vol. Commemoratif Victor Henri (1947-1948), p. 33.

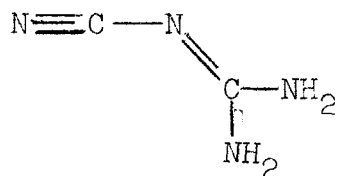
28. E. S. Ebers and H. H. Nielsen, J. Chem. Phys., 5, 822 (1937).
29. E. Amble and B. P. Dailey, J. Chem. Phys., 18, 1422 (1950).
30. Ref. 11, p. 295, 437.
31. L. H. Jones, J. N. Shoolery, R. G. Shulman, O. M. Yost, J. Chem. Phys., 18, 990 (1950).
32. R. J. Kurland, J. Chem. Phys., 23, 2202 (1955).
33. C. A. Coulson, Vol. Commomoratif Victor Henri (1947-1948), p. 15.
34. L. C. Pauling, Nature of the Chemical Bond, Cornell University Press, Ithaca, N. Y. (1948), p. 138.
35. R. D. Waldron and R. M. Badger, J. Chem. Phys., 18, 566 (1950).
36. H. M. Randall, R. G. Fowler, N. Fuson, and J. R. Dangi, Infrared Determination of Organic Structures, D. van Nostrand Company, Inc., New York (1949), p. 10.
37. R. M. Badger, Tech. Report No. 8 and Final Report, ONR contract N6ori-102, Task Order VI, Project NR-055-019, Oct. 31, 1954, p. 3.
38. W. C. Price and R. D. B. Fraser, Proc. Roy. Soc. (London) B 141, 1 (1953).
39. R. M. Badger and H. Rubalcava, Proc. Nat. Acad. Sci. (U.S.) 40, 12 (1954).

40. K. W. F. Kohlrausch and F. Köppl, Z. physik Chem., B24, 242 (1934).
41. R. Newman, J. Chem. Phys., 20, 1663 (1952).
42. B. D. Saksena, Proc. Ind. Acad. Sci., 11A, 53 (1940).
43. R. M. Badger and H. Rubalcava, Tech. Report No. 8 and Final Report, ONR contract N6 ori-102 Task Order VI, Project NR-055-019, Oct. 31, 1954, p. 74.
44. H. K. Kessler and G. B. B. M. Sutherland, J. Chem. Phys., 21, 570 (1953).
45. G. F. D'Alelio and E. E. Reid, J. Am. Chem. Soc., 59, 109 (1937).
46. J. Ladell and B. Post, Acta Cryst., 7, 559 (1954).

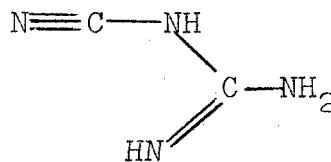
## PROPOSITIONS

1. It is proposed that the infrared spectrum of crystalline dicyanamide be studied with the aid of polarized radiation. Since the crystal structure of this substance is known (1), the spectral information may yield results applicable to the general study of solids by spectral methods.

2. It is proposed that dicyanamide be studied by means of nuclear magnetic resonance. Such a study may supply an independent check on Dr. E. W. Hughes' conclusion (1) that I, not II, is the correct structural formula.



I



II

3. An attempt to obtain the bond distances in cyanamide by means of electron diffraction should be made again. It will demand patience, but I respectfully submit, that the use of a heated nozzle, and the liberal use of film will yield the desired data.

4. A device using a train of thermal conductivity elements in a cylindrical tube can be used for determining the diffusion coefficient of binary gaseous mixtures. This device may have pedagogical use.

5. Decius (2) has observed and explained some extremely interesting phenomena in the spectra of mixtures of certain nitrates (and carbonates), for example  $\text{KN}^{14}\text{O}_3$  and  $\text{KN}^{15}\text{O}_3$ . The appearance of normally forbidden absorption bands has been attributed to destruction of the symmetry found in the pure crystals and a dipole-dipole interaction between the induced dipoles in the vibrating ions. It is proposed that a similar experiment and analysis may be applied to equimolar isotopic mixtures (using  $\text{N}^{15}$  and  $\text{N}^{14}$ ) of aliphatic amides in  $\text{CCl}_4$  solutions. This should lead to additional information applicable to the study of hydrogen bonding in aliphatic amides. See, for example, reference (3).
6. An explanation is advanced for the explosive decomposition of  $\text{HCONH}_2 \cdot \text{HCl}$ .
7. An estimate of the enthalpy of interaction between molecules such as  $\text{H}_2$  and  $\text{CO}_2$  may be obtained from intensity measurements of the infrared absorption bands of such mixtures. See (4).
8. In event that the reaction of primary amides (aliphatic) with nitrous acid is "quantitative," as stated in Sidgwick's Organic Chemistry of Nitrogen, forming nitrogen, then I propose that the Van Slyke gasometric apparatus would be useful in the determination of primary aliphatic amides.

9. Consider Figure 1:  $p_1$  and  $p_2$  are the partial pressures of components 1 and 2 of a binary liquid mixture;  $x$  is the mole fraction of 2; and the dashed lines represent the ideal pressures. A proof is presented which shows that the behavior represented by the figure is impossible.

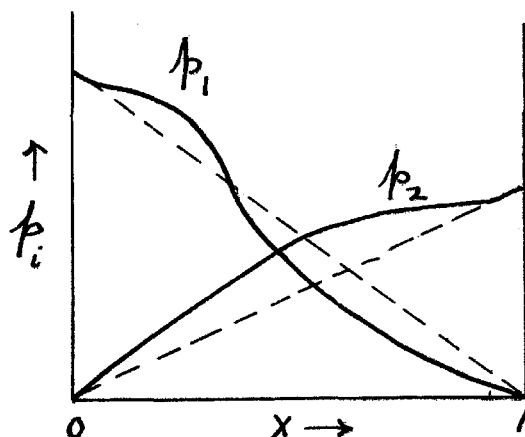


Figure 1

10. Acid ion exchange resins may be useful as column materials for vapor phase chromatography, particularly for the separation of the unsaturated hydrocarbons through  $C_4$ .

#### REFERENCES

1. E. W. Hughes, J. Am. Chem. Soc., 62, 1258 (1940).
2. J. C. Decius, J. Chem. Phys., 23, 1290 (1955).
3. R. M. Badger and H. Rubalcava, Proc. Nat. Acad. Sci., 40, 12 (1954).
4. J. Fahrenfort and J. A. A. Ketelaar, J. Chem. Phys., 22, 1631 (1954).